Decommissioning Offshore Wind Export Cables in the North Sea

Wessel Bruinsma

TU Delft

NTNU

Decommissioning Offshore Wind Export Cables in the North Sea

Master Thesis by

Wessel Bruinsma

In partial fulfilment of the requirements to obtain the degrees of

Master of Science in Offshore and Dredging Engineering at Delft University of Technology (TU Delft)

and

Master of Science in Technology- Wind Energy at the Norwegian University of Science and Technology (NTNU)

under the European Wind Energy Master programme.

To be defended in public on July 5, 2024.

Supervisors:	TU Delft - Rudy Helmons NKT - Otto Kooy NTNU - Svein Sævik NTNU - Erin Bachynski-Polić
Committee Members:	TU Delft - Geert Keetels NTNU - Bernt Leira
Student Number:	TU Delft - 4668758 NTNU - 103176
Cover:	SINTEF 3D rendering of a subsea power cable [16]

Preface

This thesis is submitted as part of the requirements for the MSc degree in Offshore and Dredging Engineering at the Delft University of Technology (TU Delft), as well as the MSc degree in Technology-Wind Energy at the Norwegian University of Science and Technology (NTNU) under the European Wind Energy Master (EWEM) programme. The thesis focuses on the decommissioning of offshore wind export cables in the North Sea, particularly addressing the technical challenges and feasibility of the cable pullout method.

I would like to express my gratitude to my supervisors, Prof. Rudy Helmons from TU Delft, Prof. Svein Sævik from NTNU, and Prof. Erin Bachynski-Polić from NTNU. Their weekly or biweekly consultations, valuable insights, and constructive feedback have been crucial in guiding my research and ensuring its academic rigour. Thanks to Rudy, the research was staged on TU Delft's social media channels, which sparked a lot of attention and interesting conversations about cable decommissioning.

The collaboration with NKT has been instrumental in the completion of this research. NKT develops and offers high-end cables, accessories and cable services such as offshore installation. NKT is well known for its offshore HVDC cables connecting offshore wind farms to onshore grids. I want to extend my gratitude to NKT and especially Otto Kooy for providing me with this opportunity and for the continuous support throughout the project. The collaboration with NKT was also valuable for other parts of the research, such as the expert interviews and the provision of the OrcaFlex software.

Special thanks go to the industry experts I had the privilege to interview. Their expertise and willingness to share knowledge on subsea cables and decommissioning practices provided essential practical insights that enriched this study and helped me to understand the basics of the industry quickly. A full list of interviewees can be found in the Appendix. I also want to thank Prof. Dave White from the University of Southampton, who helped me a lot with understanding geotechnical engineering in the context of buried pipelines and cables.

I look back at two incredible years as a European Wind Energy Master student. Except for the paperwork, it was a great experience to study at three different universities as part of one programme. Every semester was completely different and enriching. Sometimes we worked hard, other days we travelled around and had good fun. I am also grateful to my family and friends for their support and encouragement throughout this journey. Their belief in my capabilities has been a constant source of motivation.

The research conducted in this thesis is not only an academic exercise but also aims to contribute to the broader field of offshore wind energy, particularly in addressing the emerging challenges of decommissioning first-generation offshore wind farms. This research could be the start of more attention to cable decommissioning both in academics and the industry. I hope that this work will inspire further research and development in the field of offshore wind energy.

Wessel Bruinsma
Delft, June 28th 2024

Abstract

Offshore wind energy has become a crucial element of the global energy transition, with the North Sea being a major hub for offshore wind farms. As first-generation farms approach the end of their operational life, decommissioning offshore wind export cables has emerged as a significant technical challenge. This thesis focuses on the feasibility and limitations of using the cable pullout method for decommissioning offshore wind export cables, particularly examining the influence of burial depth and soil conditions.

This research is structured in two main phases. The first phase involves a comprehensive literature review to identify critical knowledge gaps and establish an overview and understanding of existing decommissioning practices. The second phase employs simulations using OrcaFlex software to model and analyze various cable pullout scenarios. These simulations focus on determining the limits and constraints imposed by burial depth and soil relative density for sandy soils commonly found in the North Sea.

Key findings from the literature study underscore the complexities of decommissioning, which encompass legal, environmental, economic, and technical considerations. One of the main conclusions is the importance of adopting a 'design for decommissioning' approach during the initial cable installation. This involves designing cables and selecting burial depths that facilitate easier future removal, thus promoting sustainability and cost-effectiveness. Additionally, this approach can help mitigate potential environmental impacts and regulatory challenges associated with cable removal.

Soil modelling plays a crucial role in understanding how burial depth and soil conditions influence resistance forces during cable pullout. Factors such as shear strength and burial depth are analyzed to determine the forces that oppose cable recovery. The model includes scenarios for fully drained, fully undrained, and partially drained uplift resistance, implemented in a Python script to simulate real-time resistance during pullout operations. To address buried cables, an external soil model is integrated into OrcaFlex, allowing dynamic simulations of soil resistance during cable pullout.

The simulation results with a 525 kV HVDC export cable reveal how soil resistance significantly increases with greater burial depth and higher soil density. These findings highlight the critical importance of burial and soil conditions in planning decommissioning operations and suggest that additional deburial techniques may be necessary when cable pullout is not feasible.

This thesis provides valuable insights and recommendations for future research and practical applications, aiming to support the offshore wind industry's evolving needs and enhance the sustainability of decommissioning processes. These findings are crucial as the industry anticipates a substantial increase in decommissioning activities, with offshore wind capacity expected to continue to grow.

Contents

List of Figures

List of Tables

1

Introduction

1.1. Background

Offshore wind energy has evolved into a vital component of the energy transition. In light of the climate crisis and worldwide increasing energy demand, boosting the global production of renewable, carbon-free electricity is essential. The North Sea, renowned for its favourable wind conditions, has emerged as a primary hub for offshore wind development in the past decades. Today, the first-generation large-scale offshore wind farms (OWFs) are approaching the end of their operational lifetime. Consequently, OWF owners will start decommissioning to restore the site as closely as possible to its original state, as this is required by the government. OWF decommissioning will significantly increase in the coming decades as total installed offshore wind capacity will grow >2000% by 2050 compared to today [7]. This is in line with the Global Wind Energy Council's forecast for the coming years presented in Figure 1.1.

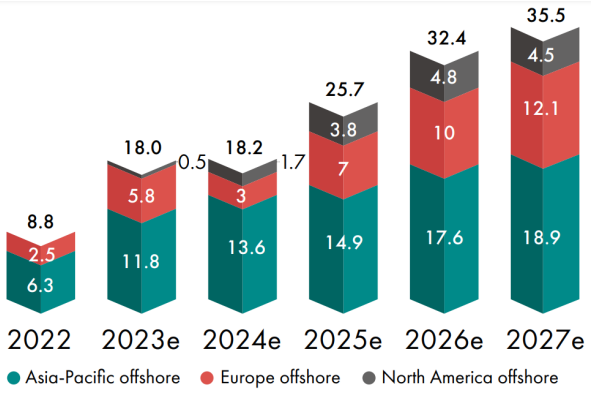

Figure 1.1: Global Wind Energy Council's forecast for estimated (e) regional offshore wind power capacity additions in GW [15]

Part of an OWF is the subsea power cable system responsible for transmitting the generated electricity to the mainland grid; see also Figure 1.2. This cable network typically consists of inter-array cables connecting individual wind turbines to at least one export cable linking the OWF to the mainland. Decommissioning these offshore wind power cables is complex and entails legal, environmental, economic, and technical constraints. This research focuses on the technical perspective of decommissioning the export cables. However, a basic understanding of the other perspectives is also important since large-scale decommissioning of subsea power cables is a relatively new and unexplored challenge. To date, only a few experimental or small wind farms have been decommissioned [25]. According to DNV, experience with the removal of subsea power cables is very limited and virtually non-existent for offshore wind farms cable systems [8]. Consequently, existing standards such as 'DNV-ST-0359 Subsea power cables for wind power plants', and guidelines, e.g. 'DNV-RP-0360 Subsea power cables in

shallow water', only shortly mention cable decommissioning with general statements and no concrete information [8], [10].

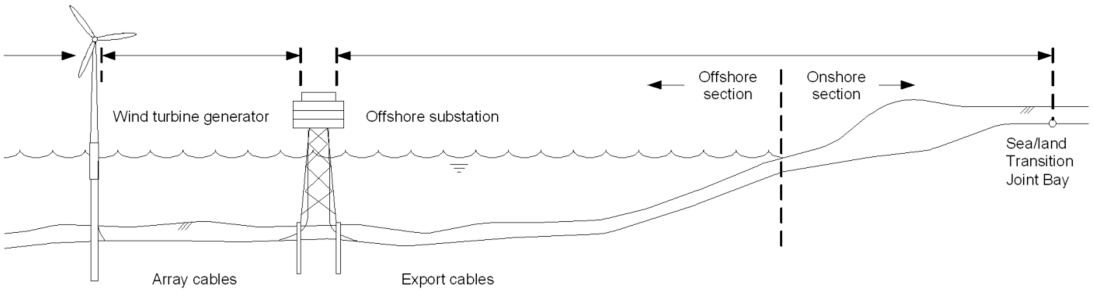

Figure 1.2: OWF subsea power cable system [8]

For the tenders of offshore wind power cables, decommissioning is currently not considered in detail (Smalt, 04-10-2023). There is usually only a lifetime requirement of around 25-30 years, which is equal to the OWF lifetime (Smalt, 04-10-2023). However, it is important to also think about decommissioning during the tender process. It is not necessary to go as far as signing decommissioning contracts 30 years upfront but cable design should take future decommissioning into account such that stripping and recycling could be more efficient. Installation for decommissioning, e.g. reducing the burial depth, could make it easier to recover the cable in the future. Nowadays, contracts require minimum burial depths to ensure proper cable protection. To obtain a broad understanding of the topic from different perspectives, interviews were conducted with industry experts. A brief overview of the insights from the experts and literature is given below to demonstrate the increasing relevance of research into decommissioning offshore wind power cables.

Legal Perspective

Although international regulations such as the United Nations Convention on the Law of the Sea (UNCLOS) stipulate complete decommissioning, implying the removal of all components and infrastructure from the marine environment, there is no strict requirement for recovering power cables [18]. Within territorial waters (up to 12 nautical miles, 22 km), national legislation governs the decommissioning requirements. Outside territorial waters, UNCLOS and customary international law do not require the removal of out-of-service (OOS) cable systems [8]. However, for the North Sea, the Convention for the Protection of the Marine Environment of the North-East Atlantic (OSPAR) decided that decommissioning includes the cables. Therefore, this research will focus on offshore wind power cables in the North Sea. Within OSPAR, cable owners may request permission to leave them in place when cable decommissioning involves severe adverse environmental or economic impacts. For the cables left in situ, it is unclear which party will be liable and here clarity should be provided.

Environmental Perspective

The complete removal of offshore wind export cables could result in considerable marine disruptions due to their extensive length [34]. On the other hand, the footprint of decommissioning would be relatively narrow. Besides, leaving the cables in place would also ignore the need for circularity of conductor materials such as copper and aluminium. Current cable permits aim to apply the installation methods that are the best solution for the environment as of today (Heemrood, 12-10-2023). However, those methods might not be the best solutions for the environment in the long term. For example, burying the cables deep (> 5 meters) could be a great short-term solution to prevent environmental impact from reburial-related maintenance. However, increased burial depth could result in more negative impacts in the case of cable repairs or decommissioning. Whereas, for limited burial depth in sandy soil in the North Sea, the environmental impact could be small and local when it is possible to pull out the cable without prior deburial (Andersen, 03-10-2023). Recovering cables from the seabed is unlikely to do more harm than laying cables in the first place. Th fact that the environmental impact of

cable laying was judged acceptable, implies it might not be sufficient to justify leaving cables in situ based on environmental concerns for the narrow cable route.

Economic Perspective

Some power cables with limited burial depth have been decommissioned mainly for their monetary scrap value and not necessarily because of legislation or environmental reasoning (Andersen, 03-10-2023). In specific cases, there was a profitable business case for decommissioning power cables with copper conductors. Nowadays, many cables contain aluminium instead, which significantly reduces their scrap value. Decommissioning is thus probably more expensive than the income from recycling in most cases (Oor, 28-10-2023). Therefore, cable owners may try to convince the government to leave the cables in place. However, the seafloor will become congested if owners do not recover their OOS cables, potentially affecting other stakeholders in the North Sea. New cable projects already encounter OOS cables, causing extra costs and delays (Oor, 28-10-2023).

Technical Perspective

The most straightforward method for subsea cable decommissioning is pulling out the cable without prior deburial. In this case, the recovery vessel can 'simply' pull the cable from the sea bed without additional deburial tools. The burial depth, soil conditions, and cable properties usually determine whether such a cable pullout is possible (Oor, 28-10-2023). For deeper buried cables, recovery first requires deburial operations. Examples of deburial methods are jetting with a jetting pig, mass flow excavation (MFE), and dredging in most extreme cases. The environmental impact on the seafloor and surroundings depends on the applied method. The industry considers decommissioning with only cable pullout as the least impactful and dredging as the most harmful to the environment (Andersen, 03-10-2023).

1.2. Problem Statement

As illustrated above, decommissioning offshore wind power cables is of increasing importance and the industry lacks experience with such projects. Therefore, there is a need to understand the reasoning, technical methods, and consequences of cable decommissioning and recycling. Moreover, cable design and burial depth during installation largely determine decommission possibilities. Ideally, cables would be designed and installed enabling quick and easy decommissioning in the future. 'Design for decommissioning' could entail designing cable armour to be especially suitable for cable pullout. Regarding 'installation for decommissioning', e.g. the burial depth could be reconsidered to enable easier future decommissioning.

Besides, an increasing number of OWFs will reach the end of their lifecycle. Regarding circularity targets, it seems unacceptable to leave cables in place after decommissioning the rest of the OWF. Deciding on the applicable decommissioning methods depends on the technical parameters as well as legal, environmental, and economic factors. For example, the environmental impact of leaving the cable on the seafloor should be compared to the disruption caused by decommissioning. This disruption depends on the composition and condition of cable materials, burial and sedimentation conditions, and the benthic environment [18]. Next to this local impact, there is also a global impact regarding the positive effects of recycling cable materials. Since cable pullout without prior deburial operations is often the preferred decommissioning method from several perspectives, it is crucial to define the limits of this decommissioning method.

1.3. Research Objective

This research aims to contribute to a more sustainable and circular offshore wind industry. To achieve this, the literature study, the first phase of this research, identified critical knowledge gaps regarding decommissioning offshore cables. After the literature study, the second phase of this research, the thesis

project, focused on increasing the understanding of the limits of cable pullout without prior deburial as a decommissioning method for offshore wind export cables. These limits were identified as a key knowledge gap after the broad analysis of the decommissioning process for offshore wind export cables in Chapter 3. The research objective was hence defined as:

"*Determine the limits and constraints on burial depth and soil conditions for cable pullout of an offshore wind export cable buried in sandy soil in the North Sea.*"

This research only considered modern high-voltage direct current (HVDC) and high-voltage alternating current (HVAC) export cables. The old-fashioned oil-filled cables were out of the current scope. Decommissioning oil-filled cables requires different methods due to the risk of environmental hazards. Besides, 95% of the market is covered when taking only cables without oil into account (Oor, 28-10-2023). Dynamic cables are more susceptible to fatigue and twists caused by hydrodynamics and have specific designs [30]. Therefore, dynamic cables are also left out of the current scope. This research focused on export cables because they are larger and longer than the inter-array cables and thus contain more raw materials. Export cables are also more relevant to investigate due to their more severe contribution to seabed congestion. However, many of the findings of this research are also applicable to inter-array cables and subsea cables in general.

Near-shore cable decommissioning is extra complicated, mainly due to the shallow water (< 10 meters water depth) and cable landings (Impola, 25-10-2023). Therefore, this research will focus on decommissioning the cable from the platform interface at the wind farm to the landfall interface. Recovering the cable end is complicated and costly, while the short amount of extra recycled cable length has little worth compared to the total length of the cable. Regarding soil type, the focus is on sandy soils, leaving out other soil types such as clay and rock since those would require different deburial methods (Oor, 28-10-2023). Furthermore, the research focused on the continuous cable pullout along the cable route. Connecting and lifting a cable end before starting with the continuous pullout is a completely different operation and would require another modelling approach. The continuous pullout can be considered a steady-state process when assuming a constant cable route regarding burial depth, soil conditions, and water depth without waves, currents, and wind.

1.4. Research Questions

To determine the most critical knowledge gaps regarding the technical feasibility of decommissioning offshore cables, the literature study covered the following questions:

- What are the characteristics of out-of-service offshore wind power cables?
- What are the state-of-the-art methods for offshore cable decommissioning and their respective limitations?
- What is a typical offshore wind power cable decommissioning scenario in the Dutch-German part of the North Sea?
- What are the governing criteria for cable pullout in such a decommissioning scenario?

For the second phase of this research, the thesis project covered research questions in order to determine the limits on burial depth and soil conditions for cable pullout:

- How do the burial depth and soil conditions influence the resistance forces during cable pullout?
- How can a dynamic model simulate the recovery of a buried offshore cable?
- For what burial depth and soil conditions is it possible to perform a cable pullout for a typical cable decommissioning scenario?

1.5. Report Structure and Research Methodology

The first three chapters were largely based on the literature study. The general characteristics of subsea cables are described in Chapter 2, and the state-of-the-art decommissioning methods are analysed to identify critical knowledge gaps in Chapter 3. A comprehensive literature search was performed using various online databases and internet search tools, including Web of Science, Science Direct, Google Scholar, and ResearchGate. The initial goal was to answer the first set of research questions with peer-reviewed scientific publications, books, theses, and non-peer-reviewed consultancy and technical reports. Due to a general scarcity of published studies on offshore cable decommissioning, much of the current knowledge is derived from industrial reports, governmental reports, and environmental impact assessments. To gather further practical insights, interviews with industry experts have been conducted. The interviews were valuable for understanding the cable industry quickly and provided insights from previous experiences related to cable decommissioning, such as cable repair operations.

As mentioned earlier, investigating the limits of cable pullout was deemed the most relevant and suitable knowledge gap to address. To determine the limits of cable pullout, a typical scenario for decommissioning an export cable is described in Chapter 4. This chapter forms the bridge between the literature study and the thesis project. Actual project data from the company NKT inspired the typical cable decommissioning scenario. To determine the limits of cable pullout without any deburial or jetting, the operation was simulated in OrcaFlex. NKT and other companies in the cable industry use this software for cable analyses, especially for offshore cable laying. OrcaFlex is useful for analysing the mechanical response of the cable from the vessel chute to the seabed. Therefore, it was relatively straightforward to model the recovery of an unburied cable, as this is basically a reverse cable-laying operation. However, OrcaFlex currently has no option to model a buried cable. Therefore, an external soil model had to be added to the OrcaFlex simulation to be able to generate the appropriate soil resistance. The construction of the model that runs these simulations was done in three different steps, as visualised in the research plan below. For each OrcaFlex modelling step, input was required, as shown in Figure 1.3. The input for steps 1 and 3 is presented in Chapter 4 and the input for step 2 in Chapter 5. Building the OrcaFlex model in step 1 and extending it with the soil model in step 2 is covered in Chapter 6. The results of the simulations in step 3 are presented and analysed in Chapter 7.

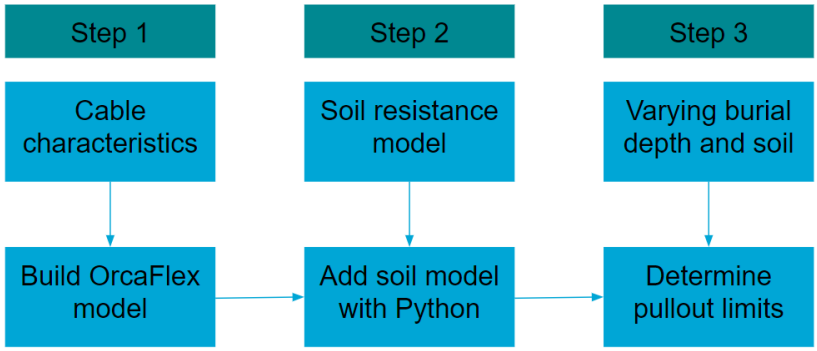

Figure 1.3: Research plan for investigating the limits of cable pullout for decommissioning export cables

Recovering a buried cable is more challenging compared to an unburied cable resting on the seabed due to the soil resistance. In Chapter 5 a soil model is introduced to calculate the resistance that has to be overcome to pull the cable out of the seabed. This soil model was partly based on existing research and adaptations of DNV guidelines for buried pipelines. This soil model was implemented in Python in order to add an external function to the OrcaFlex model. Chapter 6 details the process of constructing a standard OrcaFlex model, which includes a simple vessel, a chute, a winch, and a cable. This model first simulates the recovery of an unburied cable resting on the seabed. Thereafter, the soil model from the previous chapter is integrated to calculate soil resistance while simulation the pullout of a buried cable. Chapter 7 presents a comprehensive analysis of the final simulation results. It examines the feasibility of cable pullout across a range of burial depths and soil densities typical of offshore wind export cables. The conclusion summarizes the key findings of the research and the recommendations chapter offers specific suggestions for future research and improvements in decommissioning practices.

2

Characteristics of Out-of-Service Subsea Cables

This chapter covers the first research question: What are the characteristics of out-of-service offshore wind power cables? It provides first an overview of subsea cable applications. The section on cable elements delves into the composition of these cables, highlighting the significance of the conductor and the armour. The cable armour is described in more detail in the section with armour specifications. It explains the concepts of tensional stability, bending stiffness, and lay angles. The chapter also delves into cable protection measures, with a primary focus on burial depth, explaining its importance, complexities, and the role of cable burial risk assessments. In essence, this chapter serves as a foundation for understanding subsea cables.

2.1. Subsea Cable Applications

Subsea power cables are nowadays widely used in the oil and gas industry as well as for offshore renewables [27]. Offshore wind power cables are a specific application of this long-serving concept. Subsea cables have been around for over a century with several changes in main application areas such as supplying offshore facilities and islands and connecting power grids [37]. There are many different kinds and varieties of subsea power cables and they are often tailor-made and not off-the-shelf products [37]. Conditions can differ significantly and hence cable requirements are dependent on each individual project. Nowadays, subsea cables have several applications, according to the European Subsea Cables Association (ESCA) the most common subsea cable types are:

- DC (direct current) or AC (alternating current) interconnector cables;
- DC distribution cables;
- AC or DC transmission cables;
- inter-island power cables;
- in-field array or collector cables usually of 11 kilovolt (kV), 33 kV or 66 kV, necessary for transporting power from individual wind turbines to an offshore substation platform;
- HVAC and HVDC export cables used for the export of power from an OWF to the landing point [12].

Offshore wind farms with relatively small capacities and close vicinity to shore could connect to shore with medium-voltage cables [37]. For OWFs with many turbines, with large power output per turbine, or with a long distance to shore, a high-voltage HVAC cable is more economical. In that case, the individual wind turbines transport their power output to an offshore substation platform. The platform contains a

step-up transformer to increase the voltage from the array cables. For even longer distances with large amounts of power, wind farms can benefit from HVDC export cables because the transmission losses are lower than for HVAC cables. This only applies to distances larger than 100 km, because HVDC requires expensive offshore and onshore converter stations [37]. In the case of DC export cables, there are often two cables used together in a pair, sometimes attached or bundled and sometimes separated (Zheng-Lu, 29-09-2023).

2.2. Cable Elements

Nowadays, cables are monopolar, bipolar or three-phase systems with diameters between 5 and 30 cm and masses between 15 and 120 kg/m [30]. The most important part of the cable is the conductor, the part that transports the current. The conductor can be made out of aluminium or copper, with the latter having a 64% better conductivity [37]. In order to have an aluminium cable with the same conductance as a copper cable, the aluminium needs a larger cross-section to compensate for its lower conductivity. A subsea cable consists of several elements as can be seen in Figure 2.1. Moving outwards from the conductor we find successively:

- at least one conductor, made out of copper or aluminium;
- semi-conducting layers;
- insulation, such as cross-linked polyethene (XLPE) or ethylene propylene rubber (EPR);
- screen/sheath, made out of metal;
- optional non-metallic sheath;
- non-metallic filler material;
- optional optical fibres with protection;
- armour bedding;
- cable armour, typically metal tape(s) or wire(s) providing tensile strength and protection;
- non-metallic outer serving/sheath.

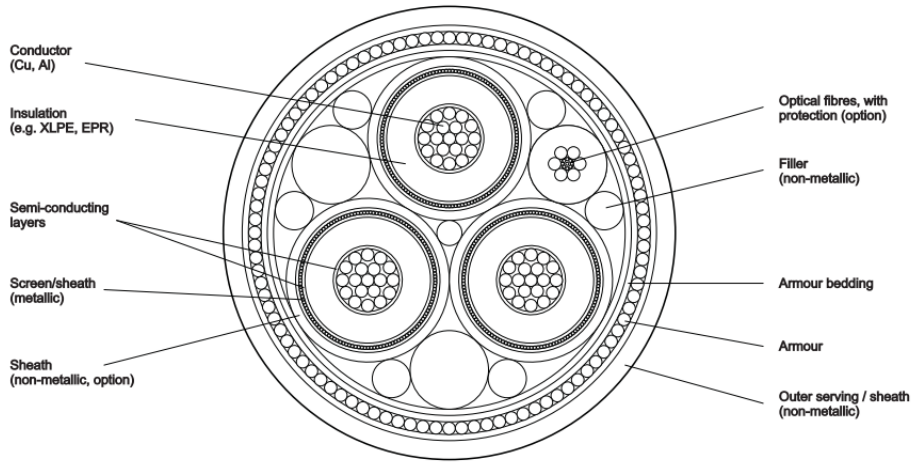

Figure 2.1: Example of a subsea three-phase AC power cable cross-section [8]

2.3. Armour Specifications

The cable armour largely determines the mechanical properties of the cable [8]. The armour is designed to enable handling of the cable during the different phases of the cable lifetime, e.g. production, storage, installation, operation, and repair/decommissioning. The armouring provides both tension stability and mechanical protection [37]. Protection of the cable is necessary for example due to fisheries, anchors,

and transport or installation tools. During installation, the cables are exposed to both the weight of the hanging cable and the dynamic forces from vertical vessel movements, potentially resulting in a total tensional force significantly exceeding the static force of a hanging cable [37]. For more details on the cable tension, see Section 3.2 and Subsection 4.2.1.

Usually, the armour is made of metal tape or wires wound around the cable in a helix [10]. The design parameters of the armour are mainly affected by the wire diameter and wire configuration [17]. The metal wires have a lay angle α and a lay length L_p also referred to as helix pitch length. See also Figure 2.2 for a visual overview of these properties.

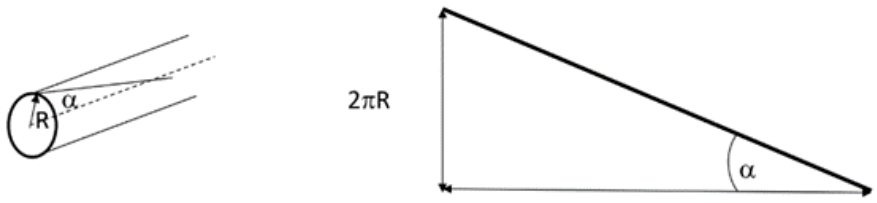

Figure 2.2: Lay angle α and lay length L_p [29]

The lay length is the distance in which the wire makes one complete turn around the cable, typically between 10 and 30 times the cable diameter [37]. The lay angle and lay length are related according Equation 2.1:

$$L_p = \frac{2\pi R}{\sin \alpha} \cos \alpha = \frac{2\pi R}{\tan \alpha} \tag{2.1}$$

where R is the cable radius. The total cross-section area of the cable armour A_a is the area of an individual armour wire A_t multiplied by the number of wires n and the cosine of the lay angle, as described in Equation 2.2. The area of a circular armour wire is simply the product of π and the wire radius r_a squared.

$$A_a = nA_t \cos \alpha \tag{2.2}$$

$$A_t = \pi r_a^2 \tag{2.3}$$

The armouring design mainly determines the tensional stability, bending stiffness, and torsion balance [37]. With helical armouring, tensional forces result in torsion forces. To limit torsion and achieve high tensional stability, long lay-length armouring is preferred. However, long lay length increases the cable's bending stiffness, which is not desirable [37]. The advantage of short lay length is a lower bending stiffness but this comes with transferring more of the force to the cable conductor [37].

Cables with unidirectional armouring are only able to absorb torsions in one direction [8]. Therefore, unidirectional armouring is also referred to as unbalanced armour, see also Figure 2.3. A double layer of armour wires with different lay directions, e.g. Z- and S-lay, provides much stronger protection than a single layer. The two layers' torsional forces counterbalance or even cancel out each other [37]. Therefore, this counter-helical double layer of armouring wires is also referred to as torsion-balanced armour. Double armoured cables are heavier and less flexible, making these more difficult to install than single armoured cables [22]. The balanced armoured cables also require turntables for storage and installation [37]. Torsion-balanced armour is therefore only applied when additional protection against the marine environment is needed such as in locations where there is a high risk of hostile seabed interventions [25].

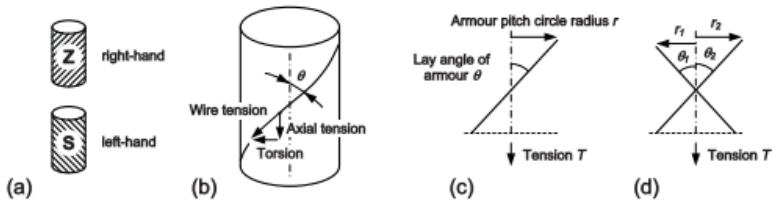

Figure 2.3: Elaboration on cable armour: (a) Z- and S-lay, (b) Forces, (c) Unbalanced armour, (d) Torsion-balanced armour [8]

Single armoured cables are typically installed in combination with cable burial to provide the cable with appropriate protection [22]. For offshore wind export cables, usually, single unbalanced armour is used. As an alternative for steel armouring, modern aramid or polyester fibres such as Kevlar can also achieve proper tensile strength [37]. Fibres have been used in the past, however, this solution has the disadvantage of offering only a little protection against fisheries and anchoring [37].

In general, external damages are not likely to cause direct breakage of the cable due to the high-strength armour [35]. However, most subsea applications such as offshore wind farms are in the open sea with salty waters and a corrosive environment. Therefore, corrosion must be considered. The steel armour wires are in most cases made of steel galvanised with a zinc coating [37]. The first protection against the impact of salt water is however the polymeric outer sheath. This sheath excludes the seawater as long as it is intact. However, when this protection layer is damaged due to for example sand abrasion, it might result in pitting corrosion from localised water current going into the wire [37]. Then the zinc layer of at least 50 μm of the galvanised steel takes care of corrosion protection. The corrosion rate of the zinc coating depends on several variables such as the temperature, the salinity and the free access to water. The last factor can be influenced to decrease corrosion rates by cable burial or protective layers. Past investigations of recovered cables from the Baltic Sea that had been exposed for decades, showed a zinc layer corrosion rate of about 1 μm/year [37]. As mentioned before corrosion-resistant materials such as polyester fibres like Kevlar could also be used as cable armour. Fortunately, corrosion affects but a fraction of armouring wires at singular spots and the other wires should still offer protection against external forces even when the tensile force has decreased [37].

2.4. Cable Protection and Burial Depth

In waters up to 1500 m deep, it is recommended to provide cables with proper protection against external aggression [13]. This protection is often achieved by the burial of the subsea cable, which means that the cable has to be pulled out of the seabed in case of decommissioning. From an operational, economic, and environmental point of view, the burial should be minimal. Other possible cable protection measures are for example pipes, concrete mattresses, and gravel/rock placement, see also Figure 2.4. However, this research focuses on the most common protection measurement in the North Sea: cable burial. In some sections of the cable route, such as the interface between the cable and fixed offshore structures like the converter platforms, infrastructure crossings or landfills, burial of the cable might be impossible or undesirable. Decommissioning of such sections would require a completely different approach and therefore these scenarios are left out of the scope of current research.

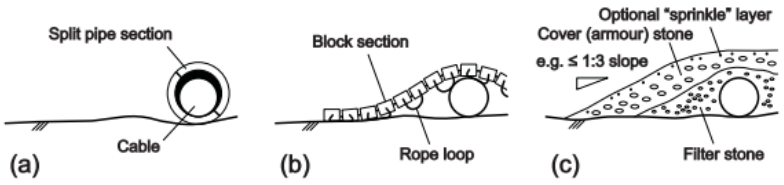

Figure 2.4: Cable protection alternatives: (a) Tubular product, (b) Concrete mattress, (c) Rock placement [8]

Regarding burial depth, specific terms are applied according to Figure 2.5. Generally, burial is described as lowering a cable into the ground/seabed [10]. The 'depth (height) of cover' is the vertical distance between the topside of the cable and the average level of the backfill above the cable. The depth of lowering (DOL) is the vertical distance between the cable's topside and the mean undisturbed seabed. The depth of the trench is defined as the vertical distance between the bottom of the trench and the mean undisturbed seabed. The material of a cable is partly selected based on the burial depth because deeper buried cables heat up more due to the isolation of the sand cover. For cables that heat up more because of larger burial depths, the preferred material is usually copper (Heemrood, 12-10-2023). Burial depths may vary along a cable route based on different local site locations and perceived risks. In some cases, the minimum burial depth depends on requirements predetermined by transmission system operators (TSOs) such as Tennet. It is also possible that local legislation requires certain minimum burial depths. Regarding decommissioning, the 'depth (height) of cover' is the most relevant parameter in Figure 2.5 and from this point, the term 'burial depth' refers to the depth of cover.

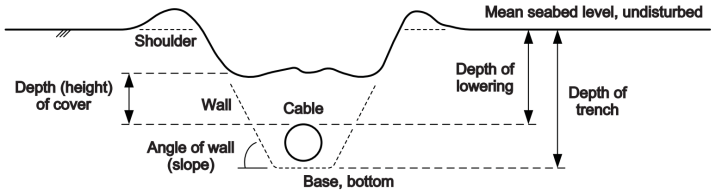

Figure 2.5: Burial depth definitions [10]

To ensure the safe installation of the cables, companies perform a cable burial risk assessment (CBRA) [11]. This risk-based approach can identify the required burial depth. Such an assessment entails potential hazards such as fishing or shipping anchors and site conditions like soil properties and seabed mobility [10]. According to the Carbon Thrust, fisheries are the main risk for subsea cables [5]. This is in line with Worzyk, who showed that more than 50% of the cable damage in the North Atlantic is the result of fishing equipment and 18% is related to anchors [37]. However, others claim that more than 50% of the encountered cable failures, cannot be proved to be caused by external factors (Andersen, 03-10-2023). In such cases, something went wrong during cable production or in the way the cable was operated. For example, OWF power cables experience high-temperature gradients due to large power fluctuations (Andersen, 03-10-2023). In such a cable failure scenario, the burial depth does not offer protection but does in fact complicate the repair process.

Depending on the results of the CBRA, it could be worth starting discussions with governments to see whether shallower burial could be allowed. Since the cost of cable supply and installation is around 10% of the capital costs (CAPEX) for offshore wind, a reduction in burial costs could result in considerable savings [5]. However, determining the optimum burial depth is a complex decision with plenty of considerations. Regarding fishing gear such as trawlers, a burial depth of 1–1.5 m offers in general good protection [37]. In the case of mobile seabeds, it might be necessary to have deeper cable burial to prevent regular maintenance with sand or rock dumping (Heemrood, 12-10-2023).

It seems obvious that a deeper buried cable has better protection but the relationship between burial depth and protection level is not linear and in some scenarios, protection level would not increase further below a certain burial depth [37]. Besides, shallower burial has quite some advantages over deeper burial:

- faster and cheaper installation with a larger choice of methods, equipment, and vessels;
- less cable and equipment stresses during installation;
- less negative environmental impact during installation and recovery in case of repairs or decommissioning;
- easier cable detection;
- easier access for cable repairs or decommissioning;
- improved cable cooling resulting in a higher cable current rating [10],[37], (Andersen, 03-10-2023).

Due to the seabed mobility, the cable burial depth at the time of decommissioning is not necessarily similar to the initial or intended burial depth. An example seabed mobility phenomenon that can affect burial depth is a sand wave. This is a large-scale depositional feature of the seabed, which is formed by sediment movement due to (tidal) currents or waves [10]. Sand waves have wavelengths ranging from 30 to 500 m [10]. They can move with a speed of dozens of meters per year and reach wave heights from 1 m up to one-third of the water depth (Snip, 02-10-2023). Other seabed features are rippled ridges and mega-rippled ridges with heights smaller than 0.1 m and wavelengths smaller than 0.6, and heights up to 1 m and wavelengths of up to 30 m respectively [10].

3

State-of-the-Art Methods for Cable Decommissioning

This chapter covers the second research question: What are the state-of-the-art methods for offshore cable decommissioning and their respective limitations? First. the installation process of subsea cables is described since the industry has way more experience with cable installation and because there are similarities between installation and decommissioning. Based on existing guidelines on subsea cable installation and subsea cable repairs, a general project overview for cable decommissioning is proposed. Next, the chapter covers the different deburial methods and the cable pullout operation. The chapter ends with a short recap of the literature study.

3.1. Subsea Cable Installation

The installation process of the offshore wind export cables largely determines the challenges for recovering the cables. Besides, the decommissioning process can be seen as reverse installation of the subsea cables. Therefore, it is important to understand cable installation properly. Before any deployment, the cable route has to be drawn based on bathymetry, soil, legislative, environmental, and economic considerations. Thereafter, the cable route has to be made ready for operation with e.g. removal of obstacles.

Installing the cable requires highly specialised equipment and is dependent on the local conditions. In soft soils such as sand, cables can be buried using ploughing or water jetting. In the case of hard or deep seabeds, cables can be laid on the seabed and stabilised with a suitable cover [30]. Installation duration depends on the applied methods and local seabed, e.g. cable laying for a flat seabed is less difficult and usually faster than routes with obstacles and elevation differences [37]. Cable laying rates can vary from 130-210 m/h for water jetting burial to 1850 m/h for free laying [24]. Laying down the cable on the seabed is done by specialized vessels. They are often equipped with a turntable for at least 4000 tons of cable and have appropriate gear [2].

A parameter of high importance during cable laying is cable tension. To control the tension, many other parameters have to be monitored and kept in check. The bottom tension, water depth, cable weight, vessel speed and wave-induced motion, bend radius, departure angle, and layback length influence the cable tension. See Figure 3.1 for the definitions of these parameters. The cable tensioner aboard the vessel controls the speed of the laying process and prevents slip of the cable [22]. The mechanical properties of the cable including tensile strength, minimum bending radius, and submerged weight should be included in the installation procedures [10]. The laying operation operability is dependent on weather conditions and the vessel's capabilities.

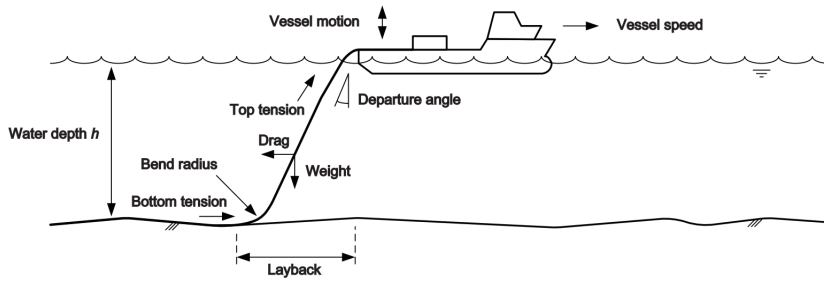

Figure 3.1: Cable laying process and cable laying parameters [8]

The type of platform chosen for laying cables depends on the project's needs. Usually, a cable-laying vessel (CLV) or barge is specially adapted for each operation, considering factors like loading capacity, deck space, handling equipment, and maneuverability. There are two common methods for the installation of subsea cables: S-lay with a chute/stinger and J-lay over the side of the vessel or through a moon pool. The S-lay chute is shaped to match or exceed the minimum bending radius of the cable. With the J-lay method, the cable is laid almost straight down to the seabed from the vessel, allowing for shorter layback lengths. The main difference between the two methods is how the cable bends from the tensioner to the seabed during deployment. With S-lay, the cable forms an S-shape, that bends over the chute and at the touch-down point (TDP) at the seabed. With J-lay the cable forms a J-shape, with no bending at the top after the tensioner and only bending at the TDP.

3.2. Cable Tension During Cable Laying

When laying the cable, several factors contribute to the total cable tension at the chute or laying wheel:

- the weight in air w_p of the cable from the chute to the sea level [29];
- the cable's weight in seawater w_s from the sea level to the touch-down point at the seabed [29];
- the bottom tension T_0 [29];
- the dynamic forces when the vessel and the chute are moving up and down [37].

The total static tension T at the chute is the sum of the first three factors:

$$T = w_p h + w_s d + T_0 \tag{3.1}$$

where h is the distance from the chute to the sea level and d is the water depth [29]. When the distance between the chute and the sea level is small, Equation 3.1 reduces to $T = T_0 + w_s y$. In the case of zero bottom tension, $T = w_s y$. The submerged weight w_s follows from applying the Archimedes law [28]. This is illustrated below in Figure 3.2.

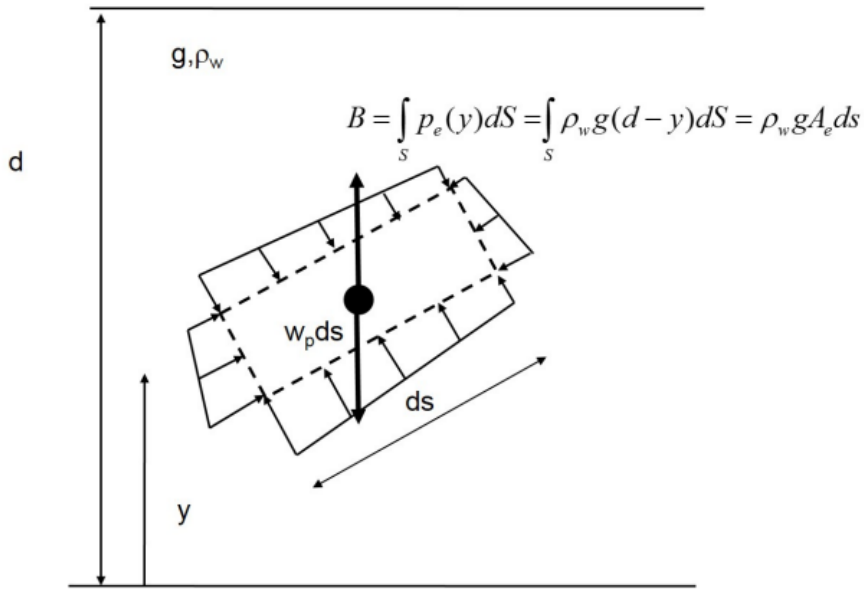

Figure 3.2: The Archimedes law for a virtual cable element in water [28]

A cable submerged in water will experience a buoyancy force equal to the weight of the displaced water. When integrating all the pressure p_e on the surfaces of a virtual submerged pipeline or cable element with length ds, the result will be the buoyancy force B:

$$B = \rho_w g A_e ds \tag{3.2}$$

where g is the is the acceleration due to gravity, ρ_w the seawater density, and A_e the external cable area. As can be seen in Figure 3.2, the submerged cable weight can be computed using:

$$w_s = w_p - g\rho_w A_e \tag{3.3}$$

Another way of coming to this conclusion is based on Figure 3.3. This method integrates the pressure field and studies the beam differential equation for the transverse equilibrium of an infinitesimal cable element in water [28]. The buoyancy acts perpendicular to the infinitesimal cable element with length ds and consists of contributions from $B1$ and $B2$. The first contribution $B1$ originates in the pressure difference between the upper part and the lower part of the cable element surface with the upper part having a lower pressure. The second contribution $B2$ is made because the area of the upper part is smaller than the area of the lower side. $B1$ is found by integrating the pressure around the entire surface of the cable and $B2$ is found by the net area difference as a result of the angular change $d\theta$ [28]. The total buoyancy can then be expressed as:

$$B = g\rho_w A_e(\cos\theta + (d-y)\frac{d\theta}{ds}) \tag{3.4}$$

where y is the distance from the seabed [28]. Considering the transverse equilibrium in Figure 3.3 gives:

$$(T + dT)d\theta + (Q + dQ) - Q + Bds - w_p \cos\theta ds = 0 \tag{3.5}$$

which by combination with Equation 3.4 and neglecting second order terms gives:

$$T\frac{d\theta}{ds} + \frac{dQ}{ds} = w_s \cos\theta \tag{3.6}$$

where T is the cable tension and $\frac{dQ}{ds}$ is the bending stiffness term [28].

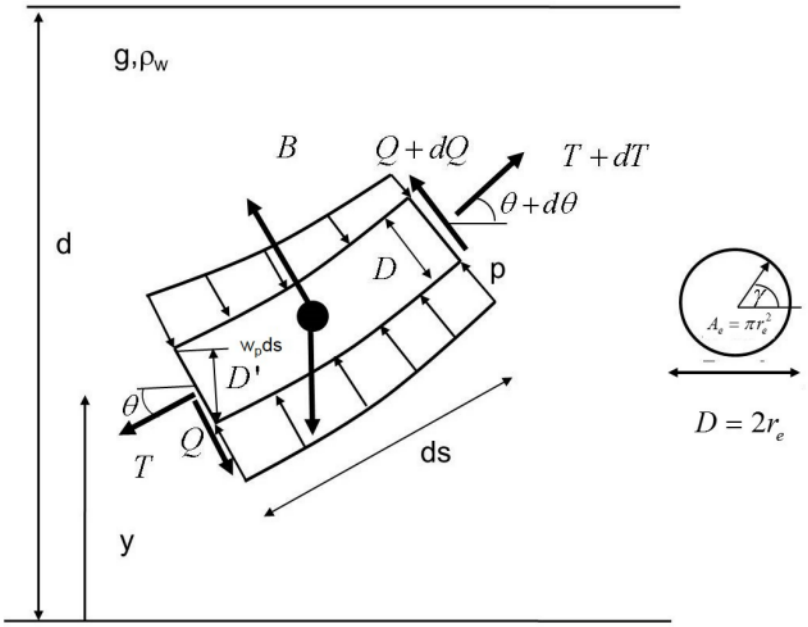

Figure 3.3: The transverse equilibrium for a infinitesimal cable element [28]

The catenary equation for installing a flexible pipeline or cable is based on neglecting the bending stiffness [28]. The catenary solution therefore represents only an approximate solution but the bending stiffness of a cable is significantly less than for a flexible pipe [29]. The global catenary geometry of the cable is shaped as shown in Figure 3.4.

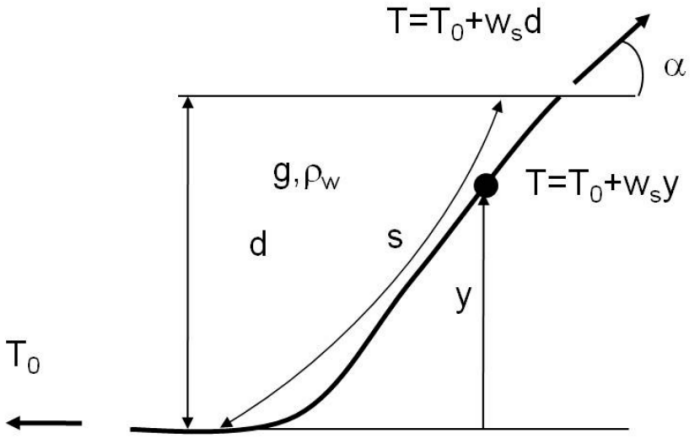

Figure 3.4: Global catenary geometry of the cable [28]

Neglecting the bending stiffness term in Equation 3.6 and some rearrangement of terms gives:

$$T = w_s \cos\theta \frac{ds}{d\theta} \tag{3.7}$$

Differentiating $T = T_0 + w_s y$ with respect to the cable element length s gives:

$$\begin{aligned} \frac{dT}{ds} &= w_s \frac{dy}{ds} \\ dT &= w_s \sin\theta ds \end{aligned} \tag{3.8}$$

Dividing Equation 3.8 by Equation 3.7 and integrating both sides gives:

$$\begin{aligned} \frac{dT}{T} &= \frac{\sin\theta}{\cos\theta} d\theta \\ lnT &= -ln\cos\theta + C \\ T &= T_0 \frac{\cos\theta_0}{\cos\theta} \end{aligned} \tag{3.9}$$

where θ_0 is the slope of the seabed at the touch-down point [28]. Assuming $\theta_0 = 0$ at $s = 0$ gives:

$$T = \frac{T_0}{\cos\theta} \tag{3.10}$$

Combining Equation 3.7 and Equation 3.10 gives:

$$\begin{aligned} ds &= \frac{T d\theta}{w_s \cos\theta} \\ s &= \frac{T_0}{w_s} \tan\theta + C \\ \tan\theta &= \frac{w_s}{T_0} s \\ \tan\alpha &= \frac{w_s}{T_0} s^* \end{aligned} \tag{3.11}$$

where α is the top angle also known as the departure angle at catenary length $s = s^*$ at $y = d$. Using that $dy = \sin\theta ds$ and inserting the first line of Equation 3.11 and Equation 3.10 gives:

$$\begin{aligned} dy &= \frac{T_0 \sin\theta}{w_s \cos\theta^2} d\theta \\ y &= \frac{T_0}{w_s \cos\theta} + C \\ d &= \frac{T_0}{w_s} \left(\frac{1}{\cos\alpha} - 1 \right) \end{aligned} \tag{3.12}$$

With the last line of Equation 3.12 one can express the total cable catenary length s^* as a function of the water depth, the bottom tension, and the submerged cable weight as:

$$s^* = \sqrt{d^2 + 2\frac{T_0 d}{w_s}} \tag{3.13}$$

and the curvature along the catenary follows from combining and rearranging Equation 3.7 and Equation 3.10:

$$\frac{d\theta}{ds} = \frac{w_s}{T_0} \cos\theta^2 \tag{3.14}$$

which has its maximum value at the touch-down point [28]. The total layback length $x^D o*$ which is the horizontal distance from the chute to the touch-down point can be computed by using that $dx = \cos\theta ds$ and applying Equation 3.14:

$$\begin{aligned} dx &= \cos\theta ds \\ dx &= \frac{T_0}{w_s \cos\theta} d\theta \\ x &= \frac{T_0}{w_s} \ln\left(\frac{1}{\cos\theta} + \tan\theta\right) \\ x^* &= \frac{T_0}{w_s} \ln\left[1 + \frac{w_s d}{T_0} + \sqrt{\left(1 + \frac{w_s d}{T_0}\right)^2 - 1}\right] \end{aligned} \tag{3.15}$$

The oscillating vertical accelerations of the chute as a result of wave-induced vessel motion add a dynamic force to the hanging cable. Assuming that the vertical vessel motions are sinusoidal gives:

$$a_{max} = \eta/2 \cdot (2\pi/P)^2 \tag{3.16}$$

where a_{max} is the maximum vertical acceleration of the chute, η is the vertical movement amplitude (peak to peak) and P is the movement period defined as the time between two wave peaks [37]. The maximum force on the hanging cable including vertical acceleration of the chute follows from:

$$T_{max} = T + ma_{max} \tag{3.17}$$

where m is the mass of the hanging cable [37]. As the force resulting from acceleration is an inertia phenomenon, the cable mass, rather than its submerged weight or weight in air, is essential for calculations. Different cable-laying vessels exhibit varying sea-keeping characteristics, indicating how they respond to waves from different directions. The key factor influencing cable top tension is the vertical acceleration of the chute, primarily affected by pitch and heave movements and in the absence of detailed ship movement data, a value of $a_{max} = 6\ \mathrm{m/s^2}$ is assumed [37].

Real waves may deviate from the sinus equation, appearing steeper in parts of the wave silhouette. Additionally, waves from different directions and causes can combine, sometimes resulting in rather steep wave fronts. In such cases, the vertical acceleration and thus the dynamic force may exceed what the sinus calculation indicates. The dynamic forces on the cable are outcomes of waves with a statistically distributed wave height. Even if the forecasted significant wave height seems acceptable, a few exceptionally large waves can generate tensions sufficient to damage the cable [37].

Estimating the contribution of the catenary and wave dynamics to the top tension separately is relatively straightforward, providing insights into the augmentation of tensional forces due to both effects. However, calculating the combined effects of a catenary line and vertical acceleration dynamics on tensional forces is a more complex task [37]. The entire length of the hanging cable, including the cable part near the touch-down point, experiences vertical acceleration. However, the inclined cable can transmit forces only in its own axial direction. Consequently, significant tensions along the cable must be transmitted to generate the vertical forces for cable acceleration near the touch-down point. For cable decommissioning the computation of the cable tension would be even more complicated due to the complex soil behaviour that resists the cable pullout and adds extra bottom tension.

3.3. Decommissioning Project Overview

An offshore wind power cable decommissioning project would have similarities to both installation and repair projects. Since there are no existing detailed applicable guidelines specifically for cable decommissioning, the decommissioning process is compared to existing cable repair and installation

guidelines from the European Subsea Cables Association (ESCA) [12], [13]. These operations can be considered more complex than decommissioning because cable integrity is of the utmost importance. For example, during repairs, it is easy to overbend the cable and have excessive tension if the cable is stuck and the vessel moves due to waves. Therefore, a direct pullout of a buried cable should be avoided during repair operations. For decommissioning, the cable is allowed to be damaged and cable integrity is thus of less concern. However, breakage of the cable should be avoided since it would be cumbersome and time-consuming to pick up the cable end again each time after it breaks. Severe damage to the cable could also make it more difficult to safely recover the cable due to for example sharp edges. Recovering the cable directly is more time-efficient than first conducting deburial. Based on the existing guidelines for similar operations, the decommissioning project would roughly entail the following phases:

- planning, surveying, and permitting;
- route clearance (when necessary);
- decommissioning vessel mobilisation;
- cable recovery operation;
- scrap metal delivery;
- post-survey.

The most relevant phase for the current research is the cable recovery operation which would consist of roughly three steps. The first step is to locate and free the OOS cable. This likely involves a bit of deburial of at least the cable end (Oor, 28-09-2023). At locations with burial depths larger than 1.5-2 mêters, deburial of the rest of the cable is also necessary (Aas, 05-10-2023), (Andersen, 03-10-2023). After the deburial, the next step is to connect the cable to the vessel. The most straightforward method for connecting the cable is using a diver but the industry prefers to work with ROVs due to safety concerns (Oor, 28-09-2023). Such an ROV should be able to perform the cable-connection operations within 15 minutes [21]. A buried cable could also be lifted using a grapnel. The decommissioning vessel can pull the cable out of the seabed with a winch or tensioner as it moves backwards along the cable route. 'Peeling out' the cable like this only works up to a certain burial depth. For larger depths, deburial methods are needed which could be carried out by a separate vessel. The last step of the recovery operation is retrieving the cable and storing it on deck or in a cable carousel.

After the recovery operation, it is important to deliver the recovered cable efficiently to the scrap metal company (Aas, 05-10-2023). It is easiest to deliver the cable in the smallest number of pieces possible in the harbour (Andersen, 03-10-2023). This is most effective for the operation because offshore time is expensive. Carousels or drums can store the cable aboard and then there is only reason to make cuts when the carousel is full. Keeping the cable as intact as possible also reduces the risk of pollution. Therefore spooling the cable into a carousel is preferred.

It might be necessary to disconnect or cut the cable first to free the cable end. The cable end could for example be at the landfall or the substation platform. If the cables are not disconnected yet, you would need a platform team to release the end of the cable at the respective interface. Usually, at the foundation of the interface, you have a cable protection system (CPS) that secures the cable at the bottom (Zheng-Lu, 29-09-2023). The old CPS types are difficult to detach but the alternative is to just cut the cable at this point (Zheng-Lu, 29-09-2023). After the CPS, inside the platform or turbine, you would have a cable hang-off to secure the cable at the top. The cable can be detached from the hang-off relatively easily but then the cable needs to be lowered down from the turbine tower or platform foundation (Zheng-Lu, 29-09-2023). To lower the cable in a controlled and safe way you would need an extra winch or similar tool. When the cable finishes at a landfall, there might be a pipe covering the cable. If this pipe also needs to be removed, the cable can be cut and left in place until the recovery of the pipe (Zheng-Lu, 29-09-2023). The processes regarding disconnecting or cutting the cable ends and decommissioning landfall pipes are not further considered in the current research.

The other phases are similar to the usual processes during cable installation as described in for example ESCA Guideline No.14 [12]. The industry expressed the need for a thorough survey before the start of the project (Andersen, 03-10-2023), (Aas, 05-10-2023). After the survey, there should be an overview of the data on the cable itself, the routing, the burial depth, the soil, and possible obstacles (Aas, 05-10-2023).

Based on this overview the decommissioning strategy can be determined and the project permit can be requested. Once the authorities give out the necessary permits, the project goes towards the final planning and start of the decommissioning operation (Aas, 05-10-2023). In some cases, subsea power and fibre optic cables are installed in entangled bundles such as in Figure 3.5. When decommissioning, one would recover the entire bundle at once because the cables cannot easily be untangled on the seabed (Andersen, 15-11-2023). Aboard you can untangle the bundle and store the fibre optic cable on a drum and the power cables in separate turntables (Andersen, 15-11-2023). Since the bundle is heavier and wider than the individual cables, the decommissioning operation is more complicated.

Figure 3.5: Installation of simultaneously bundled DC cables [20]

3.4. Deburial Methods

With a normal armoured cable, you would first try to recover it by just pulling it out of the seabed, see also the next section (Andersen, 03-10-2023). If that does not work you need to debury it first. Direct cable pullout is by far the most efficient and least environmentally damaging decommissioning method if possible (Andersen, 03-10-2023). Water clouding will be minimized but as soon as you get to a depth of 1.5-2 m, having enough force to pull out the catenary-shaped cable is challenging (Aas, 05-10-2023). In that case, one or more of the available deburial methods introduced below can be applied. A (tool-mounted) sonar head helps to locate the buried cable [21]. Such a tool is also useful for locating the cable when it has to be cut or grabbed for direct pullout.

Often water jetting with a small jetting pig, a device that moves along the outside of the cable, is the easiest way to free the cable at the touchdown point (Andersen, 03-10-2023). However, it only works if you need to remove small quantities of debris: usually, it works for jetting away material for 0.5-1 m soil (Andersen, 03-10-2023). High-pressure water jets are directed at the seabed to break up, fluidise and remove sediment around the OOS cable [13]. Water jetting can be combined with mechanical tools for more efficient deburial. Water jetting is versatile and can be applied to various seabed conditions, including sandy, muddy, or clayey substrates. It is particularly useful when precision is required. It is preferable to have an underwater pump instead of a pump aboard the vessel. One advantage is having higher manoeuvrability and a second advantage is having a controllable power cable going down from the vessel instead of a water hose (Snip, 02-10-2023). Besides, the intake pressure in the pump is larger due to the positioning near the seafloor (Snip, 02-10-2023). The downside is the high price of the underwater pump (Snip, 02-10-2023).

In case of deeper burial, you need mass flow excavation (MFE) also known as controlled flow excavation (CFE) to remove large sediment quantities (Andersen, 03-10-2023). This typically includes a remotely operated vehicle (ROV) equipped with a high-powered pump system. The pump system is designed to generate a high-velocity water flow. The flow is directed through a nozzle or jetting system that focuses the fluid stream onto the seabed. Dislodged sediments are entrained in the fluid and carried away, creating a trench around the OOS cable. The downside of this method is that you need an extra ship to operate the MFE tool which takes extra time and budget (Smalt, 04-10-2023). The MFE also has a relatively low speed of around 3 m per minute (Smalt, 04-10-2023). When doing the deburial of the sand

it has to be taken into account that you need to have at least a 45-degree angle to prevent the sand from collapsing and burying the cable again (Andersen, 15-11-2023). Consequently, the trench you create with your CFE needs to be 15 to 20 m wide (Andersen, 15-11-2023).

Some authorities, e.g. in Germany, usually prefer a suction tool over MFE/CFE that can remove the debris more locally (Andersen, 03-10-2023). Suction dredging involves using a vacuum system to remove sediment from around the subsea cables. The material is transported to the surface for disposal. Damage is probably more local but could still be comparable to MFE effects while this method is slower than MFE (Andersen, 03-10-2023).

The worst-case scenario is when you need a dredger to (partly) debury the OOS cable (Andersen, 03-10-2023). Mechanical dredging involves the use of specialized vessels equipped with dredging tools, such as suction pumps, cutter heads, or excavators. These tools remove sediment and soil from around the subsea cables. Dredging is effective in sandy or soft seabed conditions. The dredged material is transported to the surface and can be either temporarily stored or directly disposed of. Either way, dredging makes the decommissioning operation more complex. Dredging would have a relatively large impact on the environment and is expensive (Snip, 02-10-2023).

Jetting and suction can also be combined. This method involves using water jets to loosen the seabed around the subsea cables, followed by suction to remove the dislodged material. It provides both the benefits of water jetting and suction dredging. The combination of these two processes allows for efficient deburial while minimizing environmental impact. Table 3.1 compares the deburial methods for decommissioning subsea cables.

Deburial Method	Burial Depth	Advantages	Disadvantages
Water Jetting	Shallow-Moderate	Precise, versatile	Limited burial depth
Suction Dredging	Shallow-Moderate	Precise, efficient removal	Environmental impact
MFE	Shallow-Deep	Versatile, powerful	Impact, complexity
Mechanical Dredging	Moderate-Deep	Efficient for large volumes	Less precision
Jetting + Suction	Shallow-Moderate	Efficient deburial	Equipment complexity

Table 3.1: Overview of deburial methods

Deburial and cable recovery can be conducted simultaneously or as two separate operations. The latter has the advantage that a smaller, cheaper vessel can be used for the deburial operation while the cable recovery operation can be done much faster since the cable is already deburied [37]. The downside of this two-phase approach is the risk of anchors or fishing gear hooking the exposed cable in the time window between deburial and recovery. In the past, this has happened for cables that were going to be installed but were lying on the seabed waiting to be buried [37]. A simultaneous cable deburial and recovery operation could slow down the process since the burial equipment is usually slower than the cable recovery vessel. It is also important to determine a safe operating distance between the deburial equipment and the cable being pulled out. An alternative to deburial could be to just keep pulling until the cable breaks and then reconnect the cable to the vessel to start pulling again. This method is sometimes also used for decommissioning telephone cables, which are relatively thin compared to power cables (Snip, 02-10-2023).

3.5. Cable Pullout

After freeing, and deburying at least the cable end, the next step is to connect the cable to the vessel. Divers or ROVs attach the rigging equipment to the exposed section of the subsea cable. This equipment would include lifting slings or clamps to securely grip the cable. The selection of rigging equipment depends on the cable type, diameter, and the conditions at the seabed. From a safety perspective, it should be considered to always have tension on both ends of the cable and not only on the pull side (Zheng-Lu, 29-09-2023). When starting decommissioning on one end of the cable and reaching the other end, without any back tension, there is no control over the other end of the cable. In case of a loose or broken cable, you can use for example an anchor to provide the back tension for the loose end (Zheng-Lu, 29-09-2023). However, since the integrity of the cable is not important during decommissioning the

back tension is not per definition needed in contrary to cable installation.

A lifting system is employed to raise the cable from the seabed to the surface. This can include winches, cranes, or other lifting devices, either located on a surface vessel or a dedicated cable retrieval platform. The choice of lifting equipment depends on the depth of the water and the weight and length of the cable. Ideally one would have a capstan wheel to pull out the cable (Andersen, 03-10-2023). Most of the capstans are used for pipe laying and can handle up to 40-50 tons of tension (Andersen, 03-10-2023). The NKT Victoria, NKT's cable-laying vessel, has two tensioners with a capacity of 45 tons each. An example of such a tensioner is depicted below in Figure 3.6. This tensioner is designed to perform bi-directional cable lay and recovery operations. It has four tracked drives that can handle cable up to 460 mm in diameter with velocities up to 20 m/min (Zheng-Lu, 29-09-2023). The individual tensioners can be combined to achieve a total pull capacity of 90 tons. Tension sensors and monitoring systems can be employed to ensure that the tension applied during the retrieval process is within safe limits. Maintaining controlled tension helps prevent overloading the cable and minimizes the risk of damage. The speed at which the cable is lifted should be carefully controlled. Slow and controlled retrieval is essential to minimize stress on the cable and prevent any sudden movements that could lead to damage.

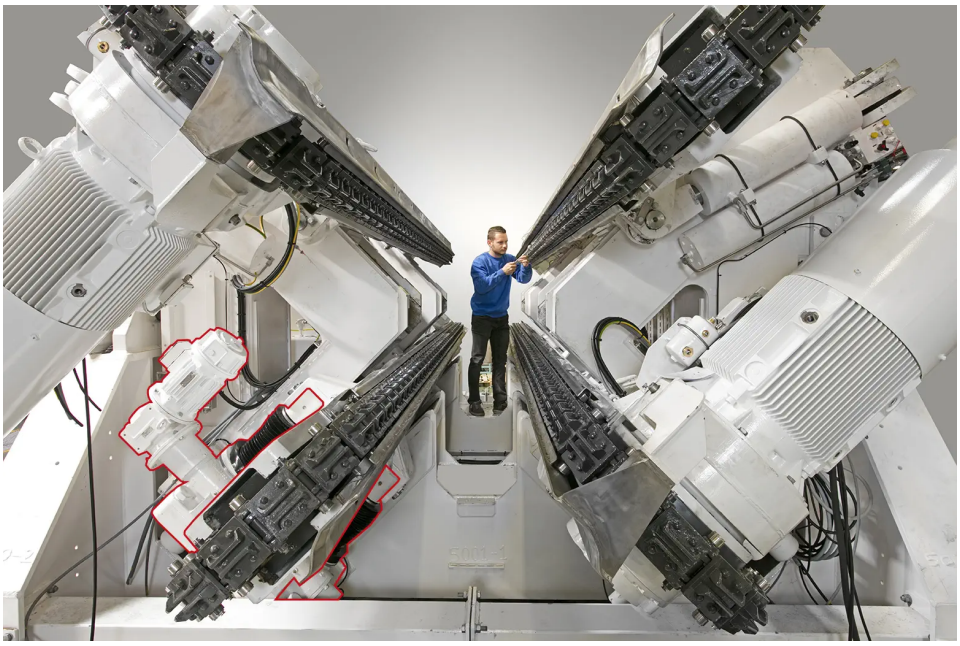

Figure 3.6: Four-track tensioner with a tension capacity up to 45 tons [20]

As the cable reaches the surface, it is carefully guided onto the deck of the retrieval vessel or platform. Tensioning systems can be used to maintain controlled tension during the final stages of the pullout operation. This helps to avoid sudden releases of tension that could lead to cable damage or unsafe conditions on the vessel (Zheng-Lu, 29-09-2023). Once on the surface, the cable is securely stowed on the deck of the retrieval vessel or platform. This may involve coiling the cable in specific patterns or using storage reels to ensure it is neatly organized and ready for further handling or transportation. Water jets onboard can clean the recovered cable at the surface before you put it in the tensioner via the chute. When you remove the sand from the cable you have more friction and less slip (Zheng-Lu, 29-09-2023).

3.6. Literature Study Summary

The goal of the broad analysis of the decommissioning process for offshore wind export cables was to get a general understanding of how to undertake such an operation and to be able to identify critical knowledge gaps. Since large-scale decommissioning of entire export cables is a new challenge with little existing research and no existing industry guidelines, several interviews were conducted

to get additional (practical) insights. It was also valuable to compare cable decommissioning to cable installation and repair procedures. The most straightforward decommissioning method is a pullout of the cable without deburial. According to industry experts, this method is usually limited by the burial depth and the soil type. However, the exact limits are not clearly defined and this leaves a critical knowledge gap. Since pure pullout would be the cheapest and most environmentally friendly decommissioning option, it is optimal to apply this method to the cable route as much as possible. Therefore at this point, it was decided to focus on modelling the cable pullout operation for a typical offshore wind export cable decommissioning scenario. The next chapter describes such a scenario and discusses the governing criteria for cable decommissioning, especially for cable pullout.

4

Case Study for a Typical Export Cable Decommissioning Scenario

This chapter first covers the third research question: What is a typical offshore wind power cable decommissioning scenario in the Dutch-German part of the North Sea? Next, it answers the fourth research question: What are the governing criteria for cable pullout in such a decommissioning scenario? To investigate the limits of cable pullout, the operation is simulated in OrcaFlex based on this chapter's input. This chapter describes the input for such a simulation for a typical export power cable decommissioning scenario. The modeling process depends on various factors including the characteristics of the export cable, soil and environmental conditions, and of course the burial depth. The first section introduces the scenario. Thereafter, the governing criteria for the cable pullout are explained. The last section touches on the OrcaFlex software and how using OrcaFlex the cable pullout operation could be simulated.

4.1. Scenario Overview

The current research focused on a simplified 525 kV HVDC subsea cable that could be used for export cables for offshore wind export cable projects such as the Tennet 2GW project. This project forms the context of the cable decommissioning scenario. After providing this context, the cable description, bathymetry, burial depth, and soil conditions are introduced.

4.1.1. Tennet 2GW Program

Tennet is the transmission system operator of the Netherlands and large parts of Germany. As a grid operator, it designs, builds, maintains, and operates more than 25,000 kilometres of high-voltage power cables both on- and offshore [31]. Its '2GW Program' is Tennet's answer to the ambitious European goals for offshore wind. The program entails at least 14 HVDC offshore grid connection systems with a transmission capacity of 2 GW each [32]. The systems will deliver electricity to the grid both in Germany and The Netherlands with a total combined capacity of 28 GW. The program's strategy is to standardise the transmission systems while also realising higher capacities. As a result, fewer connections will be required to transport wind energy from offshore to onshore. This offers advantages regarding environmental impacts, costs, construction time, and (scarce) resources. Each 2 GW grid connection consists of an onshore converter station, a 525 kV HVDC export cable system and an offshore converter station, see also Figure 4.1.1. The Tennet systems have the prerequisite to be able to join a future European offshore HVDC grid [32]. Such a European offshore grid could connect both wind farms and national grids across the North Sea.

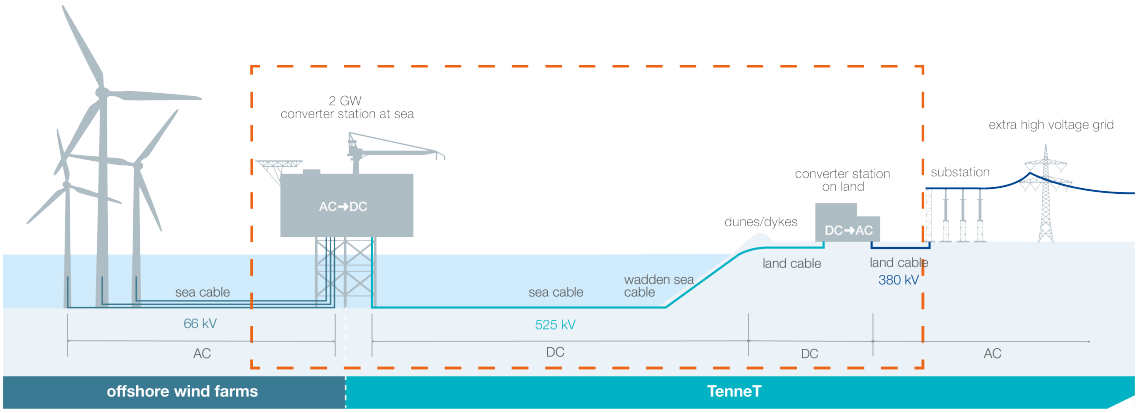

Figure 4.1: Overview of one Tennet HVDC offshore grid connection system indicated by the orange line which connects offshore wind farms to the shore [32]

As of today, the Tennet 2GW Program comprises eight Dutch offshore grid connection systems: IJmuiden Ver Alpha+Beta+Gamma, Nederwiek 1+2+3, and Doordewind 1+2 [32]. For Germany six offshore grid connection systems are planned: BalWin 3+4 and LanWin 1+2+4+5. Tennet will commission the first connections as soon as 2028 and will continue adding more connections every year until 2031. See also Appendix B for the overview of all offshore wind export cable projects that are part of the Tennet 2GW Program. More connections may be designed and added to the program in the future. Since the scale of this project is so large and as many components as possible are going to be standardized, the 2GW Program provides a relevant starting point for a decommissioning scenario. A successful cable decommission process of one 2GW Program export cable is possibly easily applied to the other export cables of the program.

4.1.2. Cable Description

The cable decommissioning scenario is based on a NKT 525 kV HVDC subsea cable as depicted in Figure 4.2. The full details of the cable are not available for publication. However, for modelling the cable pullout operation, the detailed design is not necessary since a simplified cable cross-section modelled as a beam shall be used. This model cross-section will be based on the conductor and armour characteristics of the cable. The 525 kV cable consists of a single copper conductor core with an extruded insulation system. When continuing further outwards, the other layers of the cable are extra insulation, water barriers, (metal) sheaths, armour bedding, armour wires, and the outer serving made of two layers of polypropylene yarn.

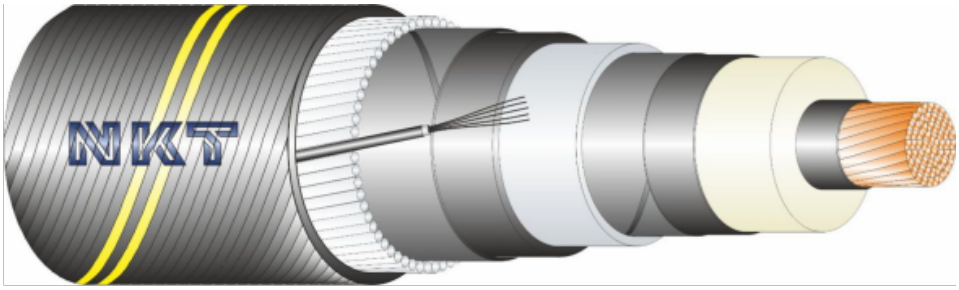

Figure 4.2: NKT 525 kV HVDC subsea cable from internal NKT cable design report

The most relevant mechanical cable properties for modelling the cable pullout operation during decommissioning are given in Table 4.1. A linear bending stiffness is assumed but in reality, the bending stiffness is non-linear. However, implementing a non-linear bending stiffness complicates the modelling while at this experimental stage, it is not necessary to include (Bodesund, 16-11-2023).

Property	Unit	Value
Outer diameter	mm	149
Mass in air	kg/m	58.4
Mass in seawater	kg/m	42.0
Axial stiffness (no rotation)	kN	390e3
Bending stiffness (linear)	kNm^2	39
Torsion stiffness	kNm^2	155
Armour material	-	Galvanized steel
Armour wire diameter	mm	5
Number of wires	-	75
Lay length (see also Figure 2.2)	mm	1570
Conductor material	-	Copper (Cu)
Conductor cross-section	mm^2	2500

Table 4.1: Cable properties of a NKT 525 kV HVDC subsea cable from internal NKT cable design report

4.1.3. Bathymetry and Burial Depth

The scenario for the current research only accounts for the offshore region because the decommissioning operation in the nearshore region would require a different approach due to the rather shallow water depth. NKT provided access to burial assessment data for several export cable tenders and projects. However, this data is confidential. Therefore, it was decided to set up a fictive cable route in the Dutch-German part of the North Sea, inspired by actual data from NKT. The bathymetry and burial depth (as the depth of cover) for this fictional cable route are shown in Table 4.2. The bathymetry is based on the lowest astronomical tide (LAT). The total length of the route is 150 km and the 8 km near the shore is left out of the analysis scenario. The bathymetry decreases at first until reaching a maximum water depth of 31 m. The tension in the cable will increase with water depth due to the increasing weight of the cable hanging in the water column. Since the effect of the burial depth on the total tension will be significantly larger than the effect of the water depth, a constant water depth of 30 m was taken for the pullout simulations (Andersen, 13-10-2023). The burial depth varies significantly along the cable route, from 1 m to 4 m cover depth, which makes it an interesting case for the cable pullout modelling.

KP from	KP to	Bathymetry (m)	DoC (m)	Route Section Length (km)
8	15	-14	2.0	7
15	17	-15	1.0	2
17	25	-22	4.0	8
25	28	-23	1.5	3
28	29	-24	3	1
29	107	-31	1.5	78
107	108	-29	3	1
108	135	-25	1.5	27
135	149	-27	1.0	14
149	150	-28	2.0	1

Table 4.2: Bathymetry and depth of cover (DoC) along a fictional cable route from Kilometer Point (KP) 8 to KP 150 inspired by actual data from NKT

4.1.4. Soil Conditions

Inspired by data and geotechnical studies previously done by NKT, assumptions on the virgin soil conditions for the decommissioning scenario have been made. The sand is mainly fine to medium-sized, poorly graded and with almost no cohesive materials. Locally, cohesive materials such as clay and silt might occur in prevalent percentages but this is ignored for the current scenario as this only may happen occasionally. Future research should look into the potential effects of the presence of such cohesive materials. Gravel is absent and gravelly-sized shell fragments are rare. The relative density of the scenario's virgin soil ranges mainly from medium dense to dense and very dense. Generally, the densities of the sand increase with water depth but locally this can be different. Relative density is a measure of the compactness of the sand and is defined as the ratio of the difference between the void ratio of a soil in its loosest state and its current state to the difference between its void ratios in the loosest and densest states. The void ratio measures the void (empty) spaces in soil relative to the volume of its solid particles. As relative density increases, the void ratio decreases. Therefore, sand in a dense state (high relative density) has smaller pore spaces and lower permeability compared to sand in a loose state (low relative density).

The information on the virgin soil's relative density from pre-laying surveying of the cable route is not very accurate for decommissioning analysis because the virgin soil was disturbed or removed during cable laying and replaced by backfill material. Assessing the soil characteristics of the backfill material is difficult after 20-30 years of service. To what extent the soil was disturbed and how long the soil takes to recover also depends on the burial method. Field data from two project locations in the North Sea indicate that the initial backfill density is very low but rises back towards the dense virgin conditions within a year [26]. As can be seen in Figure 4.3 the densification trend of the soil is different for the two locations. For site A the relative density of the backfill material $D_{R-trench}$ is 50% of the relative density of the virgin material $D_{R-virgin}$ after 200 days. For site B it takes 2000 days to regain 50% of the original relative density.

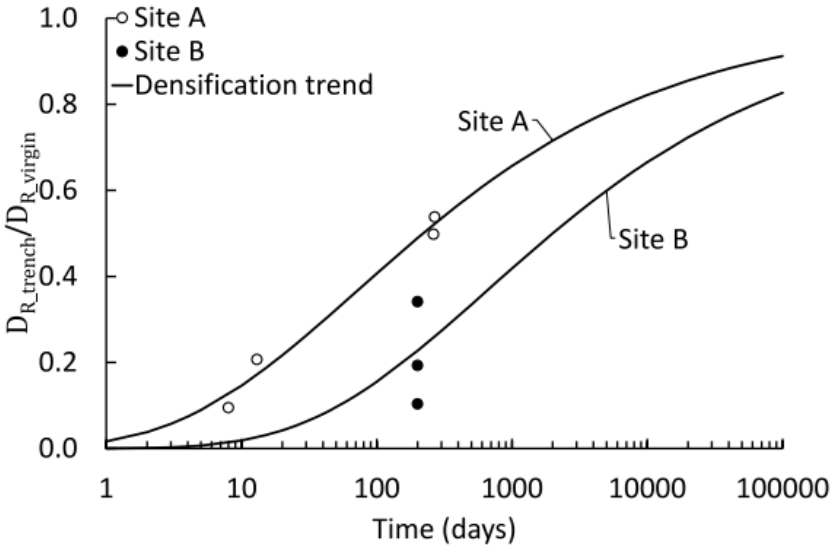

Figure 4.3: Recovery of relative density (here: D_R) back to the virgin condition [26]

For the cable decommissioning scenario, the relative density of the sand is less than 100% after 20-30 years of service. In fact, it is already conservative to assume the upper limit of the sand's relative density is no more than 80% (Snip, 02-10-2023). This is also in line with Figure 4.3. The relative density will be different along the cable route due to different virgin densities and because of different densification rates. To account for the variety in soil densities, it is valuable to model the cable pullout operation for both medium and dense sands. Here, the dense case was considered as the conservative scenario. For medium dense sand a relative density of 50% or 0.5 was taken and for dense sand, a relative density of 80% or 0.8 was assumed based on [9].

4.2. Governing Criteria for Cable Decommissioning

The exact mechanical properties of subsea cables are difficult to compute due to the presence of the helical steel armours, the interactions between the cable elements, and the nonlinear effects involved in the non-metallic parts with the composite section of the cable [27]. The expected cable loads during installation, operation, and decommissioning are also difficult to ascertain [27]. However, the mechanical properties of the cable are strongly influenced by its armour [10]. Therefore, according to DNV, the conductor, sheats, and screens shall be left out when assessing the longitudinal capacity of the cable's cross-section [8]. This could be considered a conservative approach since in reality all cable components contribute to the total cable strength [11].

Subsea cables are similar to flexible marine pipelines regarding the wire armour. Therefore, the cable overload failure mode, i.e. excessive yielding in the steel wires, is comparable to the flexible pipeline's failure mode. Since there is existing research into failure modes for flexible pipelines, it is in some ways useful to apply and adjust analytical and computational methods based on flexible pipelines for subsea power cables. However, a flexible pipeline can collapse relatively easily compared to a power cable because the pipeline does not have a conductor inside. This higher buckling limit makes decommissioning of a cable easier than a flexible pipeline (Andersen, 15-11-2023).

Similar to cables, the flexible pipeline cross-section strength is governed by the steel helix layers [14]. The design analyses are according to the requirements of the American Petroleum Institute's (API) standard *API 17J Specifications for unbonded flexible pipe* which applies the allowable stress format [1],[14]. This entails applying a load condition-specific utilization factor to the steel's yield stress to determine a stress limit for the design. The two main governing criteria for subsea cable decommissioning are the cable's ultimate tensile strength also known as the breaking stress and the cable's minimum bending radius.

4.2.1. Ultimate Tensile Strength

The maximum tension during cable decommissioning is a critical parameter to prevent breaking the cable. The ultimate tensile strength or breaking stress is the maximum stress a material can withstand while being stretched or pulled before necking. Necking occurs when the material starts contracting significantly and eventually fractures. It is expressed in units of force per unit area (MPa). The cable manufacturer usually provides the maximum allowable tension during installation and operation. However, for decommissioning the allowable tension would be significantly larger because it allows failure of all individual cable components as long as the cable as a whole does not break. The maximum tension in the cable depends on various factors, including the characteristics of the cable, the water depth, and the specific conditions of the pullout operation.

In Figure 4.4, a typical stress-strain curve for ductile materials such as metals is shown. Beyond the yield strength, metals strain harden resulting in increasing stress for increasing strain. The reversal point where necking starts is the maximum stress on the engineering stress–strain curve, which is the ultimate tensile strength. The reversal is due to the engineering stress being calculated assuming the original cross-sectional area before necking. Similarly, engineering strain is defined as the deformation divided by the initial length of the material. The true stress uses the true cross-sectional area instead, and for true strain, deformation is divided by the actual length. Therefore, true stress is larger than engineering stress and true strain is smaller than engineering strain. Since the only goal is to recycle the cable materials, the full cable integrity is not of importance anymore. Therefore, it could also be possible to go beyond the ultimate tensile strength into the necking area of Figure 4.4 but with the risk that the cable breaks and has to be reconnected to the recovery vessel afterwards. Since the operation is offshore this could result in considerable delay costs.

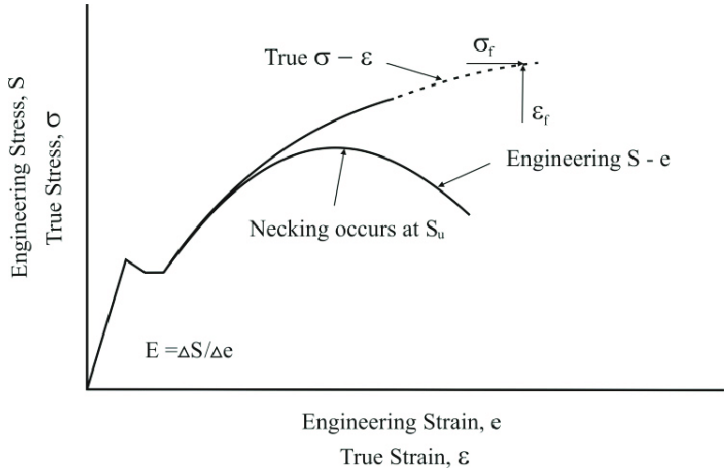

Figure 4.4: True and engineering stress versus true and engineering strain [19]

The cable's breaking load can be assumed to be a combination of the tensile strength of both the armour and the conductor (Andersen, 15-11-2023). Accounting for the conductor is a different approach to DNV's method for assessing the longitudinal capacity of the cable's cross-section explained above. However, the DNV method is not specifically made for decommissioning and gives high priority to ensuring full cable integrity. Including the conductor can make a considerable difference since strangled aluminium or copper conductors have considerable strength [37]. Assuming the armour wires and the conductor determine the break load, applying a tension force results in a cable strain ϵ and tension in the conductor T_C and armour T_A:

$$\epsilon = \frac{T_A}{E_A A_A} = \frac{T_C}{E_C A_C} \tag{4.1}$$

where E_a is the Young's modulus of the armour wires (N/mm^2 or Mpa), A_a is the total cross-sectional area of the armour wires (mm^2), see Equation 2.2, E_c is the conductor's Young's modulus of the conductor (N/mm^2 or MPa), and A_c is the conductor's cross-sectional area (mm^2). The total tension T_t is divided between the tension in the armour and the conductor:

$$T_t = T_a + T_c \tag{4.2}$$

The maximum allowable tension for the armour and the conductor follow from their respective ultimate tensile stresses $\sigma_{a,UTS}$ and $\sigma_{c,UTS}$ multiplied by their cross-section areas as shown below. Note that for the maximum armour tension, the lay angle (see also Figure 2.2) also has to be taken into account.

$$T_{a,max} = \sigma_{a,UTS} \cdot A_a \cdot \cos\alpha \tag{4.3}$$

$$T_{c,max} = \sigma_{c,UTS} \cdot A_c \tag{4.4}$$

Previous research by Ehlers et al. has investigated the ultimate tensile strength of a cable similar to the current research's NKT 525 kV HVDC cable [11]. The aim was to experimentally determine the ultimate strength in the context of safety and reliability under any operational and accidental conditions [11]. The research scenario was (emergency) anchoring of a passing vessel that resulted in an interaction between the anchor and the cable. Even though the scenario of this study was different than cable decommission, the results are still valuable for the current research and offer opportunities for comparisons. The cable used by Ehlers et al. is depicted below [11]. The cable diameter was 147 mm, almost the same as the NKT 525 kV HVDC cable, while the cable structure is also similar. The two main differences are the

different conductor material (aluminium) and the armour diameter of 6 mm instead of 5 mm for the NKT cable. The cable rate was not specified but a rating of 525 kV is assumed based on the cable structure.

Figure 4.5: Subsea HVDC power cable tested by Ehlers et al. [11]

First, the individual cable components were tested to obtain the engineering stress-strain relationships. Thereafter, the study carried out a tensile test with the complete cable. The tests were under quasi-static conditions and conducted in a strain-controlled manner [11]. The resulting engineering stress-strain relationships for the individual cable components are given below in Figure 4.6. The figure also shows the true stress-strain curves and the initial elastic behaviour. The true stress curves end at the point of failure.

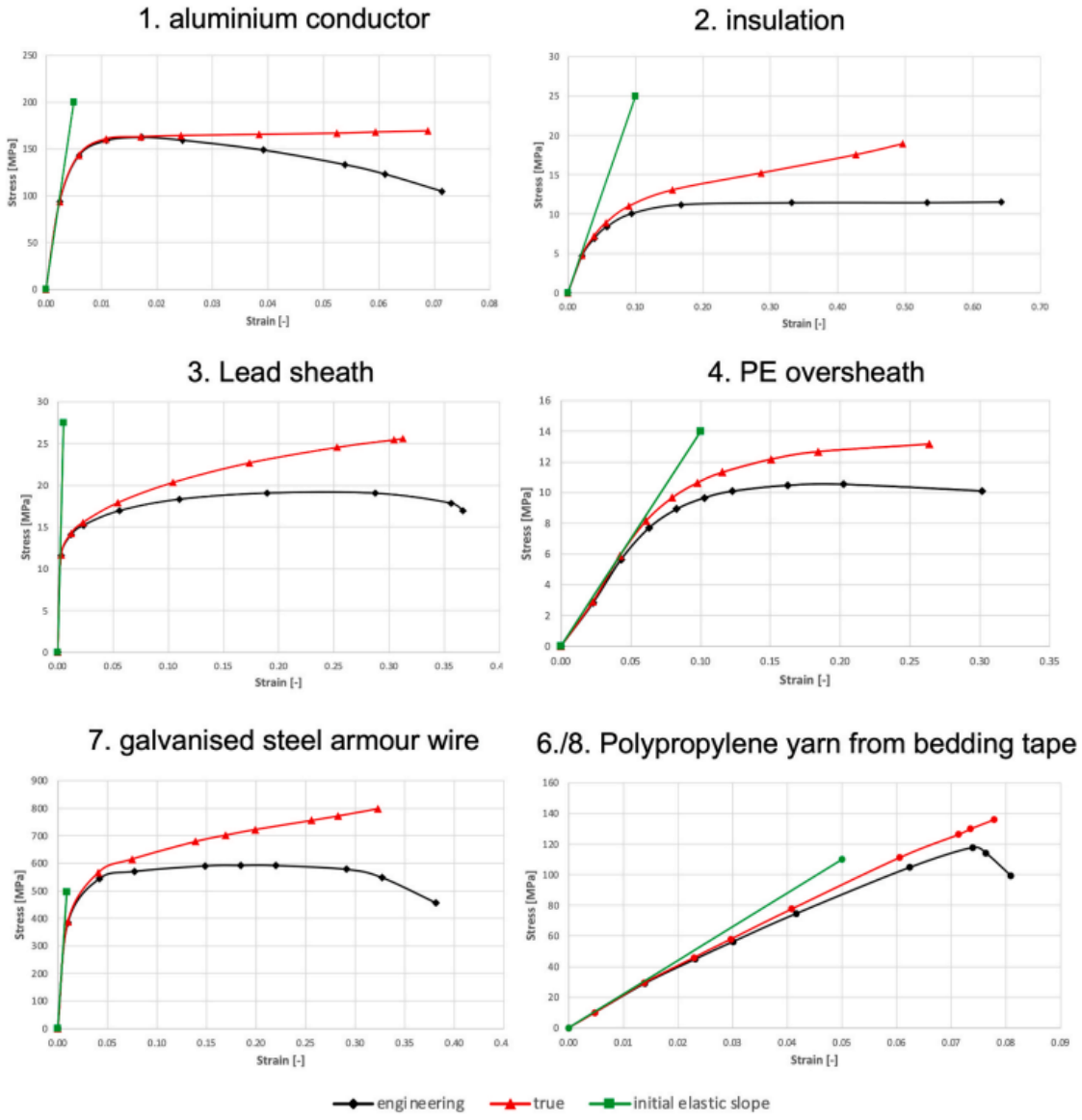

Figure 4.6: Stress-strain curves for different cable components [11]

As can be seen in Figure 4.6, the aluminium conductor and the steel armour wires have the highest ultimate tensile strength, as expected. The other cable components have relatively low ultimate strengths except the polypropylene yarn layers which are in the same order of magnitude as the conductor. However, taking the cross-section areas of the components into account, the contribution of the polypropylene yarn to the maximum tension in the cable is relatively small compared to the conductor and the armour. For the full-scale cable experiment, tension was applied to the cable utilizing terminations at the cable ends [11]. The conductor insulation and the outer serving could not be connected and thus did not contribute to the ultimate tensile strength of the cable. The resulting force-displacement graph is shown below.

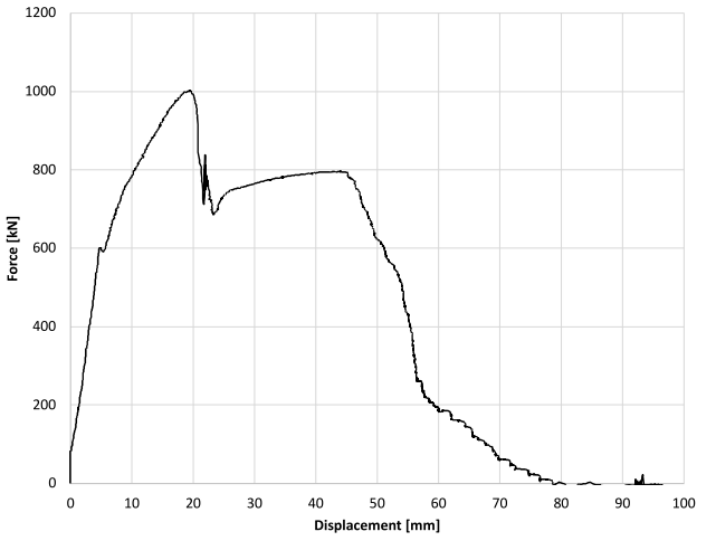

Figure 4.7: Force-displacement curve for a subsea HVDC cable [11]

When the risks related to a breaking cable are small, for example for fibre optic cables, one can go over the break load and take the risk it breaks (Andersen, 15-11-2023). If the cable holds, the decommissioning process goes relatively fast. If it breaks in a controlled way because the cable is contained in rollers there is no large risk involved (Andersen, 15-11-2023). However, the breakage probably results in delays in the operation and thus in extra costs. After breakage, one may decide to leave the rest of the cable in situ or one can connect it again and probably conduct deburial to continue decommissioning. This would be different in the case of for example an oil-filled cable that could cause considerable environmental damage if the cable breaks after exceeding the break load.

4.2.2. Minimum Bending Radius

Excessive bending of the cable can result in local buckling destruction of the cable as the armour wires interfere and touch each other [14]. The curvature radius needed to cause the locking of the armour wires is called the locking radius [1]. In most cable or pipeline handling situations, the minimum bending radius is either governed by the locking radius or by the curvature radius ρ_ϵ that results in exceeding the allowable strain in the plastic layers of the cable/pipeline [14]. However, for decommissioning, exceeding this allowable strain is of less concern. Therefore, the locking radius determines the minimum bending radius in case of decommissioning. Considering cable or pipeline armour on the compressive side at the cable radius R, the locking radius ρ_l follows from:

$$\rho_l = \frac{R}{1 - F_f} \tag{4.5}$$

where F_f is the fill factor [14]. For flexible pipeline armour, the fill factor F_f is defined by:

$$F_f = \frac{nb}{2\pi R \cos\alpha} \tag{4.6}$$

where n is the number of tensile wires, b is the width of each wire, R is cable radius, and α is the lay angle [14]. To compute the fill factor for the circular armour wires of a subsea power cable, the same formula can be applied by inserting the armour wire diameter instead of the wire width b. The American Petroleum Institute defined safety factors for the minimum bend radius during several load conditions and load type combinations [1]. For cable storage and static loading, the minimum bend radius should be at least 1.1 times the locking radius and during (quasi-) dynamic loading more safety

factors up to 1.5 are added [1]. During decommissioning operations, it is preferred to keep the bending radius larger than the applicable safety factor recommends. However, in practice, the cable can be bent till at least the minimum storage radius is reached (Andersen, 15-11-2023). This will result in electrical defects to the cores, isolation and potentially bird caging of the armouring, but the cable should not break (Andersen, 15-11-2023). Bird caging entails the armour wires becoming untwisted from the core and forming a 'cage'.

The armour of flexible pipes has a flat rectangular shape with rounded corners, while the cable armour consists of round wires. This shape difference results in less torsion in the circular cable wires compared to the rectangular pipe [29]. Therefore, the minimum bending radius for flexible pipelines is larger than for cables. The bending radius also adds to the friction: the more one bends the cable, the more friction (Andersen, 15-11-2023). The bending stiffness will increase where you have locking. Part of the cross-section will act as a continuum with a low effective height because only the wires on the compressive side will be locked to each other. Half of the wires will be able to take tension and the other half will be in compression. It requires a separate calculation outside the scope of this thesis but further detailed investigation is needed into what is going to happen when you combine the cable exposed to locking with simultaneous puling tension to the limit. For example, the break limit of the cable could go down due to the bending. When the bending the cable bending radius is below the locking radius, the original cable model is not valid anymore and you go into another domain where you don't know the limiting combination of bending curvature and tension.

4.2.3. Environmental Operability Limits

Environmental conditions might impact the cable decommissioning operation considerably. Originally, the plan was to investigate this impact as part of the current research but this proved too ambitious due to time constraints. Therefore these limits are only shortly discussed here. For cable laying projects, bad weather can force vessels to halt the operation for several weeks, which is of course costly [37]. In theory, cable decommissioning could be less susceptible to environmental conditions because of the lower precision and cable integrity requirements. However, for example, vessel movement is still dependent on the local weather. Factors influencing the operability of cable decommissioning would include:

- Surface waves: These waves can impede vessel and winch operations, particularly in the vicinity of other offshore units.
- Wind: Strong winds, especially storms, have the potential to impose restrictions on vessel operability.
- Tides: The rise and fall of sea levels due to tides, combined with storm surges, are important in shallow waters. These variations can affect navigation and harbour entry.
- Currents: Generated by rivers, tides, wind, or density differences, currents pose various challenges. They impact the position-keeping ability of the vessel and remotely operated vehicles (ROVs), as well as diving operations.
- Precipitation: Heavy forms of precipitation, including rain and snow, can adversely impact site activities.
- Fog: Impairing visibility, fog also presents challenges to marine operations.
- Turbidity: Haziness in the water, caused by suspended solid particles in the water column, can impact operations requiring visibility, such as cable cutting with divers or ROVs.

The most important operability constraint is vessel motion [8]. Examining how various vessels respond to a given wave spectrum depends both on the vessel design and the onboard equipment [37]. Each vessel with equipment can be characterized by a response amplitude operator (RAO) that considers the vessel's size, mass distribution, and other parameters reflecting its seakeeping properties. The RAO translates wave characteristics into vessel movements, with the wave heading in relation to the vessel being crucial for determining heave, pitch, and roll. Pitching and heaving have the largest influence on the vertical movement of the chute [37]. This vertical movement results in extra cable tension as explained in Section 3.2. The vessel's response to waves is highly dependent on the wave direction and

wave period. For example, regarding heave, short-period waves typically induce less significant heave due to their smaller wavelength compared to the vessel length [37]. Beam waves, waves perpendicular to the vessel, however, can cause substantial heave, even with relatively short periods [37]. During cable decommissioning activities, the vessel's heading aligns with the cable route.

Waves originate from the wind blowing over the sea. The longer the length of the route where wind can accelerate the water ("fetch"), the higher the waves can build up. In parts of the North Sea, westerly winds have a longer fetch and build up much higher waves than easterly winds [37]. The size of waves depends also on the wind duration and the water depth. Waves generated by winds can travel a far distance over the oceans. Travelling over hundreds of kilometres, the waves become less steep, having longer periods, but can conserve much of the wave height. These waves, which are generated far away are called swell. Waves from different origins can sometimes interact and create wave heights that are larger than the individual contributing waves.

4.3. Modelling Cable Pullout in OrcaFlex

To investigate the limits of cable pullout operations, an OrcaFlex model is developed to simulate the scenario described in Section 4.1. OrcaFlex is often used for cable laying analysis and NKT has experience with this software (Bodesund, 16-11-2023). This made OrcaFlex potentially a suitable software for the current research. For different burial depths and soil conditions, the influence of these factors on cable decommissioning by cable pullout had to be investigated. This section explains why it was decided to model the cable pullout operation in OrcaFlex and introduces the simulation approach.

4.3.1. OrcaFlex Introduction

OrcaFlex is a leading software for static and dynamic analysis of offshore systems and is developed by Orcina [23]. OrcaFlex is a comprehensive 3D non-linear time-domain finite element program. It has the capability to compute the dynamic response of a system based on various conditions. In static calculations, the primary objective is to determine positions and orientations for each element within the generated model to achieve equilibrium for all forces and moments. Subsequently, this static calculation serves as an initial configuration for dynamic simulations. Once the model to be analyzed is constructed within the software, the marine environment has to be defined by inputting data that includes water characteristics, water depth, seabed properties, wave motions, and current profiles [22]. Subsequently, general simulation settings are established, influencing the accuracy of results and the computational effort required.

OrcaFlex, as a tool, encompasses all the necessary functionalities for conducting installation analyses essential for inter-array cables and export cables in offshore wind projects and can do extreme response analysis under different sea states [22]. It is therefore also suitable for modelling the cable lift in the water column for cable decommissioning. However, it has its limitations regarding modelling soil interaction during cable pullout. It requires creativity and simplifying assumptions to model a buried cable in OrcaFlex. There are alternative finite element software programs where you could model the soil in more detail such as Abacus and Ansys. These methods are complex simulations and therefore advanced and computationally heavy while also requiring many parameters (Bodesund, 16-11-2023). Due to the large uncertainty and spread for input parameters, a very detailed soil mechanics model using for example PLAXIS would not be a practical solution. A model in OrcaFlex would be more convenient for quick simulations of the feasibility of the full cable pullout operation. OrcaFlex can accurately model cable and vessel responses in the water column which enables including waves and currents in the analysis. OrcaFlex has a large set of tools available and a strong Python API allowing for partly overcoming the compromise in modelling seabed interaction with buried cables. Therefore, it was decided to model the cable pullout operation in OrcaFlex.

4.3.2. Simulation Approach

It is relatively straightforward to compute the forces on the catenary in water where you have little friction (Andersen, 15-11-2023). As soon you have to pull it out of the seabed the cable would behave differently due to the friction from the soil resistance. There are currently no values available on the soil resistance for such a scenario but this friction will have a large impact on the decommissioning operation (Andersen, 15-11-2023). A possible solution would be to perform two calculations in two different models, one for the cable pullout from the seabed and one for the pullout from the water column.

In OrcaFlex, the seabed is just a surface with friction and the seabed is thus not deformable or viscous (Bodesund, 16-11-2023). When the seabed is penetrated during a cable simulation, the seabed acts as a spring with a penetration resistance that pushes the cable out again [23]. It is not possible to model a buried cable using the (nonlinear) soil model option in OrcaFlex because the soil has this spring behaviour and pushes the cable out as soon as you take away the pressure that forces the cable to penetrate the seabed. Therefore, it was necessary to work around this limitation to model a buried cable in OrcaFlex.

There are tools in OrcaFlex that could be experimented with to try to build a seabed on top of the cable to model the cable-soil interaction. For example, there is the option to add 'solid shapes' to the model. It might be challenging to capture the soil stiffness correctly by using solid shapes. The shapes are not affected by the environment and are usually used e.g. for modelling chutes (Bodesund, 16-11-2023). The shapes could represent the weight of the soil on top but would be difficult to model time-dependent soil interaction. Another option for soil modelling is using 'links'. These links act like strings and can be given a nonlinear behaviour that depends on how far they are elongated. You could have a series of links pulling the cable down mimicking the soil resistance when you start pulling on the cable. The links are probably more suitable for modelling the soil than the solid shapes (Bodesund, 16-11-2023). The links could be designed so that they behave linearly up until a certain tension or elongation and after reaching this critical point lose their stiffness, mimicking the cable breaking through the seabed. A third approach is based on adding 'applied loads'. This OrcaFlex functionality defines loads at multiple nodes along a cable and can include both forces and moments. Each load component can be constant, vary over time, or be determined by an external function [23]. The latter option allows load data to be specified by a user-defined function, such as a Python script, which is repeatedly called during an OrcaFlex simulation. After some trial and error modelling with the three different approaches the applied loads function seemed the most viable because of its flexibility and the option to calculate the soil resistance externally in Python. In Chapter 6 this modelling approach is presented in full detail.

4.4. Next Steps

This chapter presented a typical scenario for decommissioning an export cable. This information was used as input for step 1 and step 3 of the OrcaFlex modelling in Chapter 6, see also Figure 1.3. This chapter formed the bridge between the literature study and the thesis project. The cable characteristics, burial depths and soil conditions are all used as input for the OrcaFlex model. Actual project data inspired the typical cable decommissioning scenario. The main governing criteria during cable decommissioning, the ultimate tensile strength, minimum bending radius, and environmental operability limits were also introduced.

5

Soil Modelling

The soil interaction during the process of pulling out the cable from the seabed is a complex phenomenon that is crucial to take into account. The primary force opposing the recovery of a buried cable is the resistance from the seabed soil. This chapter answers the fifth research question: How do the burial depth and soil conditions influence the resistance forces during cable pullout? This resistance is determined by factors such as shear strength and burial depth. The shear strength represents the soil's resistance to deformation or failure under stress. Cohesive soils, such as clays, have high internal strength due to cohesive forces between particles, while frictional forces dominate in granular soils like sands. The burial depth determines the weight of the soil on top of the cable. This chapter introduces several soil resistance concepts that have been combined in a Python model to be able to compute the soil resistance for the OrcaFlex simulations. As was mentioned in the previous chapter, the main uncertainties for a buried pipe or cable are the soil conditions of the backfill material after 20–30 years of service.

First, this chapter introduces the models for fully drained and fully undrained uplift resistance. Thereafter, it presents how the uplift resistance can be computed for partially drained conditions based on these extremes. This computation is implemented in Python to be able to give the OrcaFlex simulation the values for the uplift resistances the cable nodes are experiencing during pullout. The Python code imports the position and velocity of each cable node from the OrcaFlex simulation for each iteration. The cable node's position is necessary to determine the instantaneous burial depth, and the node's velocity is needed for calculating the instantaneous dimensionless velocity. For the uplift resistance models mentioned below, the width of the backfill material is assumed to be infinite, which is in line with the guidelines from DNV for buried pipelines [9]. This implies that the uplift resistance is only determined by backfill material and not by virgin material.

5.1. Uplift Resistance

There is a literature gap regarding cable-soil interaction for buried cables, but the uplift resistance is also critical in upheaval buckling analyses of buried pipelines [9]. It was assumed that the cable-soil interaction would be similar to the pipe-soil interaction. Therefore, existing models are available to estimate this uplift resistance from the weight and shear resistance through the soil on top of the buried cable. For a buried pipeline or cable, such as in Figure 5.1, an applied uplift load W_t, is resisted by the sum of the buoyant self-weight of the pipeline W', and the soil uplift resistance W_u. As long as $W_t < W' + W_n$, the pipe stays in place. When a buried cable is pulled out on one end, the cable will start to bend rather than being uplifted and staying horizontal since cables are relatively flexible and have low bending stiffness. However, for starters, vertical uplift is assumed with the cable staying horizontal, simplifying the soil modelling. This results in a conservative model because pulling out a cable under an angle would mobilize less soil than pulling it out horizontally.

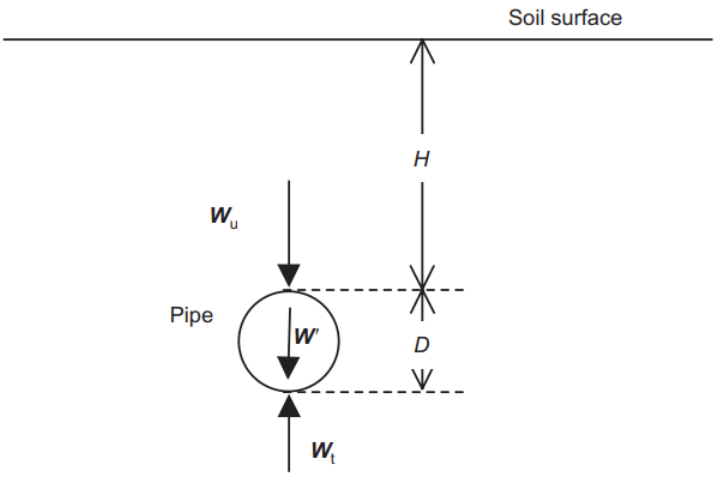

Figure 5.1: Pipeline/cable geometry and definitions [4]

The drainage condition of the sandy soil largely determines the uplift resistance, combined with the soil's relative density I_D and burial depth H. The two drainage extremes are fully drained and fully undrained. In fully drained conditions, there is sufficient time for the pore water within the soil to move and equilibrate with the applied load. Slow-loading scenarios in highly permeable soils such as sand are usually considered as fully drained [4]. In fully undrained conditions, there is insufficient time for the pore water to move in response to the applied load. Undrained conditions occur under short-term or rapid loading. In between these extremes is a transition region with a partially drained response.

Bransby and Ireland conducted the first study on the uplift resistance of pipelines for partially drained conditions [4]. They collected load-displacement data for pipeline tests carried out at different vertical velocities. Their experiments proved that low displacement rates provoked uplift resistances corresponding to (almost) fully drained conditions and that larger velocities resulted in significantly increased resistance [4]. This change in uplift load was expected to be the effect of a change in the drainage regime. Therefore, they plotted their results as normalised peak uplift resistance, i.e. the uplift capacity, $W_u/(\gamma' HD)$, with γ' as the submerged weight of the soil, against the dimensionless, i.e. normalised velocity, V, see also Figure 5.2.

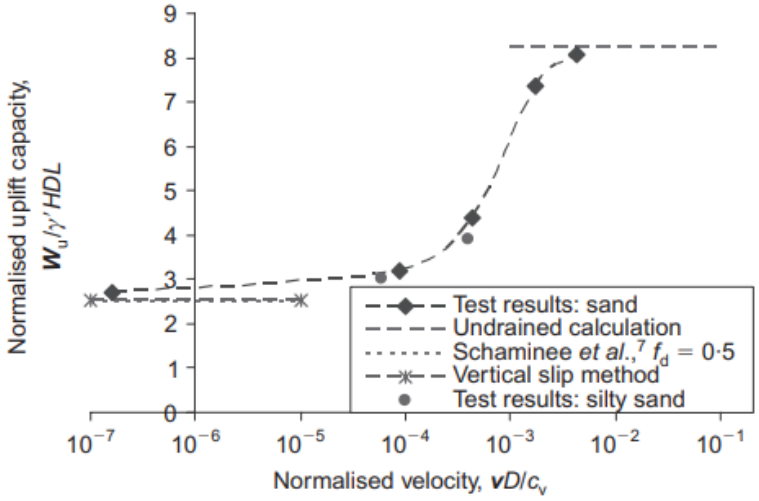

Figure 5.2: Normalised peak uplift resistance versus normalised velocity, $I_D = 0.13$, $H/D = 3$, and $D = 0.048$ m [4]

The drainage regime depends on the dimensionless velocity V defined as vD/c_v, where v is the pullout velocity, D is the pipeline or cable diameter, and c_v is the coefficient of consolidation [4]. The latter is related to the permeability of the soil which depends on factors such as the particle size and connectivity of the pores. For sandy soils, the consolidation coefficient may lie in the range 10^4–10^6 m^2/year [36]. High-permeability sands in combination with a slow pullout of the cable result in a small dimensionless velocity with drained conditions, whereas a high pullout velocity in low-permeability sands gives undrained conditions [4]. Due to the effect of shearing, dense sands dilate, which causes an increase in soil resistance [36]. Except for very loose sandy soils with high permeability, the fully drained uplift resistance is always lower than the fully undrained resistance, as is the case with the experiments from Bransby and Ireland. Therefore, it is an important objective during cable recovery to limit undrained conditions.

The resulting graph in Figure 5.2 proved the expectations and shows how for increasing dimensionless velocity, the uplift resistance increased as well [4]. This increase follows an exponential curve, which appears s-shaped on a logarithmic dimensionless velocity axis. This shape is in line with other geotechnical problems such as for shallow foundations and penetrometers [36]. Around a dimensionless velocity of 0.01, the uplift resistance curve reaches a plateau and provokes fully undrained conditions [4]. The fully drained resistance from the 'vertical slip' and 'Schaminee' methods and fully undrained resistance from the 'undrained calculation' are also plotted. These extreme values align with the curve for either relatively low (fully drained conditions) or relatively high dimensionless velocities (fully undrained conditions).

5.2. Fully Drained Uplift Resistance

When assuming vertical slip surfaces under fully drained conditions, the total drained uplift resistance F_{uD} (in kN/m) in terms of weight and integrated shear resistance follows from:

$$F_{\mathrm{uD}} = \gamma' \cdot H \cdot D + \gamma' \cdot D^2 \cdot \left(\frac{1}{2} - \frac{\pi}{8}\right) + f \cdot \gamma' \cdot \left(H + \frac{D}{2}\right)^2 \tag{5.1}$$

where γ' is the submerged weight of the soil, H is the height of cover or burial depth, D is the outer pipe diameter, and f is the uplift resistance factor which is related to the soil's relative density [9]. The first two terms relate to the soil weight, with the second term taking the semi-circular area of the cable into account. The third term relates to the shear resistance, which depends on the friction angle and therefore the relative density of the soil. See also Figure 5.3 for the definitions of the different parameters. The submerged weight of the soil γ' was assumed to have a value of 10 kN/m^3 based on the experiments of Bransby and Ireland [4].

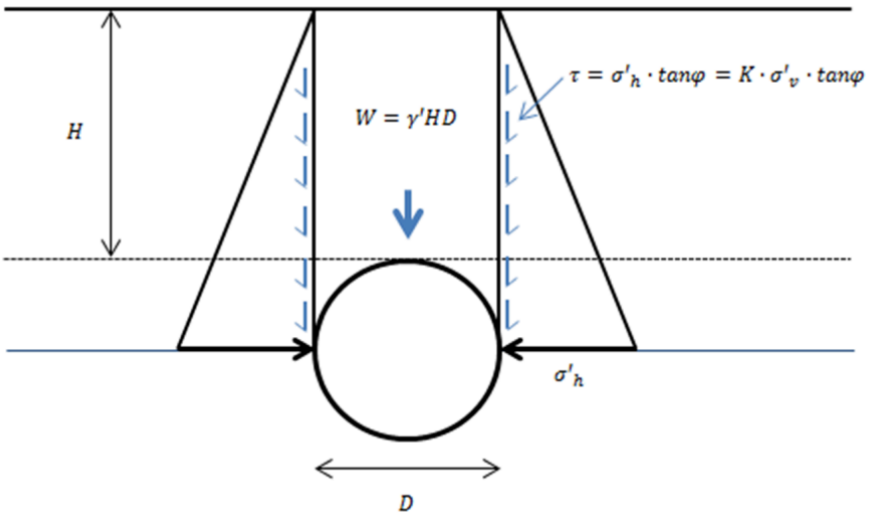

Figure 5.3: Vertical slip model [9]

The uplift resistance factor is a key parameter when it comes to accessing the uplift resistance during cable pullout. Based on uplift tests with pipelines, Equation 5.1 was fitted and estimates for the uplift resistance factor were found for sand types with different relative densities [9]. The results are shown in Table 5.1 below.

Sand Type	Relative Density	Friction Angle (degrees) ϕ	Best Estimate f
Loose	0.20	30	0.29
Medium	0.50	35	0.47
Dense	0.80	40	0.62

Table 5.1: Best estimates of the uplift resistance factor [9]

The DNV best estimates from Table 5.1 feature abrupt changes, whereas in practice, a stepwise variation in the uplift resistance factor is not realistic. Therefore, a fitted line that results in a continuous variation of the resistance factor versus relative density was suggested [26]. This fitted line connects the mid-range points for the density intervals, as can be seen in Figure 5.4. The continuous line also matched the experimental results shown in Figure 5.4. Note that in Figure 5.2 for fully drained conditions, not only the vertical slip model but also an alternative method with an empirical uplift factor, as suggested by Schaminee et al., was used to compute the fully drained uplift resistance [4]. Since the results from this method are similar, this method was not further considered in the current research.

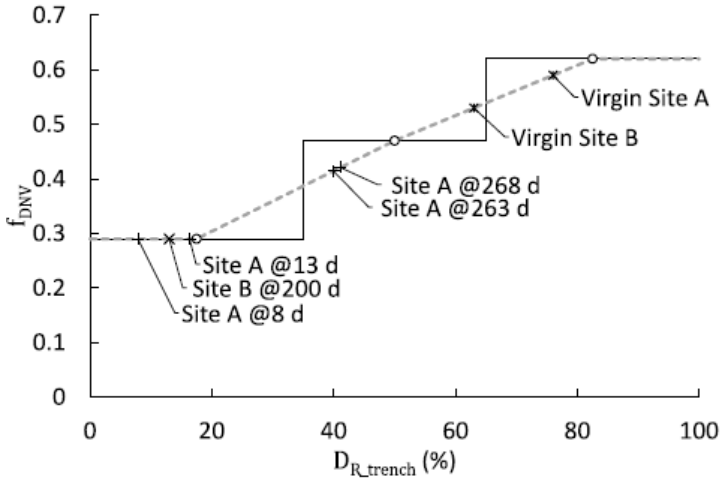

Figure 5.4: Recommended uplift resistance factor vs relative density [26]

Applying Equation 5.1 in combination with Figure 5.4 allows computing the drained uplift resistance of the 525 kV export cable described in Chapter 4 for different burial depths and relative soil densities. The results for different burial depths for different soil conditions have been plotted in Figure 5.5. For the drained resistance, the burial depth has a larger effect than the relative density. Note that, although barely visible in Figure 5.5, the uplift resistance is non-zero for zero burial depth due to the second and third terms of Equation 5.1. Both terms have non-zero values for zero burial depth as long as the cable diameter D is non-zero. According to DNV, the definition of the uplift resistance factor and hence Equation 5.1 has a validity range with respect to the soil cover ratio H/D up to $H/D = 8.0$ [9]. This implies that using this definition of the uplift factor for larger soil cover ratios gives rise to uncertainties. However, using this definition is assumed to be conservative because it is likely that for larger soil cover ratios, a local failure mode would prevail over global failure, modelled here with the vertical slip model. This local failure mode would have lower soil resistance than the global failure mode for large burial depths. This is similar to the local failure mode for undrained conditions, which is explained in the next section.

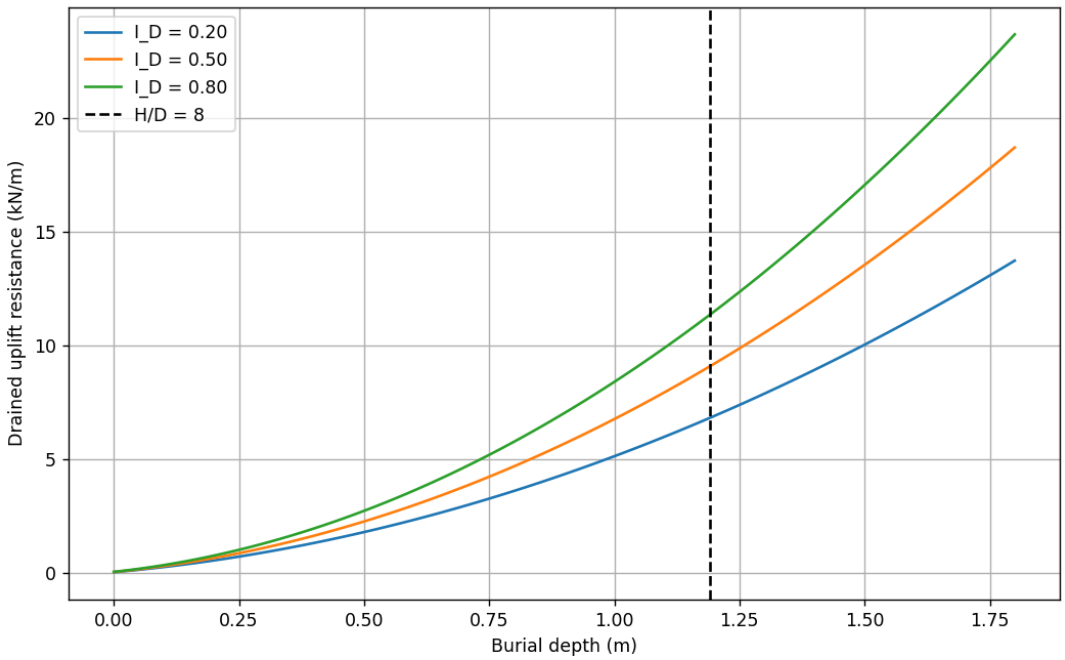

Figure 5.5: Drained uplift resistance versus burial depth H with $D = 0.149$ m for different relative densities (loose, medium, and dense) with the dashed line indicating the validity range according to DNV [9]

5.3. Fully Undrained Uplift Resistance

The above section explains drained uplift resistance where the uplift process does not generate excess pore pressures. If pore pressure is generated, it will dissipate within seconds [26]. If the uplift resistance is mobilised over periods comparable to or less than the soil drainage period, then undrained uplift resistance could be mobilised [26]. In very loose contractile sandy soil the undrained uplift resistance is smaller than the drained value, whilst for dense sand it is larger. Very loose sands contract and therefore generate positive excess pore pressure during shearing which reduces the resistance compared to drained conditions. Dense sands, however, expand and generate negative excess pore pressure and pore water suction caused by dilation. Because the dense material dilates, the uplift resistance increases.

For fully undrained conditions two different failure modes govern the uplift resistance [9]. The first mode is global soil failure where a wedge extending to the surface of the soil is lifted together with the cable or pipeline [9]. The second mode is local soil failure where the soil directly above the cable is displaced around and under the cable. Global failure can be modelled with a vertical slip model where the total uplift resistance is a combination of the weight of the soil block directly above the cable and the sliding resistance on the two vertical planes on either side of that block. These planes run from the seafloor down to the equator of the cable, as shown before in Figure 5.3 for drained conditions. When local failure of soil flowing around the cable is preferable, i.e. has a lower resistance, than global failure, the uplift resistance is a function of the local shear strength at the depth of the cable [9]. The two failure modes are illustrated below in Figure 5.6. For shallow burial, the resistance from the global vertical slip model is less than the resistance for a local flow-around failure, so the vertical slip mechanism occurs preferentially. For global failure, the resistance increases with burial depth whereas local failure resistance is independent of burial depth. Therefore, at a certain burial level, local failure has a smaller resistance and thus replaces global failure.

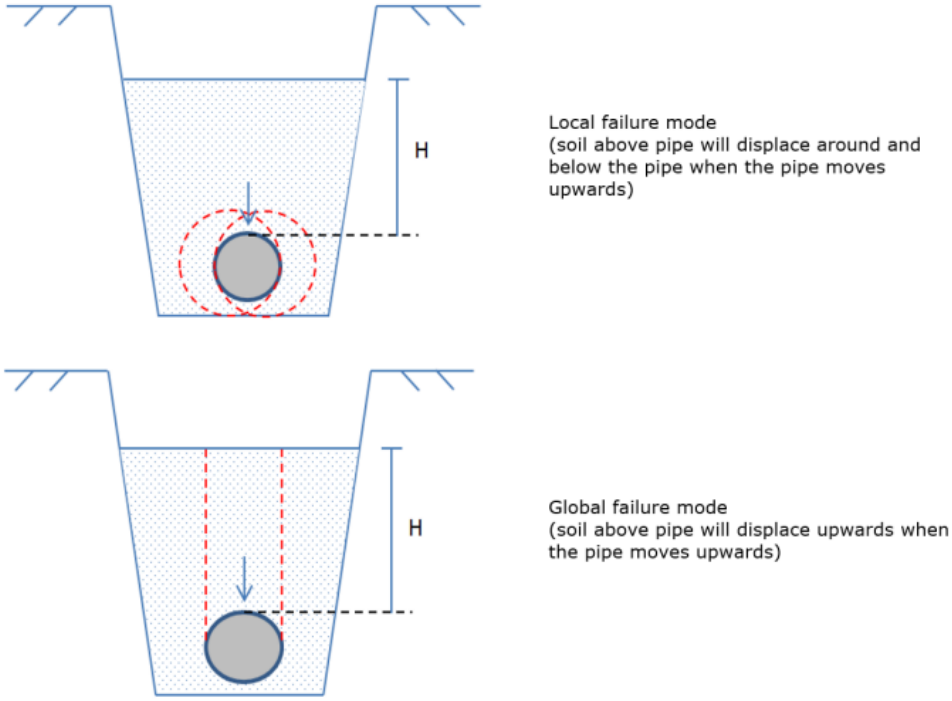

Figure 5.6: Uplift resistance failure modes for undrained conditions [9]

The initial undrained uplift resistance F_{uU0} for global failure is similar to the drained resistance model. However, the shear resistance through the soil above the cable is governed by the undrained shear strength s_u along the vertical failure planes:

$$F_{\mathrm{uU0}} = \gamma' \cdot H \cdot D + \gamma' \cdot D^2 \cdot \left(\frac{1}{2} - \frac{\pi}{8}\right) + 2 \cdot s_u \cdot \left(H + \frac{D}{2}\right)^2 \tag{5.2}$$

Local failure resulting in undrained uplift resistance is a function of the shear strength around the cable or pipeline:

$$F_{\mathrm{uU0}} = N_c \cdot s_u \cdot D - \gamma' \cdot A_p \tag{5.3}$$

where N_c is the bearing capacity factor and A_p is equal to πD^2 with this last term accounting for a soil buoyancy effect [9]. The value for N_c is typically in the range between 9-12 and can be taken as an intermediate 10.5 [4]. Both failure modes are governed by the undrained shear strength s_u. This shear strength depends on the relative density of the soil and can be computed by applying Bolton's correlations in the following way:

$$I_R = I_D(Q - \ln p') - 1 \tag{5.4}$$

where I_R is the relative dilatancy, I_D is relative density, Q is the crushing strength parameter, commonly taken as 10, and p' is the mean stress at failure in kPa [3],[36]. For undrained failure the dilation angle must be zero, so $I_R = 0$ [36]. After rewriting Equation 5.4 this results in

$$p' = \exp\left(Q - \frac{1}{I_D}\right) \tag{5.5}$$

which can be used to compute the undrained shear strength:

$$s_u = \frac{1}{2} p' \left(\frac{6 \sin \phi_{cv}}{3 - \sin \phi_{cv}} \right) \tag{5.6}$$

where ϕ_{cv} is the constant volume or critical state friction angle which can be taken as 32 degrees [36]. The result from applying the formulas above to the NKT 525 kV export cable is the undrained uplift resistance as plotted below in Figure 5.7. Opposite to drained conditions, the relative density has a larger effect on the resistance than the burial depth. This follows from the exponential term in Equation 5.5. The fact that the uplift resistance is non-zero for zero burial depth is due to the second and third terms of Equation 5.3. Both terms have non-zero values for zero burial depth as long as the cable diameter D is non-zero. The resistance curves reach their plateau at approximately 0.7 m burial depth. Below 0.7 m, the resistance is governed by the global soil failure mode which increases with burial depth. For larger depths, the local failure mode dominates which results in the resistance being independent of burial depth. Comparing Figure 5.7 to Figure 5.5 it is evident that the undrained resistance is significantly larger than the drained resistance for loose, medium, and dense sand.

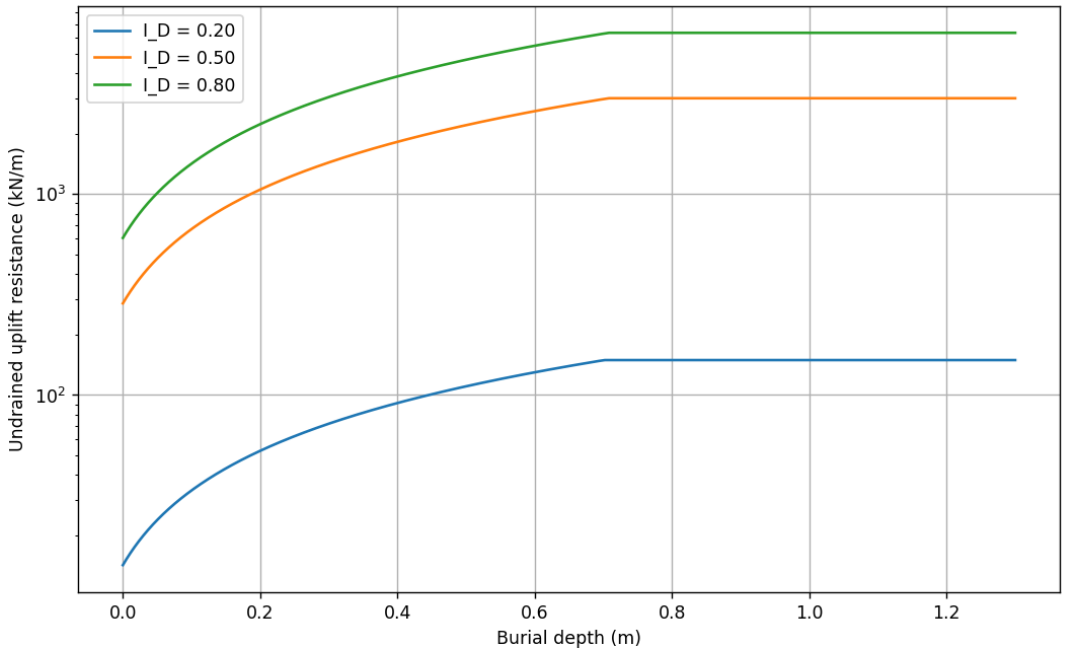

Figure 5.7: Unrained uplift resistance versus burial depth H with $D = 0.149$ m for different relative densities

Apart from the local failure mode, there is a limit to the dilating behaviour of dense sands that could cap the resistance increase due to dilation. The potential negative excess pore pressure is bounded through the cavitation of the pore water, limiting further decrease of the pore pressure. The water will vaporize if the pore pressure reduces to the water's vapour pressure and thus the pore pressure does not further reduce. In a water column, pressure increases with depth due to the weight of the water above (hydrostatic pressure). Therefore the likelihood of cavitation increases with decreasing water depth. Shallower water depths correspond to lower hydrostatic pressures. Taking cavitation into account in further research could potentially make the undrained uplift resistance calculation more accurate and less conservative for shallow water depths. It was left out of the scope of this thesis because pore pressure development was not a focus of the research.

5.4. Partially Drained Uplift Resistance

The dilation experiments of Bransby and Ireland investigated uplift resistance for loose sand with a relative density of 0.13 [4]. Based on their test results, the exponential curve in Figure 5.2 was constructed. This exponential curve appears s-shaped on the logarithmic dimensionless velocity axis. Equipped with F_{uD} and F_{uU0} it is possible to generate similar curves for other relative densities showing the general initial uplift resistance F_{u0} for at any dimensionless velocity. These responses again follow an exponential curve:

$$F_{u0} = F_{uU0} + (F_{uD} - F_{uU0}) \left(\frac{1}{1 + \frac{V}{V_{50}}} \right) \tag{5.7}$$

where V_{50} is the dimensionless velocity that lies halfway between the drained and undrained limits which is approximately 0.01. This method of constructing resistance curves stems from the backbone curves previously created for free fall penetrometer resistances for different relative densities [36]. Applying Equation 5.7 for different relative densities gives resistance curves as shown in Figure 5.8. Here, the diameter of the cable is 0.149 m and burial depth is taken as 0.450 m to have a similar H/D ratio as with the experiments of Bransby and Ireland. Note that the initial undrained uplift resistance is not normalised as in Figure 5.2, because the input for the OrcaFlex simulation requires the non-normalised values for uplift resistance.

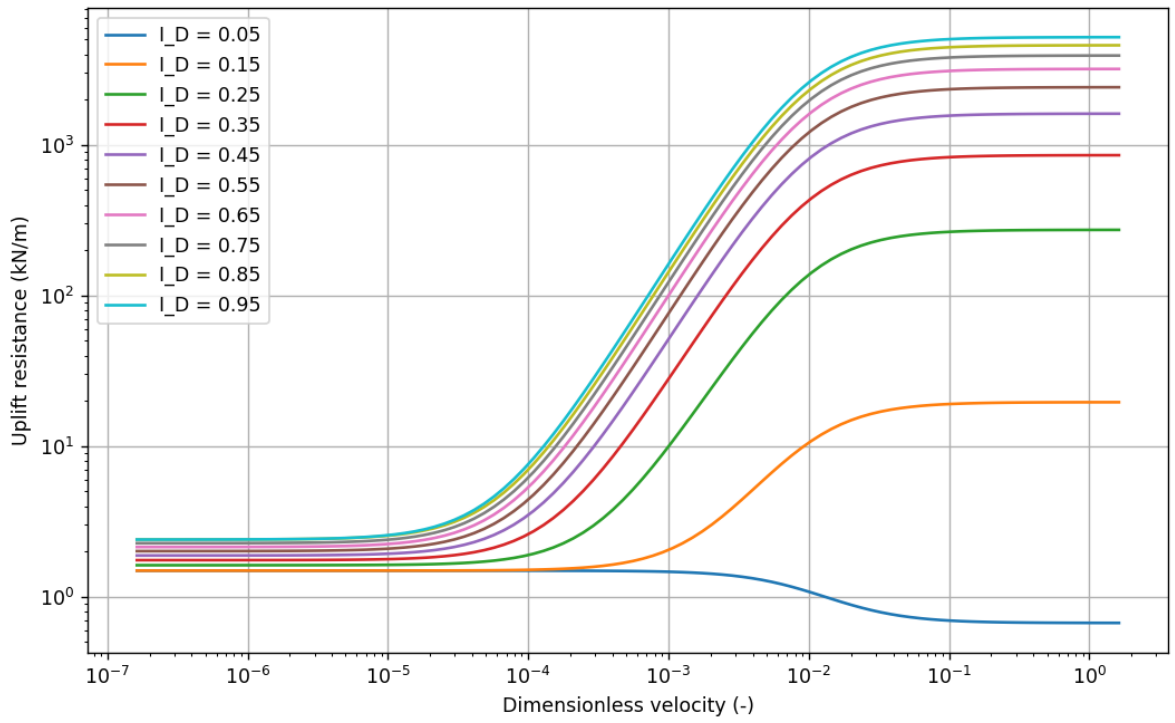

Figure 5.8: Resistance curves for uplift resistance versus dimensionless velocity for different relative densities with H = 0.450 m, and D = 0.149 m

Very loose sands, e.g. with a relative density of 0.05, generate positive excess pore pressure during shearing because very loose sands reduce in volume. Dense sands, however, dilate and generate negative excess pore pressure and pore water suction caused by dilation. These events explain the divergent shapes at low and high relative densities in Figure 5.8. For very loose sands, the undrained resistance is smaller than the drained resistance, whereas, for dense sands, the undrained resistance has a larger value. This aligns with the effects of dilatancy, where the dense material expands, leading to

an increase in effective stress and uplift resistance under undrained conditions. There is a transitional relative density above which any increase in uplift velocity would increase the uplift resistance due to negative pore pressure developments. This transitional relative density ranges between 10% and 20% according to previous research [26]. This is in line with Figure 5.8. As was mentioned in Chapter 4, having loose sand conditions is already unlikely, and therefore very loose sands are not expected during cable pullout.

The transition from fully drained to fully undrained conditions occurs over approximately three to four orders of magnitude of V, which is comparable to the experimental results of Bransby and Ireland. Below a dimensionless velocity of around 10^{-5} the sand is fully drained, and above approximately 10^{-1} the sand is fully undrained. Once you start pulling the cable upwards quickly enough to mobilize an undrained or partially drained response, water will start flowing due to the excess pore pressure created.

When the sand is not very loose, the sand dilates, the excess pore pressure is negative and with time passing water starts flowing in relieving the pressure difference. When the water flows in and drainage increases, the density and the undrained strength reduce due to the particles spacing out more. To capture this effect, there are two assumptions: (1) ultimately, the resistance will converge towards the drained value and (2) this progression will follow a typical consolidation curve with time. These assumptions allow for the definition of a changing undrained resistance F_{uU} which depends on the time t since the cable started moving, i.e. initial failure:

$$F_{uU} = F_{uD} + (F_{uU0} - F_{uD}) \left(\frac{1}{1 + \frac{T}{T_{50}}} \right) \tag{5.8}$$

where T is the dimensionless time defined in the same way as dimensionless velocity, $T = c_v t / D^2$, and T_{50} is the dimensionless time for which 50% of the excess pore pressure has dissipated which is approximately 0.5 [36]. This definition of F_{uU} matches usual consolidation approaches [6]. When t increases, the instantaneous undrained resistance F_{uU} converges from the initial untrained resistance F_{uU0} towards the drained resistance F_{uD}. Figure 5.9 shows this convergence due to the time-dependent drainage.

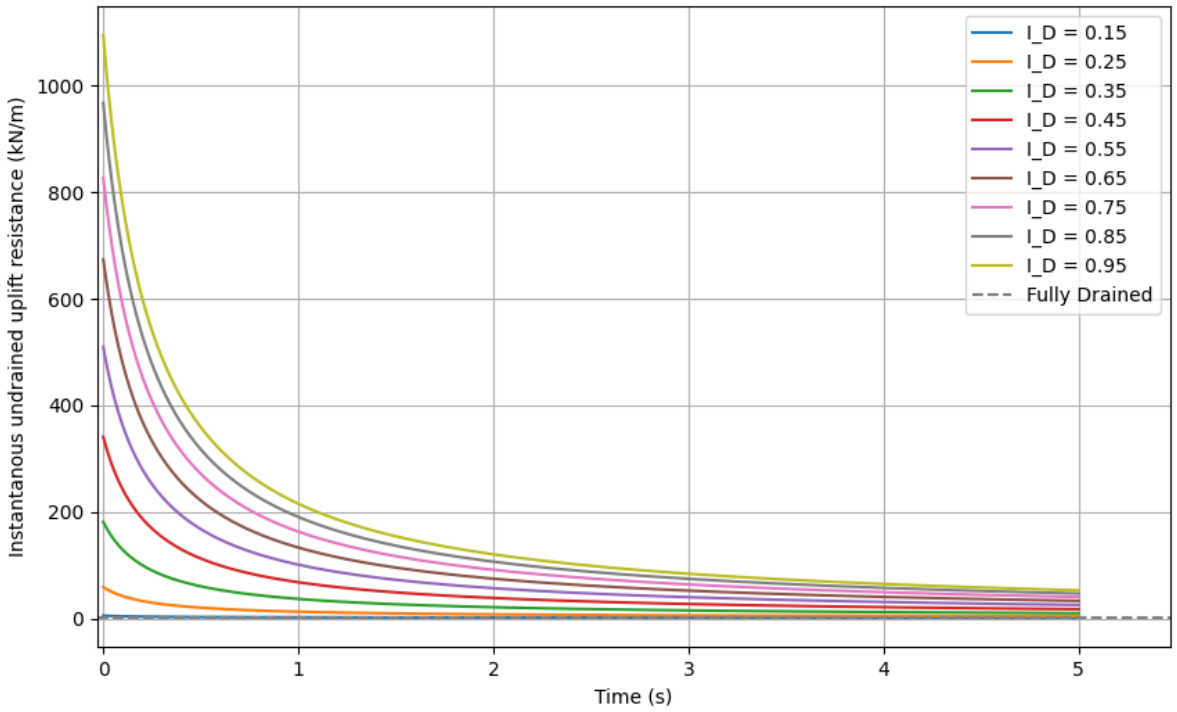

Figure 5.9: Instantaneous undrained uplift resistance vs. time with $V = 0.326$, $H = 0.450$ m, and $D = 0.149$ m

When taking the effect of increasing drainage into account, the uplift resistance can be computed at any time by applying the changing undrained resistance F_{uU} to the formula for the initial uplift resistance F_{u0}. The result looks rather similar to Equation 5.7:

$$F_u = F_{uU} + (F_{uD} - F_{uU}) \left(\frac{1}{1 + \frac{V}{V_{50}}} \right) \tag{5.9}$$

where F_u is the time-dependent peak uplift resistance at any dimensionless velocity. This implies that for each point in time after the initial failure, the resistance curves from Figure 5.8 have a different upper limit since the fully drained resistance decreases with time. Compare for example, the resistance curves below in Figure 5.10 with the curves in Figure 5.8. You see that after five seconds since the initial failure, the fully undrained resistance plateaus are significantly lower than the initial fully undrained resistance plateaus in Figure 5.8.

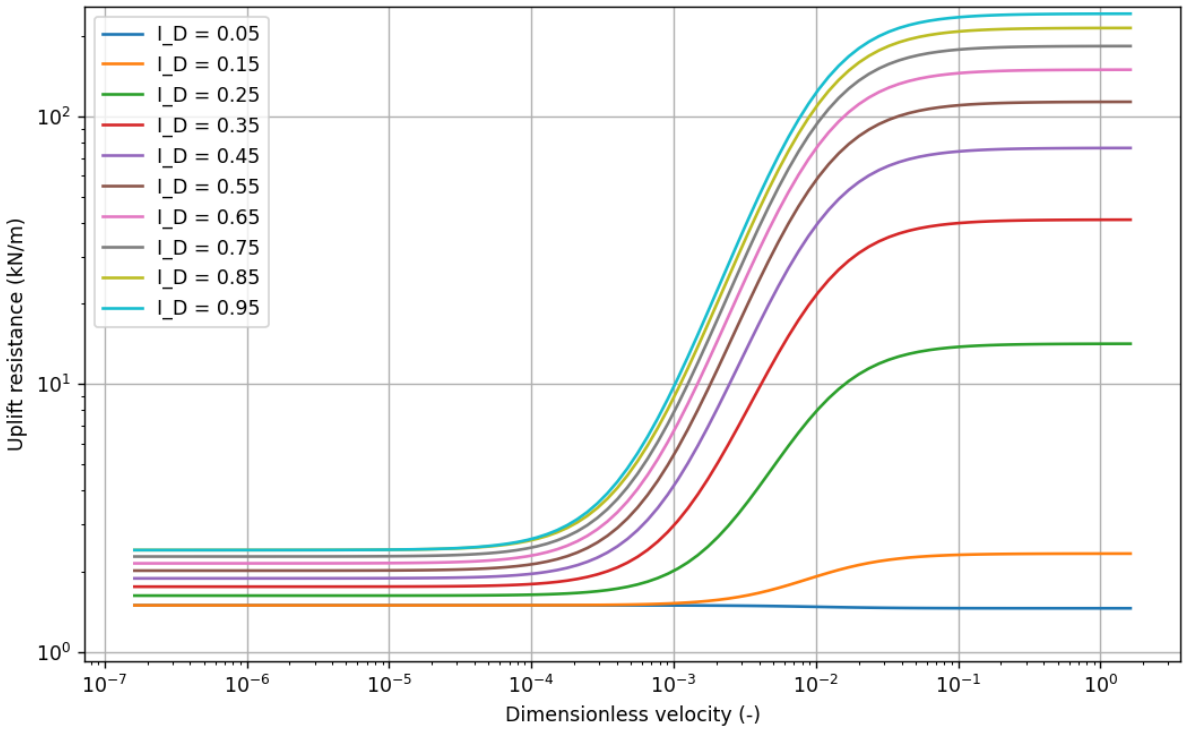

Figure 5.10: Resistance curves for uplift resistance versus dimensionless velocity for different relative densities after 5 s since initial failure with $H = 0.450$ m, and $D = 0.149$ m

5.5. Mobilisation Distance

The mobilisation distance z_{mob} is the displacement required to mobilise the peak uplift resistance. According to DNV this required displacement is uncertain for sand [9]. For gravel and rock backfill, a z_{mob} of 0.01 times the burial depth H is recommended but this value would be conservative for sandy soils [9]. At first, this value was used for the current research, which resulted in unstable simulations. Bransby and Ireland found that the mobilisation distance in sandy soil is not only dependent on the burial depth but also on the velocity, see also Figure 5.11. They showed with their experiments that for uplift velocities larger than 0.01 m/s, the mobilisation distance can be of the order of $0.1H$ for sandy soils [4]. This result matches other studies indicating that z_{mob} can be as large as $0.1H$ for sandy soils [33].

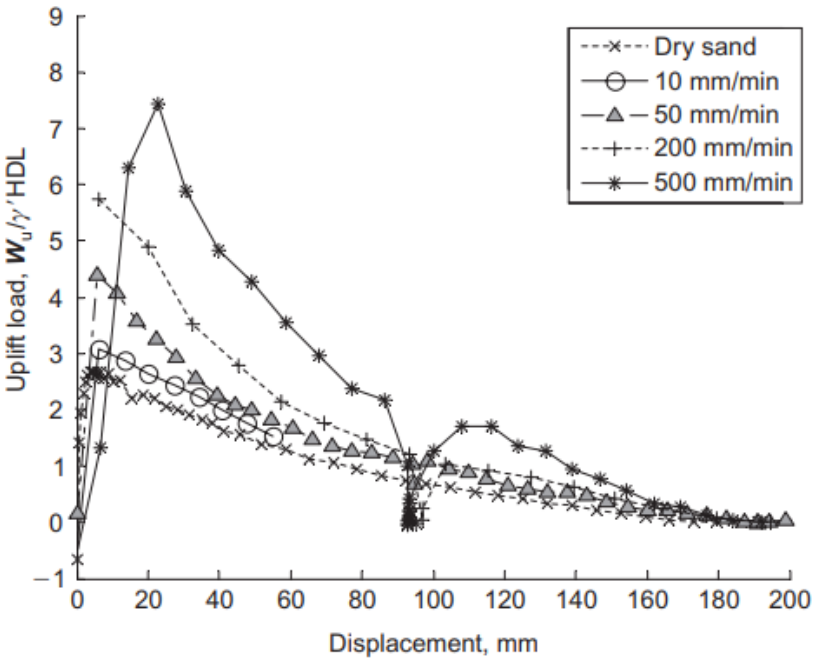

Figure 5.11: Normalised uplift resistance vs. displacement for pipeline tests carried out at different vertical velocities with saturated sand, $H/D = 3$, and $D = 0.048$ m [4]

During cable decommissioning, the pullout velocity would be several times larger than 0.01 m/s, for example, 0.2 m/s (Zheng-Lu, 29-09-2023). No experimental data on mobilisation distances is available for such velocities so the exact appropriate mobilisation distance remains uncertain. Based on the trend observed in Figure 5.11, it is likely that for velocities larger than 0.01 m/s, the mobilisation distance continues to increase since there is no sign of having reached a plateau for z_{mob}.

Before the mobilisation distance is reached, the cable's real uplift resistance F is not yet at its peak value F_u. To model the effect of the mobilisation distance, a simple approach is relating the uplift resistance F to the upward displacement z of the cable by:

$$F = \min(kz, F_u) \tag{5.10}$$

where F_u is the time-dependent general uplift resistance at any dimensionless velocity as calculated using the methods above, and k is an upward spring stiffness. This k can be defined on the initial undrained resistance F_{uU0} and the mobilisation distance:

$$k = \frac{F_{uU0}}{z_{mob}} \tag{5.11}$$

Combining Equation 5.10 with the partially drained resistance equations results in Figure 5.12. The x-axis is the vertical displacement z normalised with the initial burial depth H_0. While the cable is being pulled out, the value for z increases. The instantaneous burial depth H decreases with increasing z but the initial burial depth is constant. For simplicity, the effect of increasing drainage is neglected in this figure. Therefore, the plotted uplift resistance is larger than in reality. Figure 5.12 has three evident transition points. The first one is after a vertical displacement z equal to the mobilisation distance. At this point, the uplift resistance is fully mobilised and starts to decrease because the burial depth decreases. Before this point, the uplift resistance increases despite the decreasing burial depth due to the mobilisation. The second transition is after a vertical displacement equal to the initial burial depth H_0. At this point, there is no more soil on top of the highest part of the cable, but there is still soil above the rest of the cable due to its circular shape and also around the cable. When the vertical displacement

reaches a distance equal to the initial burial depth plus the cable diameter, the uplift resistance is finally zero.

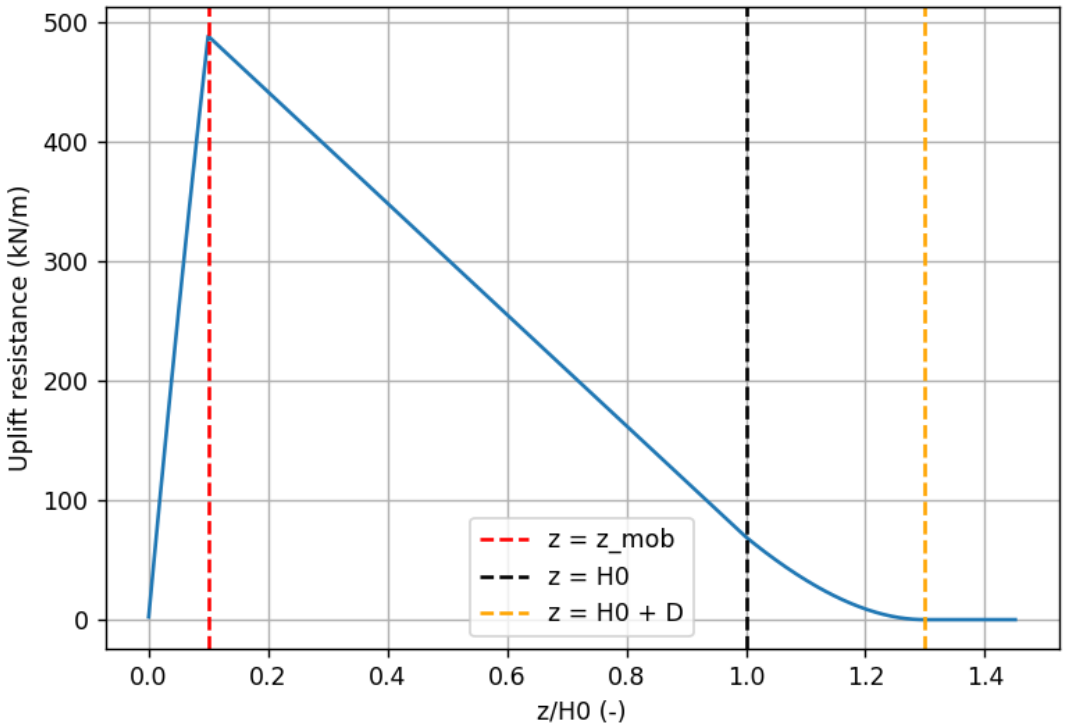

Figure 5.12: Uplift resistance vs. normalised displacement z/H_0 with $H_0 = 0.5$ m, $I_D = 0.5$, $v = 0.2$ m/s, and $D = 0.149$ m

5.6. Soil Modelling Summary

This chapter introduced the concept of partially drained uplift resistance. With the derived formulas, it is possible to compute the soil resistance, which depends on the burial depth, relative density, and dimensionless velocity at every time instance. The soil modelling also considered the mobilisation distance by introducing an upward spring stiffness. The soil model formulated in this chapter was used as input for step 2 of the OrcaFlex modelling in Chapter 6, see also Figure 1.3.

6

OrcaFlex Modelling

This chapter answers the sixth research question: How can a dynamic model simulate the recovery of a buried offshore cable? The OrcaFlex modelling was done in three steps, see also Figure 1.3. First, a 'standard' OrcaFlex model was built with a simple vessel, a chute, a winch, and a cable based on the specifications listed in Table 4.1. This basic model was able to simulate the recovery of an unburied cable resting on the seabed. The soil model constructed in the previous chapter was implemented in Python and connected to the OrcaFlex model by using external functions as a variable data source. This OrcaFlex extension was first tested with a simplified cable segment. Thereafter, the governing criteria are computed and an overview of all the underlying assumptions is given. Based on the assumptions, full results of a base case cable pullout in medium dense soil with a burial depth of 1 m are presented. Next, the results of sensitivity analyses on the effect of the time step, segment length, and dimensionless velocity are shown and analysed.

6.1. Model Set-Up

The modelling of a cable pullout operation started with a decommissioning vessel. For simplicity, the default OrcaFlex vessel model was used, see also Figure 6.1. All properties were left to the default settings and it was initially positioned at the origin of the OrcaFlex simulation. The vessel was equipped with a chute at the stern of the vessel. To model this chute, the shape function was used to add an elastic solid cylinder. The chute was connected to the vessel. To store the cable, a block shape was added to the ship to function as a simplified deck. A winch with a specified payout range of -0.2 m/s was responsible for pulling the cable out of the seabed and recovering it on board the vessel. The full summary of the data from the different components of the OrcaFlex model is given in Table 6.1.

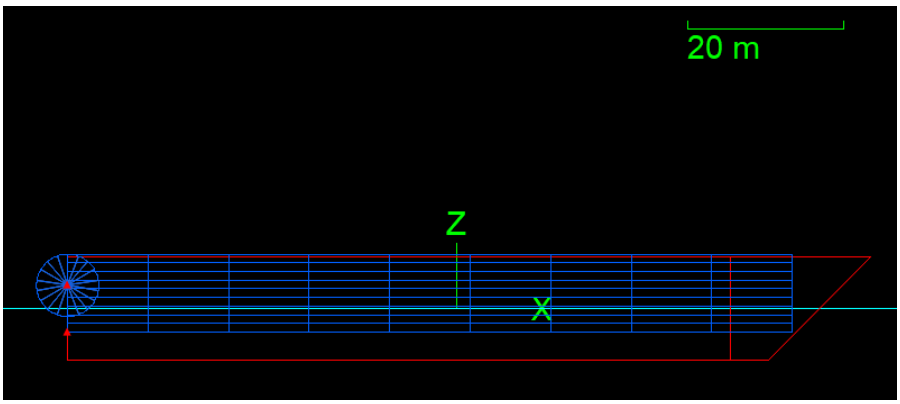

Figure 6.1: Default OrcaFlex vessel (red) with an added chute and deck (both blue)

Property	Unit	Value
Vessel Data		
Vessel properties	-	Default
Position	m	0,0,0
Line Type Data		
Outer diameter	m	0.149
Mass per unit length	te/m	0.0584
Bending stiffness	kN m^2	39
Axial stiffness	kN	390e3
Torsional stiffness	kN mm^2	155
All other properties	-	Default
Line Data		
Length	m	110
Segment length	m	0.05
End A connection	m	Free: -40, 0, 7.0745
End B connection	m	Anchored: -130, 0, 0.745
Chute Shape Data		
Type	-	Elastic solid
Shape	-	Cylinder: 20 m length, 8 m diameter
Connection	m	Vessel: -50, -10, 3
Azimuth	degrees	90
Declinations	degrees	90
Normal stiffness	kN/m/mm^2	40e3
Deck Shape Data		
Type	-	Elastic solid
Shape	-	Block: 95 x 20 x 10 m
Connection	m	Vessel: -50, -10, 3
Normal stiffness	kN/m/mm^2	40e3
Winch Data		
Winch wire stiffness	kN	100e3
Control type	-	By stage
Statics	-	Specified length: 73 m
Payout rate	m/s	-0.2

Table 6.1: Summary of data of the OrcaFlex model components

The NKT 525 kV HVDC cable was modelled using the 'line type'. The cable data provided by NKT and presented earlier in Table 4.1 were converted into the units used by OrcaFlex, as shown above in Table 6.1. Based on a line type, lines can be added to the OrcaFlex simulation. Within OrcaFlex, a finite element model for lines is used. The line is divided into a set of line segments, which are modelled by straight massless segments with a node at each end [23]. This is shown in Figure 6.2 below. The model segments account solely for the axial and torsional characteristics of the line. All other attributes (mass, buoyancy, etc.) are concentrated at the nodes, as shown by the arrows in the figure above. The nodes and segments are numbered sequentially from end A to end B, starting with 1, 2, 3, and so forth. Each node functions as a short, straight rod that represents the two half-segments on either side of it and forces and moments are applied at the nodes [23]. There is an exception for the end nodes, which only represent one half-segment since they are adjacent to just one.

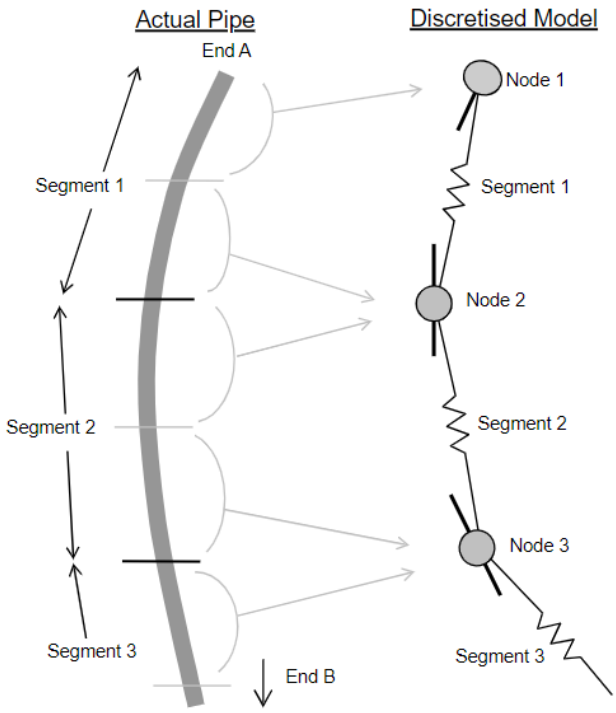

Figure 6.2: OrcaFlex line model with nodes and massless segments [23]

Based on the line type, a line was added to the OrcaFlex model to represent a cable to be decommissioned. This results in a cable model with a total length of 110 m and a segment length of 0.05 m. The first end of the cable, End A, was attached to the winch and End B was anchored at the seabed at the stern side of the vessel. To ensure that the anchoring point would not affect the simulation results, different cable lengths were tested. Based on the scenario provided in Chapter 4 the water depth was set to 30 m. The flat elastic seabed was given a relatively large stiffness of 10e6 kN/m/m^2 to model a fully consolidated soil. For the current research, a calm sea was assumed with no waves, currents or wind. All other environmental data, such as the water density and temperature, were left at their default value.

With this line model and the default vessel, it was possible to simulate the recovery of an unburied cable; see also Figure 6.3. First, a static calculation in OrcaFlex finds the positions and orientations for each model element such that all forces and moments are in equilibrium [23]. This provides a proper starting configuration for the dynamic simulation. The line static calculation is computed in two steps. Step 1 gives a reasonable starting shape for the line. In step 2, the 'full statics' calculation takes the result of step 1 and finds an equilibrium position for the model. For step 1, the spline method was used to give the line an initial shape based on user-defined input.

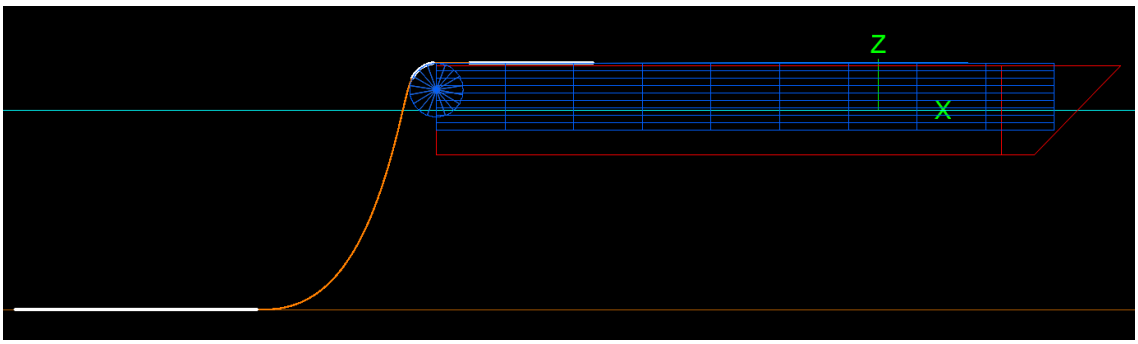

Figure 6.3: OrcaFlex simulation of recovering an unburied cable (orange) from the seabed with the white colour indicating contact between the cable and any surface

From the static equilibrium, the dynamic simulation can start. Time domain simulations are conducted in several stages, each lasting a specific duration [23]. Typically, the initial stage is a build-up period where the simulation is gradually increased from zero to prevent abrupt transients at the start of the simulation. This initial build-up stage is designated as stage 0, with time recorded as negative during this phase. Consequently, the first main stage is numbered 1 and begins at time t = 0 s. In Figure 6.4, the winch tension is plotted for both the build-up stage and stage 1. After the build-up stage, the winch tension clearly converges towards a steady state.

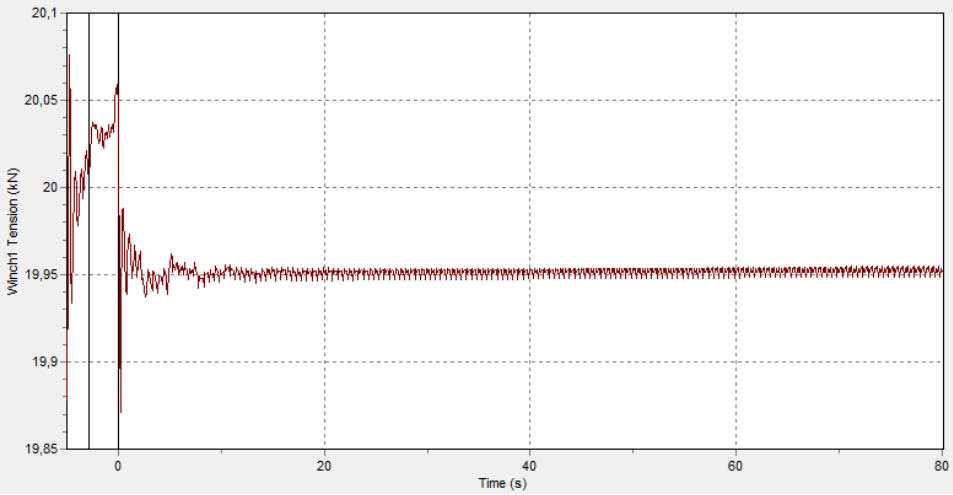

Figure 6.4: Time history graph of the winch tension during recovery of an unburied cable

OrcaFlex offers two time-domain dynamic integration schemes, explicit and implicit. Because implicit integration requires an iterative solution method, it consumes significantly more computation time than the explicit scheme [23]. However, the implicit scheme is typically stable for larger time steps, which often means that it is faster than the explicit scheme [23]. Therefore, at first, the implicit scheme was used with a standard timestep of 0.01 s.

Since the goal was to model steady-state cable recovery, the vessel velocity was set to a constant value of -0.2 m/s due to operational constraints. The velocity was negative because the cable was assumed to be recovered using a stern-side chute. The winch payout rate was therefore also set to -0.2 m/s. During stage 0 the vessel was given a speed change of -0.2 m/s, meaning that the vessel would accelerate during this stage until a speed of -0.2 m/s was reached at -0.2 m/s. While in stage 0, the winch payout rate accelerated in a similar way as the vessel. The simulation duration of stage 0 was set to 5 s and of stage 1 to 80 s.

To check the validity of the OrcaFlex simulation, the resulting maximum cable tension of 19.95 kN in Figure 6.5 can be compared with the analytical result from Equation 3.1. The analytical method returns a total tension of 20.01 kN which is only slightly more (0.25%) than the OrcaFlex result. The effect of the chute on the cable curvature can be seen in Figure 6.6. The cable nodes that have passed the chute have a maximum cable curvature of 0.25 1/m which corresponds to the chute radius of 4 m and thus a chute curvature of 1/4 = 0.25 1/m.

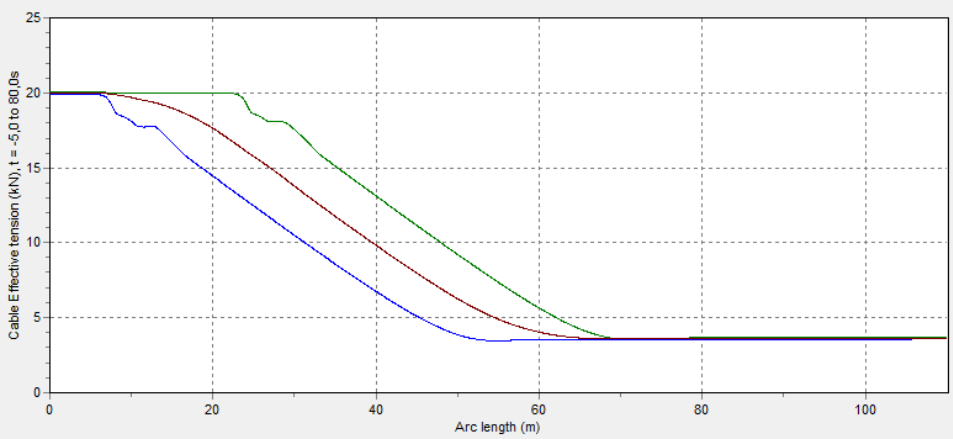

Figure 6.5: Range graph of the cable tension during recovery of an unburied cable with blue as minimum, red as mean, and green as maximum tension

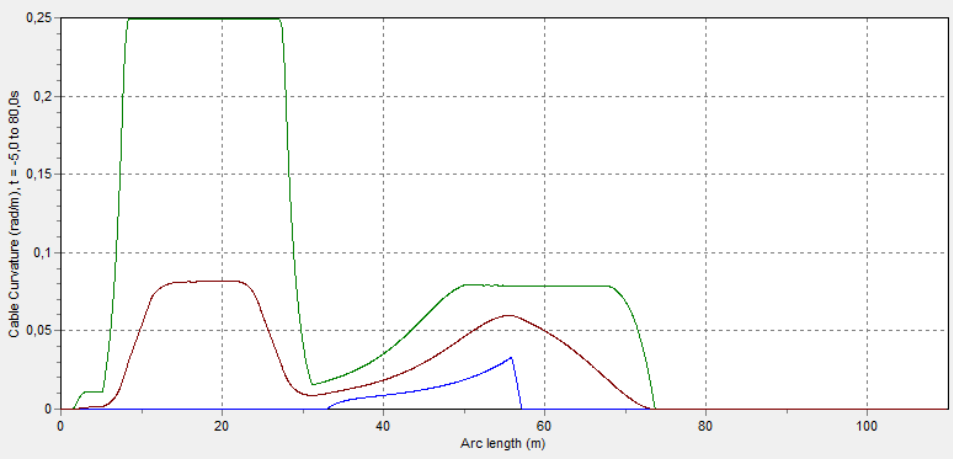

Figure 6.6: Range graph of the cable curvature during recovery of an unburied cable with blue as minimum, red as mean, and green as maximum curvature

6.2. External Function for Soil Resistance

Simulation of cable pullout of a buried cable required an extension of the OrcaFlex model described above. The idea was to use the OrcaFlex seabed as the lower boundary and to create a virtual seabed on top. For pullout simulations, the cable would start resting at the original seabed during the static calculation. The result of the static calculation would hence be equal to the static result for an unburied cable. In the dynamic simulation, the cable would be pulled out by the winch and would experience soil resistance from the virtual seabed. Several possibilities for constructing the virtual seabed were introduced in Chapter 4 but the most viable option seemed to be 'applied loads'. With this OrcaFlex functionality, it is possible to define loads at multiple nodes along a line. The point of application of each applied load follows from the arc length measured relative to either end A or end B of the line [23]. The loads can be applied with respect to global axes or to local node axes but for this application, the loads follow the global axes.

The applied loads can have both applied forces and moments. Since it was assumed that vertical uplift resistance is dominant and resistance in other directions can be neglected, the only load component needed was a vertical force. Each load component may be constant, vary with time or follow from an external function [23]. The latter allows the load data to be specified by a user-defined function, for example, in a Python script. The external function is called repeatedly during the OrcaFlex simulation. The soil model described in Chapter 5 was implemented in Python and connected to cable nodes in the

OrcaFlex model with external functions. The virtual seabed and resulting soil resistances are visualised in Figure 6.7. Each node loads its own version of the Python script as its external function. The external Python function can be reviewed in Appendix E. This makes it possible to have different soil resistances for the different nodes, which is necessary because the cable nodes are not pulled out simultaneously but one by one similar to a zipper.

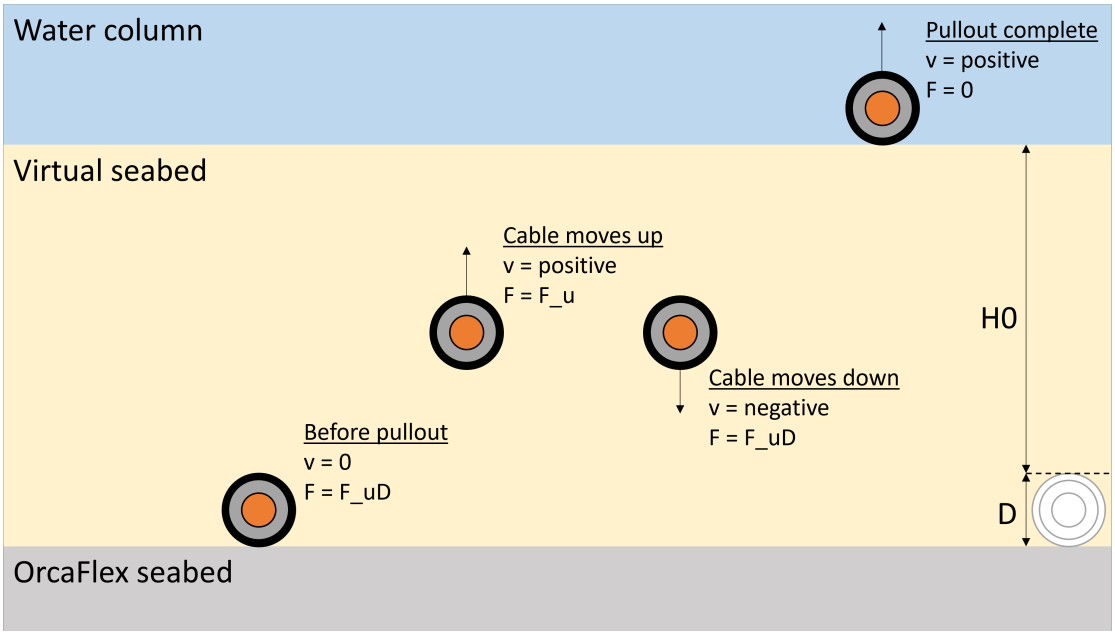

Figure 6.7: Visualisation of the resulting soil resistances in the virtual seabed computed by the external Python function

The Python script imports the current time, velocity, and vertical position of each node from OrcaFlex each iteration. Based on the vertical position, the script computes the current burial depth. With the current time, it calculates the time since the initial failure. The virtual seabed's soil parameters, such as the relative density, are assumed to be constant for each simulation. They are provided as Python variables inside of the script (and thus outside and independent of the OrcaFlex model). The input from OrcaFlex combined with these soil parameters enables the Python script to compute and return a soil resistance to OrcaFlex for each node for each iteration of each time step. This soil resistance value then acts as an applied force to each cable node.

During the static calculation, the external functions are inactive, which means that during this phase the cable does not 'feel' any effects of the burial in the virtual seabed and it rests on the OrcaFlex seabed as in Figure 6.3. Once the dynamic simulation starts, the external functions activate. During this phase, the cable nodes resting at the OrcaFlex seabed are not moving, but they start to feel the weight of the virtual seabed on top of them because the external function returns a force F equal to the drained uplift resistance F_{uD} for a burial depth equal to the initial burial depth H_0. See also the left cable cross-section in Figure 6.7. The cable is pushed down, but the elastic OrcaFlex seabed acting as a linear spring pushes back, which results in an equilibrium.

Once the first cable node starts to move due to the winch pulling on the cable, the Python script receives a positive velocity from OrcaFlex and saves the timestamp of this initial failure. Now the uplift resistance is not simply the fully drained resistance but most likely somewhere in the partially drained regime. By combining Equation 5.9 and Equation 5.10 the Python script computes the uplift resistance F_u for each iteration. From the start of the upward movement, the burial depth decreases. However, at first, the uplift resistance increases due to the mobilisation distance and acceleration of the upward movement. After reaching a maximum, the resistance decreases due to the time-dependent drainage and the decreasing burial depth.

During the simulation, the cable might also move down. When this happens, the Python script returns the drained resistance. Here, the cable still feels the weight from the soil above but no resistance from the soil beneath. For this model, it was thus assumed that the cable could move down freely until reaching the OrcaFlex seabed. In reality, the downward cable movement would result in opposing soil resistance. Once a cable node reaches the water column and is completely pulled out from the virtual seabed, the resistance has decreased to zero. Inside the water column, the external function has no longer any effect on the cable node.

To test and improve the external Python function responsible for computing the soil resistance, a simple OrcaFlex model was made that consisted of a line segment with only two nodes. This line was attached to an OrcaFlex 'constraint' to be able to force the line to move upwards with a constant velocity. This modelled a perfect vertical pullout of a cable, whereas for the full pullout simulation, the cable would not be pulled out perfectly vertically and also not with a constant velocity. However, it was a valuable way to do quick experiments with the external Python function. For these experiments, an initial burial depth H_0 of 0.5 m was used.

The line segment started the simulation resting on the OrcaFlex seabed and at $t = 0$ s the line was given a constant upward velocity of 0.1 m/s, see also the second graph of Figure 6.8. As soon as the nodes experience this upward velocity, the uplift resistance starts increasing from the fully drained resistance until the peak uplift resistance is reached when the vertical displacement is equal to the mobilisation distance z_{mob} as shown the third graph of Figure 6.8. As explained in Chapter 5, the mobilisation distance is assumed to be $0.1H_0$ which in this case equals 0.05 m. This distance is reached after 0.5 s with a velocity of 0.1 m/s. Due to the combination of both increasing drainage and decreasing burial depth, the uplift resistance decreases rapidly after hitting its peak. After 5 s and a vertical displacement of 0.5 m, the instantaneous burial depth H is equal to zero. After this point, the only uplift resistance left comes from the soil around the circular cable, which is completely out of the virtual seabed after 6.5 s.

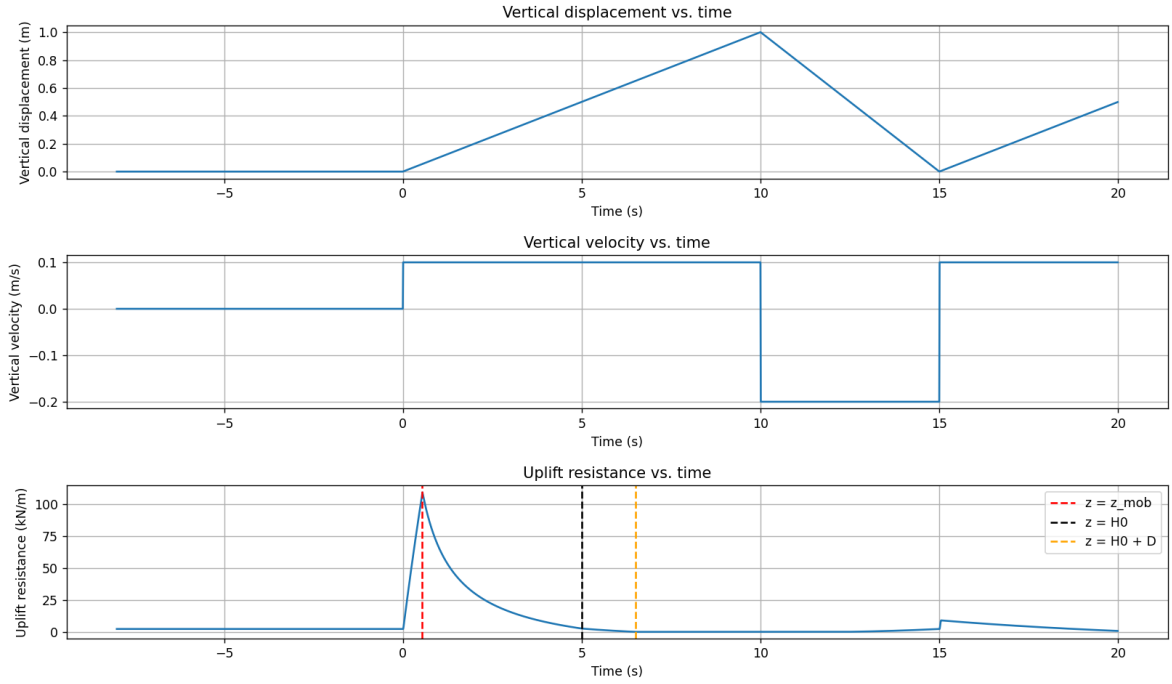

Figure 6.8: Resulting vertical displacement, velocity, and uplift resistance as computed by the external Python function for a cable segment with two nodes with $D = 0.149$ m, $H_0 = 0.5$ m, and $I_D = 0.5$

After 10 s, the line segment is given a constant downward velocity of 0.2 m/s. Such movements are not expected during actual cable decommissioning, but it helps to understand how the soil model works. After 11.8 s, the cable starts to 'feel' the soil again. In real life, the soil would resist the downward movement of the cable, but this simplified soil model only resists upward movement because uplift

resistance limits the pullout operation. The uplift resistance starts to increase slowly until the line segment is back at the initial burial depth after 15 seconds. At this point, the uplift resistance is also equal to the initial fully drained resistance since this value is independent of time. At $t = 15$ s, the constraint is again given an upward velocity of 0.1 m/s. This time, the peak uplift resistance is much lower due to the time-dependent drainage that decreases the undrained resistance dramatically. This shows that the soil model is only applicable for a continuous cable pullout after the initial movement of the cable. In a scenario where the pullout is paused for a while, according to the model, the uplift resistance would drop to the fully drained resistance, which would underestimate the actual uplift resistance.

6.3. Governing Criteria

In Chapter 4 the ultimate tensile strength i.e. the maximum allowable tension and the minimum bending radius were introduced as the governing criteria for the cable pullout. The environmental operability was out of the scope of the current research. For each simulation, the results were analysed to check whether these governing criteria were within their limits. It is undesirable to break the cable during the operation so the tension in the cable should stay below the ultimate tensile strength. It was assumed in Chapter 4 that the armour wires and the conductor determine the ultimate tensile strength. The maximum allowable tensions for the armour and the conductor of the NKT 525 kV HVDC cable follow from their respective ultimate tensile stresses. Applying Equation 4.3 to compute the armour tension and Equation 4.4 for the conductor tension results in a maximum allowable tension of 525 + 719 = 1244 kN. For the armour, a typical ultimate tensile strength of galvanised steel of 510 MPa was assumed. For the conductor, an ultimate strength of 210 MPa was assumed. The experiments by Ehlers et al. on a similar cable resulted in a maximum allowable tension of around 1000 kN [11]. However, this cable had an aluminium conductor with an ultimate strength of only 90 MPa. When doing the same calculation again but with an aluminium conductor to make a better comparison, the maximum allowable tension is 944 kN. The assumption that the armour wires and the conductor determine the ultimate tensile strength seems to be largely true and is on the conservative side.

Excessive bending of cables can cause local buckling, where armour wires interfere and touch each other (locking), leading to potential damage. The critical radius at which this occurs is the locking radius. Detailed investigations are needed to understand the effects of combining bending at the locking radius with pulling tension, as the cable's break limit might decrease under these conditions. Below the locking radius, standard cable models are invalid, requiring new assumptions and understanding. Therefore the locking radius was taken as the minimum bending radius. Based on the cable data provided in Table 4.1, the lay angle was calculated using Equation 2.1. With a cable lay angle of 16.6 degrees, according to Equation 4.6, the fill factor is 0.836. When applying Equation 4.5, this results in a locking radius of 0.909 m. Because it is more convenient to evaluate the simulated cable curvature than the cable bending radius in OrcaFlex, the locking curvature was used instead of the locking radius. The locking curvature κ is simply $1/\rho_l$. For the NKT 525 kV HVDC cable, the locking curvature is thus 1.01 1/m.

A third governing criterion follows from the maximum pull capacity of the equipment on the decommissioning vessel. For example, for the decommissioning of fibre optic cables, the tensioners are usually limited to 20 tons of pull capacity. However, the NKT Victoria has a total capacity of 90 tons, see also Chapter 3. For the current research, a maximum tensioner capacity of 90 tons or 900 kN was assumed based on NKT Victoria's equipment. When you account for the effect of waves, this pull capacity would be larger, since the upward movement of the ship would result in extra tension on the cable. For each simulation, the winch tension was checked in a similar way as the cable tension. The governing criteria are summarised in Table 6.2.

Governing Criteria	Unit	Value
Maximum allowable tension	kN	1244
Locking curvature	1/m	1.01
Tensioner capacity	kN	900

Table 6.2: Governing criteria for cable pullout of a NKT 525 kV HVDC cable

There is one other important constraint for the cable pullout. This constraint is the vessel velocity during cable recovery. The initial assumption was that the cable could be decommissioned at a rate of 1 m/s, hence a vessel velocity of 1 m/s. However, since the retrieved cable must be stored in a turntable or reel, the crew needs enough time to store the cable while maintaining a safe work environment. As seen in Figure 6.9, the crew is inside the turntable to ensure space-efficient cable storage. Therefore, the cable pullout velocity should be limited to approximately 12 m/min or 0.2 m/s (Zheng-Lu, 29-09-2023). In case of damage to the cable, such as bird cages, it might also be necessary to cut parts of the cable during the pullout operation. In such scenarios, it is also crucial to limit the pullout velocity.

Figure 6.9: Cable loading on a turntable on the NKT Victoria [20]

6.4. Assumptions Overview

To be able to model the cable pullout in OrcaFlex, assumptions were made which often simplified reality. Most of these assumptions have been introduced earlier in this report in different sections. It is important to be aware of these assumptions because they result in limitations of the applicability, accuracy, and certainty of the modelling results. Therefore, the underlying assumptions are summarised in this section. The effects and limitations of these assumptions on the simulation results are discussed in Chapter 7.

- The simulations were conducted with zero waves, currents, and wind.
- To compute the soil resistance, a continuous vertical uplift with a horizontal cable was assumed, as with the experiments of Bransby and Ireland. Hence, the curvature of the cave was neglected, and the soil resistance existed as only a downward-facing uplift resistance.
- Hysteresis during pullout velocity oscillations was neglected, and the downward movement of the cable during the pullout was assumed to not mobilise any upward-facing soil resistance.
- For each simulation, all input variables, such as burial depth, relative density, and vessel velocity, were kept constant. The seabed was flat with constant water depth and the potential influence of cavitation was not included. The backfill material was assumed to be infinite.
- The sandy soil was assumed to contain only purely non-cohesive sand.
- For all soil cover ratios, a vertical slip failure mechanism was assumed for fully drained conditions.
- The submerged weight of the sandy soil γ' was assumed to have a value of 10 kN/m^3 and the coefficient of consolidation c_v was assumed to be equal to 3e6 m^2/year based on [4]. The crushing strength parameter Q was taken as 10, and the constant volume or critical state friction angle ϕ_{cv} was taken as 32 degrees [36].
- The initial undrained resistance was assumed to converge with time towards the drained value following a typical consolidation curve.
- The mobilisation distance was assumed to be $0.1H_0$ and for constant velocity an upward linear soil spring stiffness k was taken [4].

- Regarding the cable, the breaking load was assumed to be a combination of the tensile strength of both the armour and the conductor. The cable-soil interaction was assumed to be similar to the pipe-soil interaction. The bending stiffness was assumed linear and was together with the other cable properties provided by NKT.
- The cable was modelled with a finite element model dividing it into a set of line segments, which are modelled by straight massless segments with a node with a concentrated mass at each end.
- On the operational side, cable handling constraints limited the maximum vessel and thus the coupled pullout velocity to 0.2 m/s. A stern-side chute with a radius of 4 m was used, and a maximum tensioner capacity of 90 tons or 900 kN was assumed based on the NKT Victoria's equipment.

6.5. Base Case Cable Pullout Simulation

The vessel and the cable model were now used to simulate a cable pullout; see also Figure 6.10. The green line was added to visualise the upper boundary of the virtual seabed. The lower boundary of the virtual seabed is the original OrcaFlex seabed. For this simulation, the burial depth was 1 m and the relative density was 0.5. The water depth for all simulations was set to 30 m. Waves, currents, and wind were not included. The effect of the virtual seabed and thus the soil resistance on the shape of the cable catenary is shown in Figure 6.11. Due to the soil resistance, the bottom tension increases significantly and the cable straightens in the water column. In the virtual seabed, the cable curvature rises in the part of the cable that is being pulled out of the seabed.

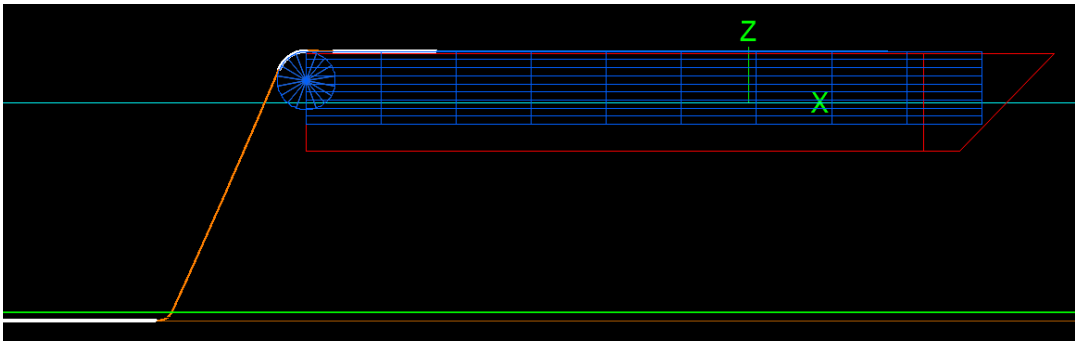

Figure 6.10: OrcaFlex simulation of pulling out a buried cable from the virtual seabed (green) with $H_0 = 1$ m and $I_D = 0.5$

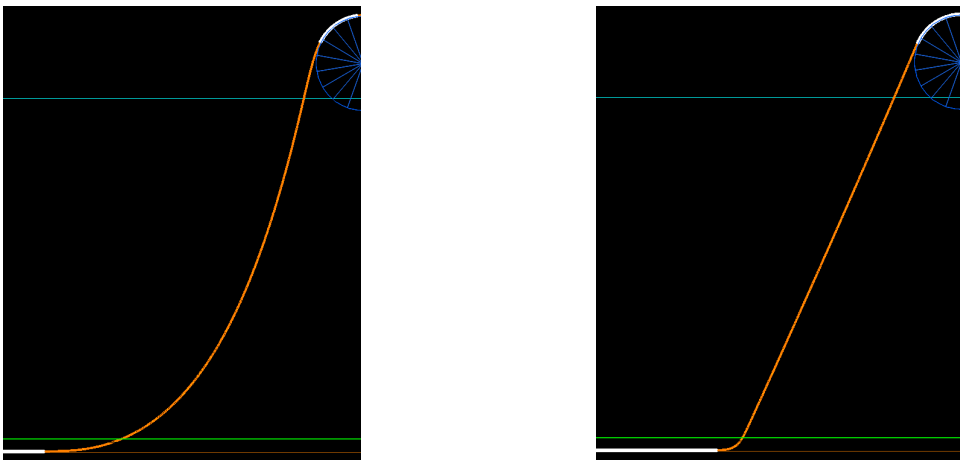

(a) Before applying soil resistance

(b) During applying soil resistance

Figure 6.11: Comparison of the cable catenary before (a) and during (b) applying soil resistance to the cable nodes with the white colour indicating contact between the cable and the OrcaFlex seabed or chute

The first cable node with an applied force through an external Python function is located at an arc length of 58 m. From this point onwards, an external force is applied at every 0.5 m along the cable. The segment length L is thus 0.5 m, which was recommended by an OrcaFlex expert (Bodesund, 16-11-2023). Note that this segment length for the externally applied forces is different than the line segment length, which was set to 0.05 m to model the cable. At the start of the dynamic simulation, all nodes have an applied load equal to the drained resistance. Once the node at 58 m arc length starts moving, the partially undrained resistance is applied, which increases with increasing displacement and velocity at first until it starts decreasing due to time-dependent drainage and the declining burial depth; see also Figure 6.12. One by one, the nodes are mobilised. After mobilisation of the seventh node located at an arc length of 61 m starts after around 47 seconds, the simulation enters an approximate steady state where the uplift resistance of each node follows the same pattern. Within this steady state, the velocity still oscillates but each node again follows the same pattern. The goal of the research was to investigate the limits of such a steady-state cable pullout. Therefore, the results obtained before reaching this steady start were considered start-up effects, which are not included in the result analyses.

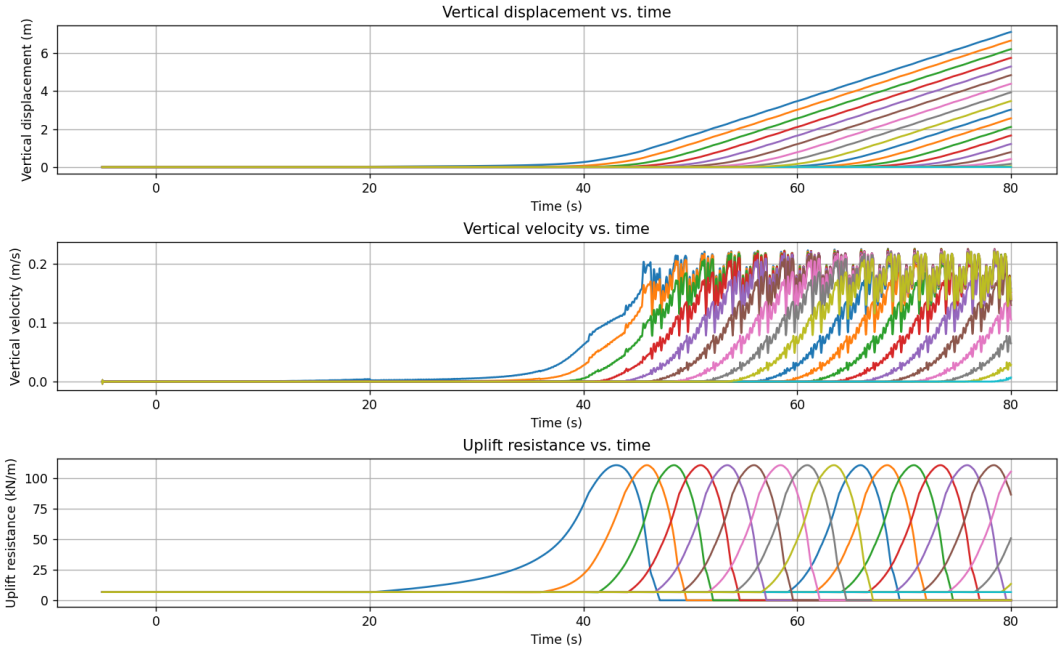

Figure 6.12: Resulting vertical displacement, velocity, and uplift resistance as computed by the external Python function for each node of the cable with $t = 0.01$ s, $L = 0.5$, $H_0 = 1$ m, and $I_D = 0.5$

The time history graph of the winch tension in Figure 6.13 also shows how the steady state for this simulation scenario is reached after around 47 seconds. The range graph of the cable tension in Figure 6.14 shows that the cable tension has its maximum at End A (arc length 0 m) which is at the winch connection. The maximum cable tension is thus equal to the maximum winch tension. The cable curvature peaks at an arc length of 58 m as can be seen in the range graph of the cable curvature in Figure 6.15. However, since at this point, the steady state has not been reached, this peak is only a start-up effect and is not taken into account for the results. Note that the winch tension oscillations have a period of 2.5 s and thus a frequency of 0.4 Hz. This period follows from the vessel velocity of 0.2 m/s and the segment length of 0.5 m: every 0.5/0.2 = 2.5 s, a new node is mobilised. The segment length also determines the pattern of the cable curvature of the mobilised nodes: every 0.5 m along the cable there is a peak in curvature.

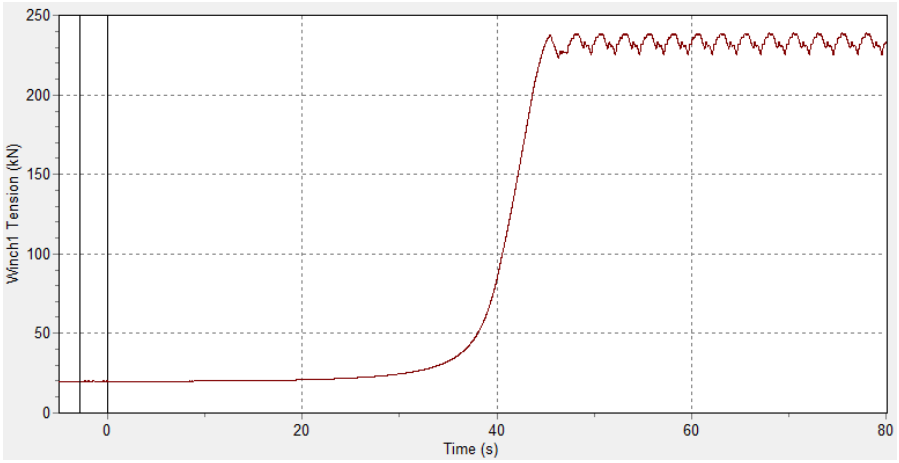

Figure 6.13: Time history graph of the winch tension with $t = 0.01$ s, $L = 0.5$, $H_0 = 1$ m, and $I_D = 0.5$

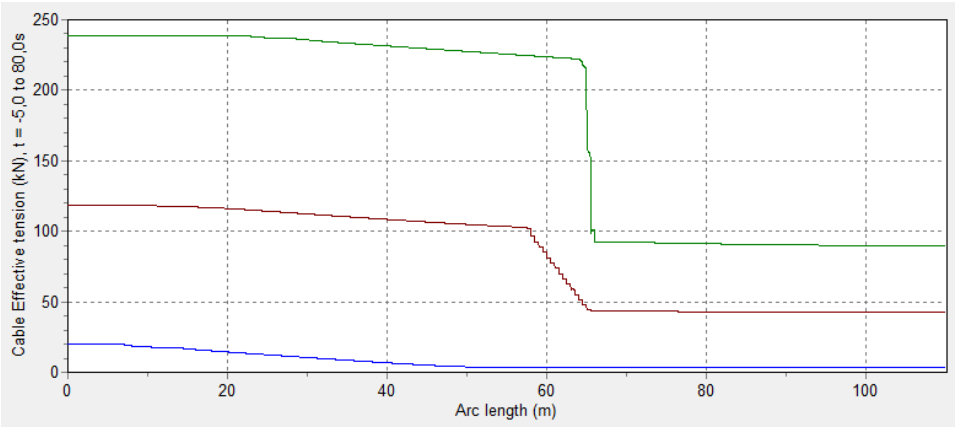

Figure 6.14: Range graph of the cable tension with blue as minimum, red as mean, and green as maximum tension

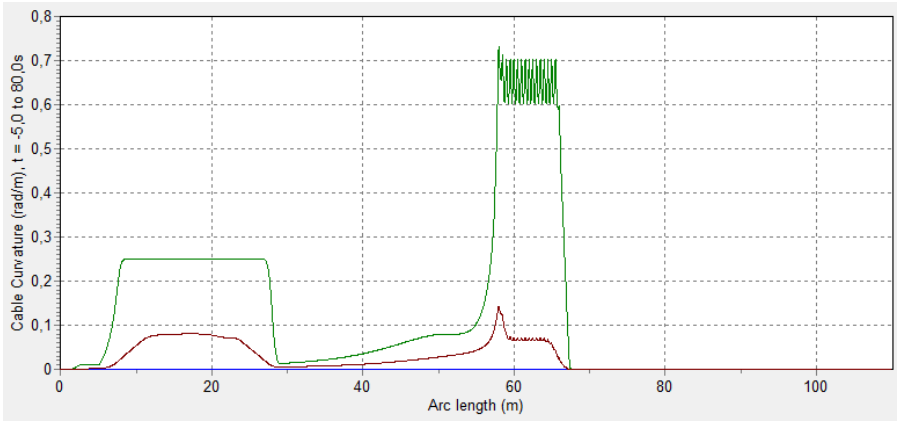

Figure 6.15: Range graph of the cable curvature with blue as minimum, red as mean, and green as maximum curvature

6.6. Sensitivity Analyses

Several sensitivity analyses were conducted to test the model for the base case described in the previous section. The results should smooth and converge for smaller time steps and shorter segment lengths. Therefore, both parameters have been investigated. The dimensionless velocity depends on both the

vessel velocity and the coefficient of consolidation and was therefore also interesting to analyse. For a larger vessel velocity, the dimensionless velocity increases and thus the partially undrained resistance should increase as well. For larger coefficients of consolidation and thus higher permeabilities, the dimensionless velocity decreases and the partially undrained resistance should converge towards the drained uplift resistance. The parameters for the final simulations in Chapter 7 with different burial depths and relative densities were based on the results of these sensitivity analyses.

6.6.1. Segment Length

The base case segment length L was 0.5 m. To investigate the effect of different segment lengths, the base case simulations were conducted again with segment lengths of 0.1 m and 1 m. To compare the results of both simulations, Figure 6.16 and Figure 6.17 zoomed in at winch tension and curvature in the steady state. As expected, the results for a smaller segment length are smoother with fewer oscillations. The maximum winch tension for $L = 0.1$ m (and for $L = 0.5$ m) is significantly smaller than for $L = 1$ m but the average winch tension is similar. The periods of the winch tension oscillations are directly related to the segment length: for $L = 0.1$ m every $0.1/0.2 = 0.5$ seconds a node is mobilised and for $L = 1$ m this happens every $1/0.2 = 5$ seconds. This corresponds to a frequency of 2 Hz for $L = 0.1$ m and a frequency of 0.2 Hz for $L = 1$ m.

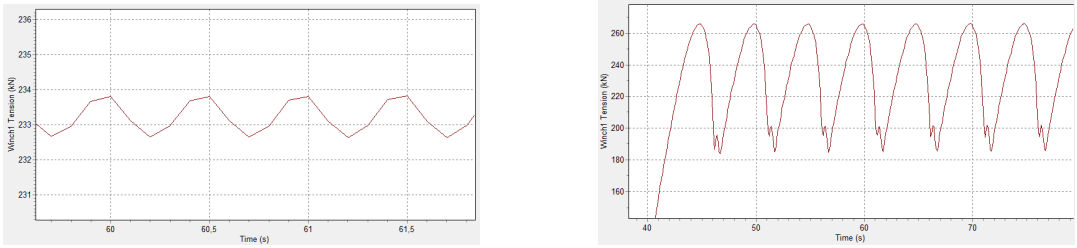

(a) Segment length = 0.1 m **(b)** Segment length = 1 m

Figure 6.16: Comparison of the steady-state winch tension for different segment lengths

Similar to what we saw with the winch tension, the maximum curvature is smaller for $L = 0.1$ m than for $L = 1$ m. For the cable curvature, the average value is also smaller for $L = 0.1$ m compared to $L = 1$ m and also slightly smaller compared to $L = 0.5$ m. The oscillations in curvature along the cable arc length are repeated every 0.1 m for $L = 0.1$ m and every 1 m for $L = 1$ m. The full results can be reviewed in Appendix C. With $L = 0.5$ m, the cable has only two segments per meter which could make it difficult to properly capture the cable curvature which has an order of magnitude of 0.5 1/m. Therefore, although tension differences between the simulations with $L = 0.5$ m and $L = 0.1$ m were small, it was decided to conduct the final simulations with $L = 0.1$ m.

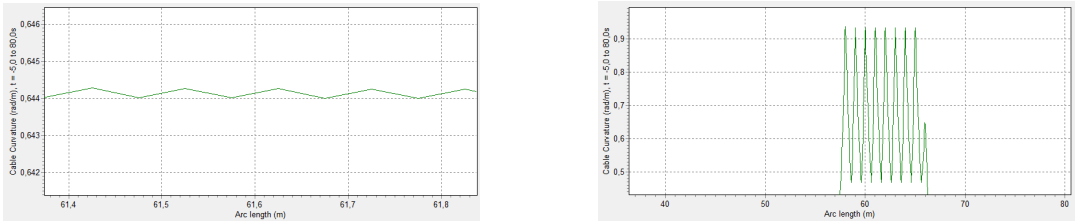

(a) Segment length = 0.1 m **(b)** Segment length = 1 m

Figure 6.17: Comparison of the steady-state cable curvature for different segment lengths

6.6.2. Time Step

The base case simulation used a time step of 0.01 s. To investigate the time step sensitivity, the base case simulation was repeated with time steps of 0.1 s and 0.001 s. For the smaller time step, more

detailed simulation results were expected for the winch tension since the external function would be able to adjust the soil resistance more precisely. To compare the results of both simulations, Figure 6.18 zoomed in at winch tension in the steady state for both simulations. The full results can be reviewed in Appendix C. As expected, applying the smaller time step gives a more detailed result with more small tension peaks. The frequency of the repeating oscillations pattern is 0.4 Hz corresponding to a period of 2.5 s for all time steps. Changing the time step does not result in significantly different minima or maxima of the winch tension. Since the computation time of the simulations decreased from around 10 minutes for a time step of 0.01 s to around 1 minute for a time step of 0.1 s, it was decided to conduct the simulations with a time step of 0.1 s instead of 0.01 s.

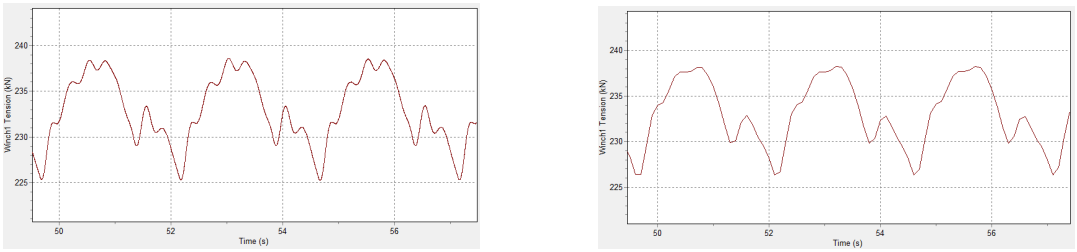

(a) Time step = 0.001 s

(b) Time step = 0.1 s

Figure 6.18: Comparison of the steady-state winch tension for different time steps

6.6.3. Dimensionless Velocity

The section on partially drained resistance in Chapter 5 explained how the uplift resistance depends on the dimensionless velocity $V = vD/c_v$. For infinite permeability, the coefficient of consolidation c_v would also be infinite [4]. With infinite permeability, the drainage regime is always fully drained. Therefore, the cable's peak uplift resistance should converge towards the fully drained value for large values of c_v and thus V. Increasing the dimensionless velocity with a factor of 100 in Figure 6.19 and with a factor of 10000 in Figure 6.20 shows how the peak uplift resistance converges towards the drained value for increasing permeability. In Appendix C it can be seen how the decreasing uplift resistance also results in less tension and curvature.

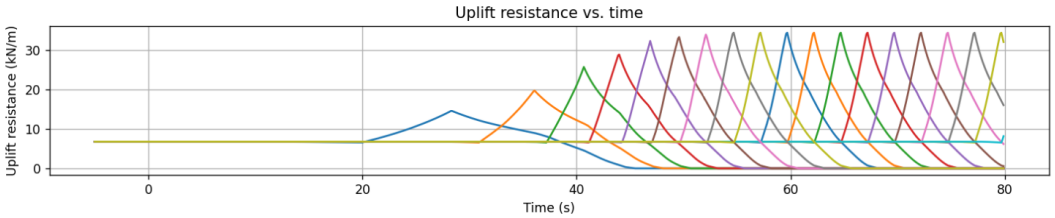

Figure 6.19: Resulting uplift resistance with c_v = 3e8 m^2/year

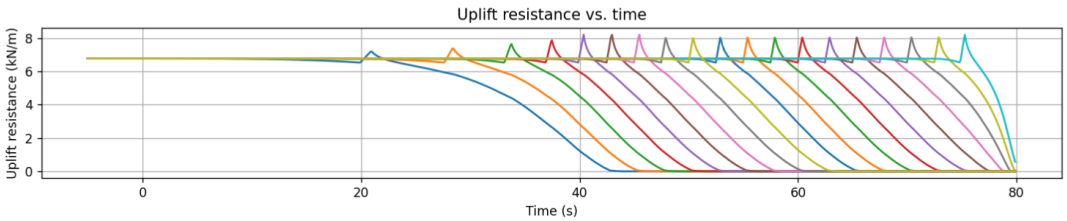

Figure 6.20: Resulting uplift resistance with c_v = 3e10 m^2/year

If innovations in cable handling methods and systems improve the limiting constraints on the cable recovery velocity, the pullout operation might be done at larger velocities than 0.2 m/s. As explained before, increasing the velocity also increases the partially undrained resistance, and thus the resulting winch and cable tension are also expected to increase. To investigate whether cable pullout could also be feasible with larger velocities, the base case was repeated with a vessel velocity of 2 m/s instead of 0.2 m/s. As can be seen in Figure 6.21, the tension did indeed increase with the larger velocity compared to Figure 6.13. However, the tension is still far below the critical limit of 900 kN. Therefore, for the base case simulation, the uplift resistance would not immediately be the limiting factor for increasing the pullout velocity under the assumed conditions. Due to the larger velocity the approximate steady state is reached faster than with a velocity of 0.2 m/s. The last node with an applied force has left the seabed already after less than 7 s which results in the steep drop in winch tension as seen in the figure below.

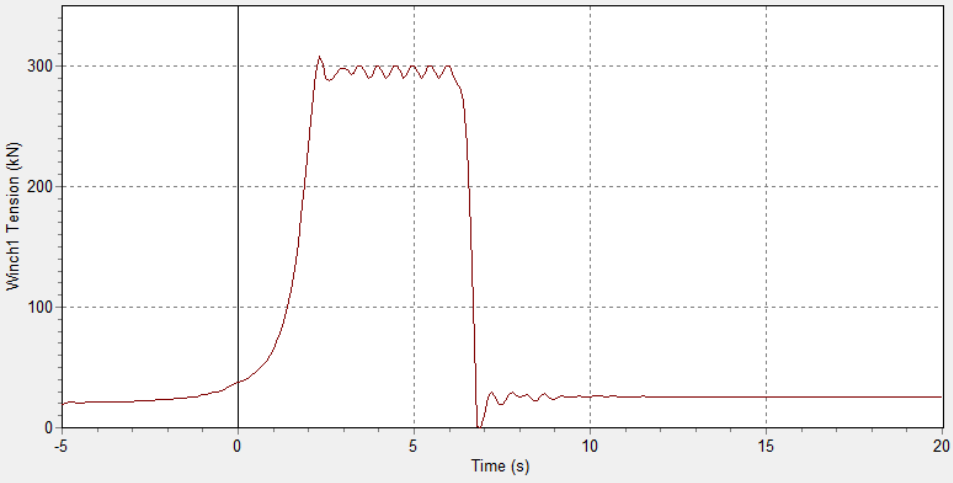

Figure 6.21: Time history graph of the winch tension for a vessel velocity of 2 m/s

7

Simulation Results and Discussion

With the decommissioning scenario as described in Chapter 4 and the OrcaFlex model with external Python functions introduced in Chapter 6 as input, the last step is to determine the actual limits of cable pullout. This chapter answers the final research question: For what burial depth and soil conditions is it possible to perform a cable pullout for a typical cable decommissioning scenario? With the parameters based on the results of the sensitivity analyses, OrcaFlex simulated the full range of burial depths and soil densities of the typical cable decommissioning scenario. This resulted in finding limiting combinations of relative densities and burial depths. The full set of resulting figures from the OrcaFlex simulations can be reviewed in Appendix D. The first section of this chapter shows how the results provided the values for the governing criteria of cable pullout for one particular simulation. The second section gives the total overview of the results compared to the governing criteria for all simulations. Finally, the implications of the underlying assumptions and their influence on the results are discussed.

7.1. Cable Pullout Results in Medium Dense Soil

Based on the sensitivity analyses the base case simulation as discussed in the previous chapter was improved by changing some of the parameters. For faster computation, the timestep was changed to 0.1 s instead of 0.01 s. In order to better capture the cable curvature, the segment length L changed to 0.1 m instead of 0.5 m. The latter increased the number of nodes with an applied force by a factor of five which resulted in more nodes being mobilized simultaneously, see also Figure 7.1. Since the uplift resistance was computed as force per meter, the resistance of each node did not change but the applied force per node decreased due to the smaller segment length.

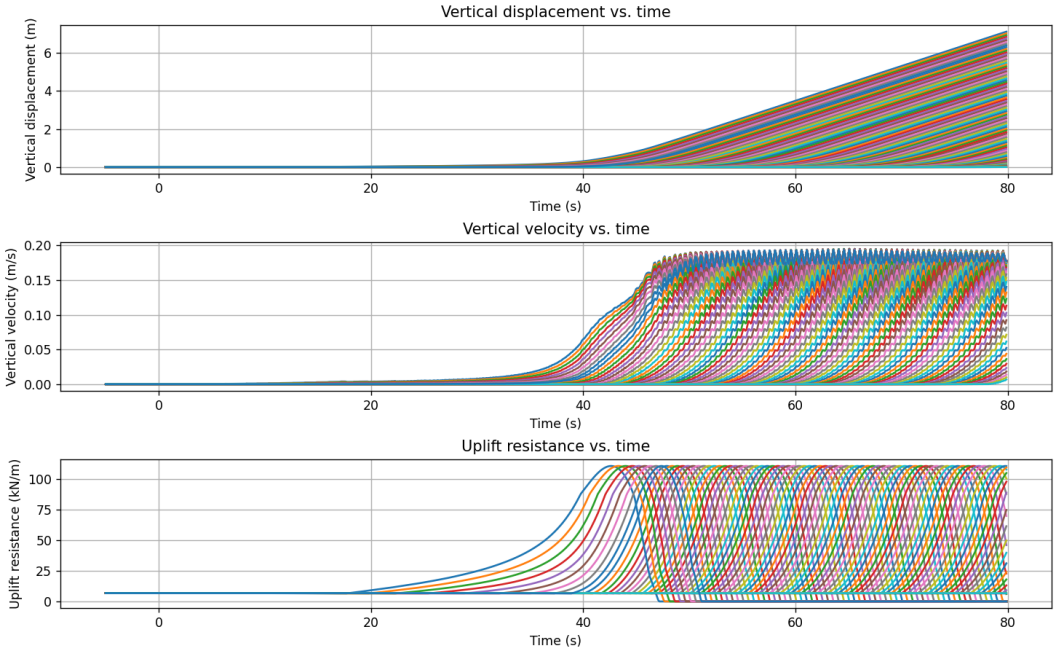

Figure 7.1: Resulting vertical displacement, velocity, and uplift resistance as computed by the external Python function for each node of the cable with $t = 0.1$ s, $L = 0.1$, $H_0 = 1$ m, and $I_D = 0.5$

The time history graph of the winch tension in Figure 7.2 also shows how the approximate steady state for this simulation scenario is reached after around 47 s. The maximum winch tension is 234 kN, far below the limit of 900 kN and thus the equipment criterion is not a problem for this cable pullout scenario without wind, waves or currents. The maximum cable tension is again equal to the maximum winch tension as shown in Figure 7.3. After reaching a steady state, the maximum curvature is 0.64 rad/m and therefore does not exceed the locking curvature of 1.01 rad/m, see also Figure 7.4. The winch tension oscillations occur with a period of 0.5 s. This period results from the vessel's velocity of 0.2 m/s and a segment length of 0.1 m: every $0.1/0.2 = 0.5$ s, a new node is mobilized. The segment length also determines the curvature pattern of the cable at the activated nodes, creating a small peak in curvature every 0.1 m along the cable.

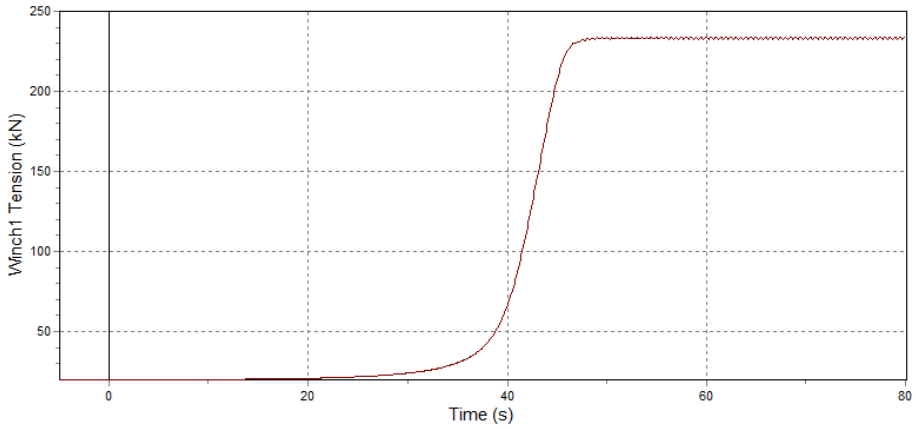

Figure 7.2: Time history graph of the winch tension with $t = 0.1$ s, $L = 0.1$, $H_0 = 1$ m, and $I_D = 0.5$

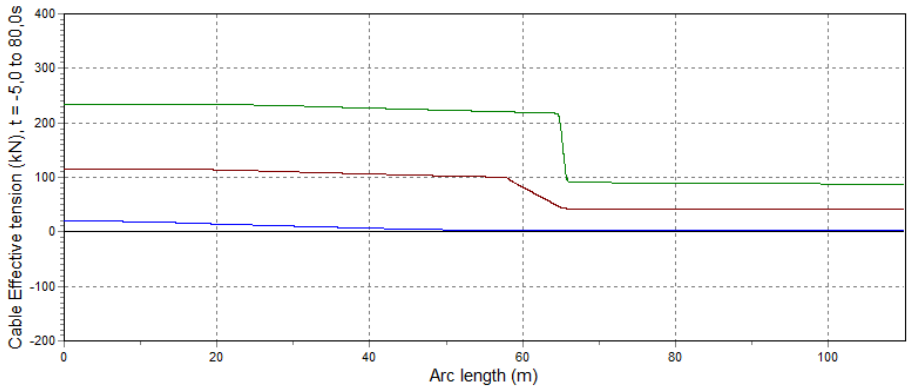

Figure 7.3: Range graph of the cable tension with blue as minimum, red as mean, and green as maximum tension

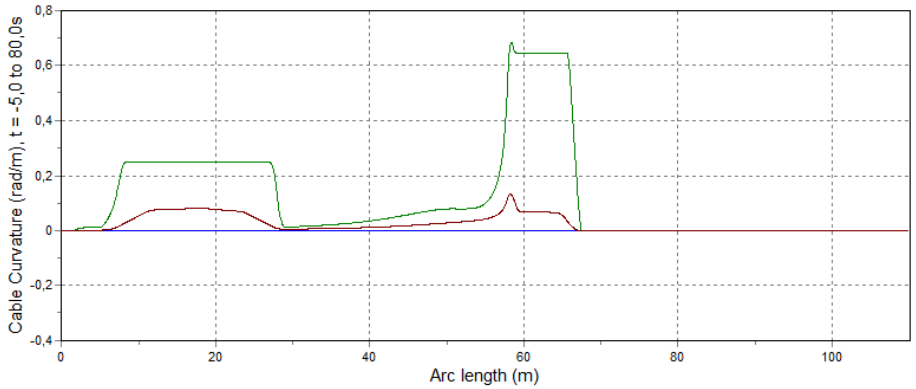

Figure 7.4: Range graph of the cable curvature with blue as minimum, red as mean, and green as maximum curvature

It is also interesting to see how many nodes are being pulled out of the seabed at the same time. Since nodes are mobilised one by one, the first node has already left the seabed once the final node starts to move. According to Figure 7.1, there are around 20-25 nodes simultaneously experiencing a partially undrained uplift resistance, of which the first nodes are already very close to leaving the seabed. This means that with a segment length of 0.1 m, only around 2-2.5 m of the cable is actively being pulled out in the steady state. This is valuable information to consider in case other decommissioning methods, such as jetting, are required to recover the cable. When only 2.5 m of the cable is pulled out of the seabed, it is beneficial to fluidise the soil in this 2.5 m range. However, fluidising along the cable further than 2.5 m away from the touchdown point does not contribute much to the operation.

7.2. Varying Burial Depth and Relative Density

With a segment length of 0.1 m, a vessel velocity of 0.2 m/s and a time step of 0.1 s, a set of simulations was carried out to determine the limiting combinations of burial depth and relative densities for the typical cable decommissioning scenario described earlier in Chapter 4. For the burial depth, a range between 1 m and 4 m was taken. Regarding the soil density, medium and dense sand were assumed with relative densities of 0.5 and 0.8 respectively. The full results are presented in the same manner as the results for the simulation above. These results can be reviewed in Appendix D. These graphs show for example that the steady state is reached later for increasing burial depth. This is due to the larger necessary displacement of the first nodes to leave the seabed. The results are summarised in the table below. The maximum cable tension was equal to the maximum winch tension for all simulations. As expected, tensions increase for both increasing burial depth and increasing relative density. The limitations of the results due to the underlying assumptions are discussed in the next section.

Burial Depth (m)	1	1.5	2	3	4	1	1.5	2
Relative Density (-)	0.5	0.5	0.5	0.5	0.5	0.8	0.8	0.8
Max Winch Tension (kN)	234	410	592	961	1350	471	829	1193
Max Cable Tension (kN)	234	410	592	961	1350	471	829	1193
Max Cable Curvature (1/m)	0.64	0.67	0.70	0.72	0.75	0.68	0.71	0.74

Table 7.1: Resulting tensions and curvatures for different combinations of burial depth and relative density

The maximum winch tension increased for both increasing burial depth and increasing relative density, see also Figure 7.5. The maximum winch tension strongly depends on both the burial depth and the relative density. With constant relative density, the maximum tension increase seems almost linear versus the burial depth. This can be explained by the fact that during the pullout, the local failure mode is most of the time dominant for burial depths over 1 m, which results in a constant peak undrained uplift resistance, see also Figure 5.7. Therefore, the total tension increase largely depends on the number of nodes mobilized at the same time, which scales approximately linearly with the burial depth.

For medium dense sand with a relative density of 0.5, a burial depth of 3 m results in a winch tension of 961 kN, which means that the assumed tensioner capacity of 900 kN is not enough to perform the cable pullout. In theory, a tensioner with a capacity of up to 1000 kN could be designed to decommission cables in medium dense sand with burial depths of around 3 m. However, once the burial depth is 4 m, the cable tension is so large that a pullout operation would result in breaking the cable. For dense sands with a relative density of 0.8, the winch tension is already 1193 kN for a burial depth of 2 m. Therefore, to perform a cable pullout in dense sands, the burial depth should not be much more than 1.5 m. Because the limit was already reached, the simulations for burial depths of 3 m and 4 m were not conducted. It is important to note that these results were obtained assuming zero waves, currents, and wind. For example, wave-induced heave motions of the vessel could result in cable snatching which affects the workability. Cable snatching entails that the cable becomes slack and has little tension during downward heave motion and then suddenly becomes very tight with a peak in tension with upward heave. The forces might then exceed the cable-breaking load or the equipment capacity for lower burial depths than discussed above.

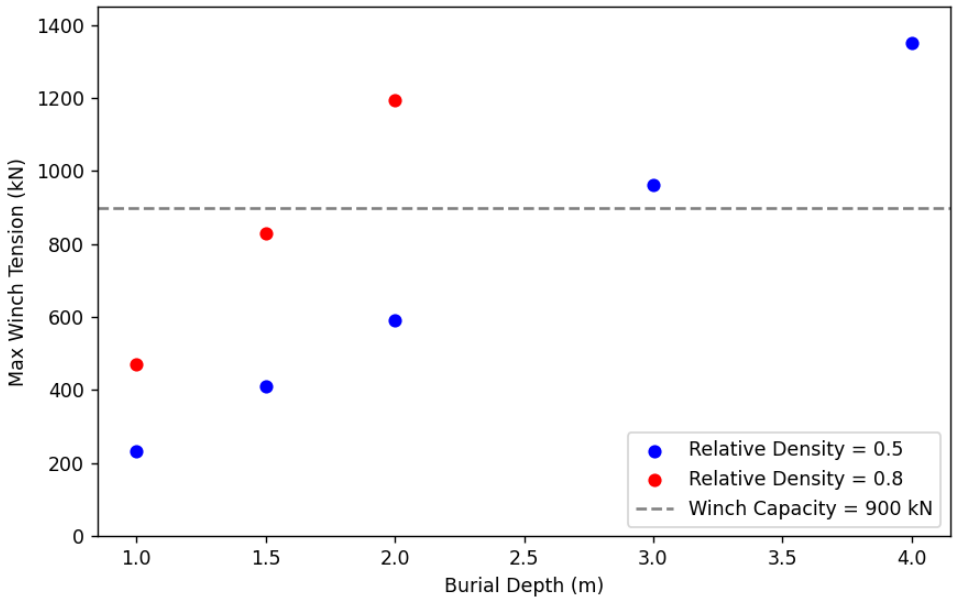

Figure 7.5: Maximum winch tension vs burial depth for medium and dense sand

Fortunately, the cable curvature does not reach the locking curvature for any of the simulations performed, as shown in Figure 7.6. The cable curvature was expected to follow the same pattern as the

tension, with increasing curvature for increasing burial depth and relative density. This is indeed the case but the curvature increase is relatively small with the smallest curvature equal to 0.64 1/m and the largest curvature equal to 0.74 1/m. It might be possible that the cable is also being straightened by the increasing tension in the cable itself hence limiting the increase in curvature. During cable pullout more curvature of the cable results in a sharper pullout angle and thus less simultaneously mobilized soil resistance. It would hence be favourable to minimize the bending stiffness of a cable in the context of soil resistance against cable pullout.

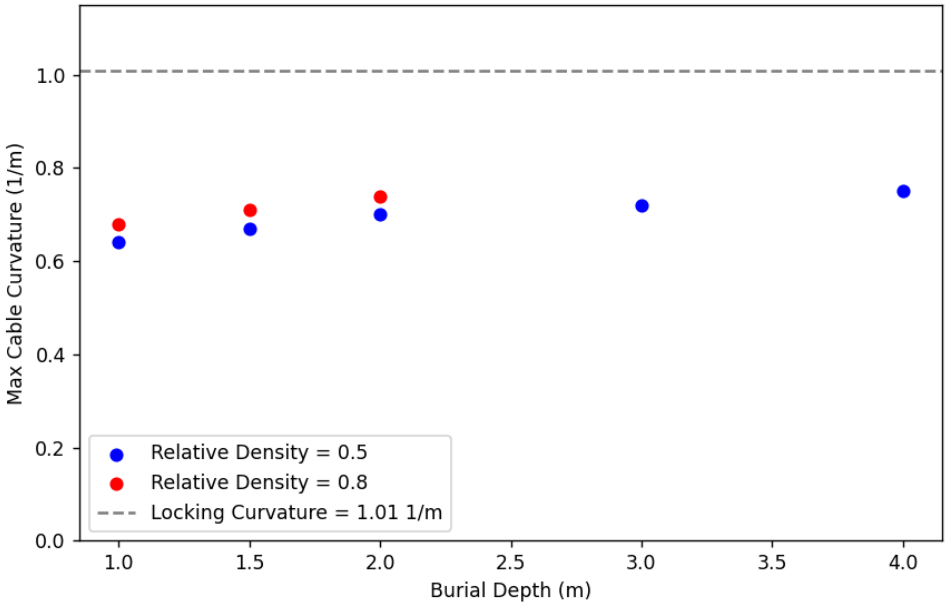

Figure 7.6: Maximum cable curvature vs burial depth for medium and dense sand

7.3. Assumption Implications

As was explained in Chapter 6, modelling the cable pullout operation in OrcaFlex is not straightforward and comes with a set of assumptions. This is especially due to the complex cable-soil interaction. Therefore, it is important to experiment with different ways of modelling soil behaviour and to also conduct physical experiments. The assumptions made in the OrcaFlex cable pullout simulations significantly simplify the complex interactions between the cable and the seabed. While these assumptions provide a manageable starting point for modelling, they also limit the accuracy and applicability of the results. The thesis would benefit from more validation of the simulation results. Unfortunately, there are no real-world data or case studies to validate the findings from the OrcaFlex simulations yet. However, the results were in line with industry experts who stated that pullout should be possible up to around 1.5 m burial depth (Andersen, 15-11-2023).

Each assumption has its implications and considerations for the accuracy and applicability of the model. Firstly, the simulations were conducted without accounting for waves, currents, and wind. This assumption simplifies the model by eliminating dynamic environmental forces that can significantly impact cable behaviour during the pullout. In reality, these forces can induce additional stresses and strains on the cable, potentially affecting the pullout efficiency and the cable's structural integrity. The absence of environmental forces may lead to an underestimation of the actual resistance and forces encountered during pullout. However, waves could also be useful to increase the pulling capacity during the upward movement of the vessel.

Secondly, the model assumes a continuous vertical uplift with horizontal cable segments, similar to the pipeline experiments of Bransby and Ireland instead of pulling out the cable under an angle [4]. This assumption partly neglects the curvature and potential bending moments of the cable, simplifying the soil resistance to a purely downward force. This results in a conservative prediction of the actual

soil resistance because less soil would be mobilized in reality. Incorporating the curvature effects would provide a more realistic assessment of soil-cable interactions. For a discontinuous instead of a continuous cable pullout, the soil model would probably underestimate the uplift resistance for cable nodes that stand still after initial movement due to the time-dependent drainage.

The model also neglects hysteresis during pullout velocity oscillations and assumes that the downward movement of the cable during the pullout does not mobilize any upward-facing soil resistance. This assumption simplifies the model by ignoring the complex behaviour of soil resistance during cyclic loading and unloading (hysteresis). Neglecting hysteresis can result in an oversimplified model that doesn't capture the energy dissipation and potential changes in soil resistance over time. Including hysteresis effects could improve the accuracy of the soil resistance predictions.

Furthermore, the model keeps all input variables, such as burial depth, relative density, and vessel velocity, constant. The seabed is assumed to be flat with constant water depth, and the backfill material is assumed to have infinite width. By keeping these variables constant, the model ignores variations in seabed topography and soil conditions that can affect cable pullout. Real-world scenarios always involve variable conditions, for example, the burial depth could change a lot along the route due to mobile seabeds. Incorporating these variations would provide a more comprehensive understanding of the challenges and feasibility of cable pullout operations under different conditions. Varying the water depth instead of keeping it constant could affect the results in two ways. Firstly, increasing water depths give increasing cable lengths in the water column, resulting in more tension. However, the tension is significantly more dependent on the burial depth and relative density than on water depth. Secondly, taking cavitation into account could potentially make the undrained uplift resistance calculation more accurate and less conservative for shallow water. By assuming an infinite width of the backfill material, a potential influence of adjacent virgin material is neglected. As was explained in Chapter 4, the virgin material is most likely more dense and could increase the soil resistance.

The sandy soil is assumed to be purely non-cohesive sand, which simplifies the soil model but ignores the presence of other soil types, such as clay, which have different resistance properties. In reality, the soil exists seldom of purely non-cohesive sediments. Including different soil types would enhance the model's applicability to various seabed conditions, providing more generalizable results for different offshore locations.

A vertical slip failure mechanism is assumed for fully drained conditions. This assumption simplifies the failure mechanism to a vertical slip, ignoring potential lateral or rotational failures that could occur. Fixed values for soil properties, such as submerged weight, coefficient of consolidation, crushing strength, and friction angle, provide a baseline for simulations but may not reflect site-specific conditions. Conducting site-specific geotechnical surveys to obtain accurate soil properties would improve the precision of the model. Sensitivity analyses could also be conducted to understand the impact of varying these parameters.

The model assumes that the initial undrained resistance converges with time towards the drained value following a typical consolidation curve. This simplifies the consolidation process, potentially overlooking intermediate stages of soil behaviour. More detailed modelling of the consolidation process, including intermediate stages, would enhance the accuracy of the soil resistance predictions during different phases of the pullout operation.

A mobilisation distance of $0.1\,H_0$ and a linear soil spring stiffness are assumed. This provides a simplified representation of soil resistance mobilization. However, soil resistance is often nonlinear and can vary significantly with displacement. Besides, the actual mobilisation distance is uncertain. Incorporating a more detailed soil spring model that accounts for nonlinearity and variable stiffness would provide more accurate resistance predictions.

Regarding the cable properties, the breaking load is assumed to be a combination of the tensile strength of both the armour and the conductor. The cable-soil interaction is assumed to be similar to the pipe-soil interaction, and the bending stiffness is assumed to be linear. These assumptions simplify the model but may not fully capture the unique characteristics of cable behaviour. More detailed modelling of cable properties, including nonlinear bending stiffness and specific cable-soil interaction mechanisms,

would improve the accuracy of the simulations.

Finally, operational constraints limit the maximal vessel and pullout velocity to 0.2 m/s. A stern-side chute with a radius of 4 m is used, and a maximal tensioner capacity of 90 tons or 900 kN is assumed based on NKT Victoria's equipment. These constraints are realistic for current operations but exploring the impact of varying these operational parameters could provide insights into optimizing the pullout process and identifying potential improvements in equipment design and operation strategies. This would enable larger pullout velocities and thus a faster decommissioning operation.

8

Conclusion

It is concluded that the industry is currently not taking decommissioning into account sufficiently during the design and installation of offshore wind export cables for several reasons. In Chapter 1 the legal exceptions for leaving cables in situ, environmental concerns, and the unfavourable business case explained the limited experience with export cable decommissioning. This limited experience is also partly because most export cables have been installed recently. Another reason for the low priority given to cable decommissioning is the lack of existing literature or industry guidelines. This makes it hard for cable design and installation companies to consider decommissioning in the early development stages of export cable projects. This research aimed to contribute to a more sustainable and circular offshore wind industry. To achieve this, the literature study identified critical knowledge gaps regarding decommissioning offshore cables. Investigating the limits of cable pullout was deemed the most relevant and suitable knowledge gap to address. The second phase of this research, the thesis project, focused on increasing the understanding of the limits of cable pullout as a decommissioning method for offshore wind export cables. The research objective was defined as:

"*Determine the limits and constraints on burial depth and soil conditions for cable pullout of an offshore wind export cable buried in sandy soil in the North Sea.*"

The short conclusion to this research objective is that for a medium dense soil with a relative density of 0.5, cable pullout would be possible up to a burial depth of around 3 m based on the developed OrcaFlex model with the external Python functions to compute the soil resistance. For dense soil with a relative density of 0.8, cable pullout would be possible up to a burial depth of around 1.5 m. However, this conclusion is bound to the limitations of the underlying assumptions of the OrcaFlex model and the decommissioning scenario as discussed in Chapter 7. For example, by assuming a completely flat sea, potential effects from waves, currents, and wind were not included.

To arrive at this final conclusion to the research objective, the study was guided by several research questions. The first research question was: What are the characteristics of out-of-service offshore wind power cables? This question was addressed in Chapter 2 where a comprehensive overview of subsea cable applications, elements, and protection measures was provided. The chapter detailed the various types of subsea cables used in the offshore wind industry, their construction, and the significance of their components, such as conductors and armour. Understanding these characteristics is essential as they directly impact the decommissioning process and the feasibility of different decommissioning methods.

The second research question asked: What are the state-of-the-art methods for offshore cable decommissioning and their respective limitations? Chapter 3 delved into the existing decommissioning techniques, including jetting, mass flow excavation, and dredging. The analysis highlighted the environmental and economic impacts of these methods. It was also valuable to compare cable decommissioning to cable installation and repair procedures. Since a cable pullout would be the cheapest and most

environmentally friendly decommissioning option, it is optimal to apply this method to the cable route as much as possible. The burial depth and the soil type usually influence this method's feasibility. However, the exact limits are not clearly defined, leaving a critical knowledge gap. Therefore, at this point, it was decided to focus on modelling the cable pullout operation.

The third research question was: What is a typical offshore wind power cable decommissioning scenario in the Dutch-German part of the North Sea? This scenario was outlined in Chapter 4, where specific conditions such as burial depth, soil characteristics and bathymetry were considered. The 525 kV export cable was also introduced here. The chapter provided a detailed case study that formed the basis for the simulation studies conducted using the OrcaFlex software. This typical scenario helped in understanding the practical challenges and requirements for decommissioning cables in this region. This chapter also covered the fourth research question: What are the governing criteria for cable pullout in such a decommissioning scenario? The maximum allowable tension and the minimum bending radius were introduced as the governing criteria for the cable pullout. The environmental operability was out of the scope of the current research. In Chapter 6, the tensioner capacity was added to the governing criteria to account for the maximum pull capacity during decommissioning.

In Chapter 5 the fifth research question was investigated: How do the burial depth and soil conditions influence the resistance forces during cable pullout? This chapter introduced a comprehensive soil model to calculate the resistance forces that need to be overcome during the cable pullout process. The study found that both burial depth and soil relative density are critical factors that significantly affect the resistance encountered during decommissioning. Specifically, as burial depth increases, the resistance force also increases, making cable pullout more challenging. Similarly, higher soil densities result in greater resistance forces. The model includes scenarios for fully drained, fully undrained, and partially drained uplift resistance, implemented in a Python script to simulate real-time resistance during pullout operations.

The sixth research question asked: How can a dynamic model simulate the recovery of a buried offshore cable? This was addressed through the development and validation of a model using the OrcaFlex software, as detailed in Chapter 6. The chapter described how the model was constructed to simulate the mechanical response of the cable during recovery operations, integrating external Python functions to compute real-time soil resistance. This modelling approach allowed for the simulation of cable pullout, considering various operational parameters and environmental conditions. The OrcaFlex simulations provided valuable insights into the mechanical behaviour of cables under different decommissioning scenarios, demonstrating the feasibility of using dynamic models to predict and optimize cable recovery processes.

The final research question was: For what burial depth and soil conditions is it possible to perform a cable pullout for a typical cable decommissioning scenario? This was explored through a series of simulations presented in Chapter 7. The results indicated that the feasibility of cable pullout depends heavily on the burial depth and soil conditions. The findings emphasize the importance of considering both burial depth and soil characteristics during the design and installation stages to ensure that future decommissioning can be carried out efficiently and effectively. The current ongoing research could contribute to determining optimal cable decommissioning methods for projects in the near future, but also for long-term projects. When the limits of cable pullout and other decommissioning methods are better understood, decommissioning could be considered more easily. This could result in optimised 'cable design for decommissioning' and 'cable installation for decommissioning'.

9

Recommendations

Based on the conducted literature review and the interviews with industry experts, there were some recommendations for research into other knowledge gaps related to decommissioning export cables:

- Since the subsea infrastructure is getting increasingly entangled and at the same time the cable lifetime is usually way longer than the wind farm lifetime, it seems like a waste of resources to remove expensive export cables. If these cables are still fully functional, it could be interesting to reuse this infrastructure. Reusing has many limitations but could be interesting for example for innovation projects for floating solar or wave energy converters.
- There seem to be possibilities for the optimization of cable design regarding decommissioning but also regarding recycling. With the layered cables, it is a complex operation to split the different layer materials to be able to recycle them.
- In case deburial is necessary, it is important to determine the optimal deburial method. The modelling of deburial operations is left out of the current research scope but is of course relevant to cable decommissioning.
- Another deburial-related question is whether deburial and pullout should be done simultaneously or as two separate operations. When conducted simultaneously, the safe distance between the touchdown point and detrenchers or other deburial devices has to be investigated.
- The minimum required burial depth is a parameter that largely affects cable decommissioning. The trade-off between better cable protection and more difficult cable decommissioning should be more clear than it is today. To properly define this trade-off it is also important to have a proper understanding and statistical overview of the reasons for cable failure.
- Lastly it is important to be able to improve prediction models on mobile seabeds. For example, sand waves can increase the depth of cover of a buried cable considerably and make it hard to decommission such cable sections.

As was stressed before, modelling of the cable pullout in OrcaFlex required many assumptions. Therefore, it would be valuable to conduct further research in the following directions:

- Proposing and conducting physical experiments is crucial to gather empirical data. This data would validate OrcaFlex results and refine the inputs to the external soil resistance function, ensuring that the simulations reflect real-world conditions more accurately.
- More detailed soil modelling using tools like PLAXIS is also necessary. The current models may oversimplify soil behaviour, and a more nuanced approach could provide better predictions of soil resistance during cable pullout. For example, more certainty on the mobilisation distance is required. Additionally, different soil types, such as clay, should be considered to broaden the applicability of the findings.

- Investigating the effects of different water depths on the cable pullout process is critical as well. Different depths could significantly alter the mechanical and hydrodynamic forces acting on the cable, affecting the feasibility and strategy of the pullout operation. Including cavitation effects in the undrained uplift resistance calculations could lead to more accurate and less conservative estimates, particularly for shallow water depths.
- The inclusion of environmental factors such as waves, currents, and wind in the simulations is important. While these factors could increase pull capacity, they also pose the risk of cable breakage. A thorough analysis of these dynamics is needed to establish safe operational limits. OrcaFlex is a useful tool for doing these analyses and therefore this future research could profit from the fact that the current research used OrcaFlex already.
- Further research should examine the uplift resistance factor for soil cover ratios larger than 8.0 and develop a local failure model for drained conditions. Current models may not accurately reflect the complexities involved in high soil cover scenarios which probably resulted in too conservative results.
- The bending stiffness of the cable significantly affects soil mobilisation and resistance. Research should investigate how varying stiffness influences the ease of vertical pullout and overall decommissioning efficiency.
- The effects of soil fluidisation techniques, such as jetting, should be integrated into simulations. This would help in understanding how these techniques can facilitate or complicate the cable pullout process. Additional methods could extend the feasibility of cable decommissioning to larger burial depths.
- Cables are often dirty and damaged, which can significantly influence tensioner performance. Understanding how these factors affect the decommissioning process is vital for developing more robust and reliable methods.
- Determining the optimal depths at which it is more practical to leave cables in situ rather than pulling them out is necessary. This decision involves balancing environmental impact, cost, and technical feasibility. Identifying the circumstances under which cable pullout presents a viable business case is crucial. Economic analysis should consider factors like scrap value, operational costs, and potential environmental penalties.

By addressing these recommendations, future research could significantly advance the understanding and practices related to the decommissioning of offshore wind power cables, ensuring that the industry is better prepared for the challenges ahead.

References

[1] American Petroleum Institute. *API 17J Specifications for unbonded flexible pipe*. Tech. rep. 2008.

[2] M. Ardelean and P. Minnebo. *HVDC Submarine Power Cables in the World*. Tech. rep. 2015. DOI: 10.2790/95735.

[3] M. D. Bolton. "The strength and dilatancy of sands". In: *Geotechnique* 36.1 (Mar. 1986), pp. 65–78. ISSN: 17517656. DOI: 10.1680/geot.1986.36.1.65.

[4] Mark Fraser Bransby and Jamie Ireland. "Rate effects during pipeline upheaval buckling in sand". In: *Proceedings of the Institution of Civil Engineers: Geotechnical Engineering* 162.5 (Oct. 2009), pp. 247–256. ISSN: 13532618. DOI: 10.1680/geng.2009.162.5.247.

[5] Carbon Trust. *Cable Burial Risk Assessment Methodology*. Tech. rep. 2015.

[6] Santiram Chatterjee, David J. White, and Mark F. Randolph. "Coupled consolidation analysis of pipe-soil interactions". In: *Canadian Geotechnical Journal* 50.6 (June 2013), pp. 609–619. ISSN: 00083674. DOI: 10.1139/cgj-2012-0307.

[7] DNV AS. *DNV ENERGY TRANSITION OUTLOOK 2023*. Tech. rep. 2023.

[8] DNV AS. *Recommended practice — DNV-RP-0360 Subsea power cables in shallow water*. Tech. rep. 2016. URL: www.dnvgl.com..

[9] DNV AS. *Recommended practice — DNV-RP-F114 Pipe-soil interaction for submarine pipelines*. Tech. rep. 2021.

[10] DNV AS. *Standard — DNV-ST-0359 Subsea power cables for wind power plants*. Tech. rep. 2016.

[11] Sören Ehlers et al. "Experimental and numerical investigations of the ultimate strength of two subsea power-transmission cables". In: *Marine Structures* 88 (Mar. 2023). ISSN: 09518339. DOI: 10.1016/j.marstruc.2022.103346.

[12] ESCA. *ESCA Guideline No.14 Power Cable Installation*. Tech. rep. 2018.

[13] ESCA. *ESCA Guideline No.15 Power and Renewable Energy Cable Repair Guidelines*. Tech. rep. 2023.

[14] Dag Fergestad et al. *Handbook on design and operation of flexible pipes*. 2017. ISBN: 9788271742850.

[15] Global Wind Energy Council (GWEC). *GLOBAL WIND REPORT 2023*. Tech. rep. 2023.

[16] Øystein Hestad and John Olav Tande. *"Hybrid cables" explained*. Apr. 2022. URL: https://blog.sintef.com/sintefenergy/hybrid-cables-explained/.

[17] Meng Chang Hsieh et al. "Determining optimal number of cores in a submarine power cable". In: *International Journal of Naval Architecture and Ocean Engineering* 14 (Jan. 2022), p. 100463. ISSN: 2092-6782. DOI: 10.1016/J.IJNAOE.2022.100463.

[18] ICPC. *Management of Decommissioned and Out-of-Service Cables*. Tech. rep. 2020. URL: http://www.iscpc.org.

[19] Peter Kopas et al. "A Plastic Strain and Stress Analysis of Bending and Torsion Fatigue Specimens in the Low-cycle Fatigue Region Using the Finite Element Methods". In: *Procedia Engineering*. Vol. 177. Elsevier Ltd, 2017, pp. 526–531. DOI: 10.1016/j.proeng.2017.02.256.

[20] NKT. *Simultaneously bundled DC cables*. URL: https://www.nkt.com/products-solutions/high-voltage-cable-solutions/installation/offshore-installation.

[21] Offshore Magazine. *Rotech completes trenching, cable cut and recovery at offshore wind farm*. Jan. 2023. URL: https://www.offshore-mag.com/subsea/article/14288662/rotech-completes-trenching-cable-cut-and-recovery-at-offshore-wind-farm.

[22] L Okkerstrøm, O T Gudmestad, and E Pedersen. "Simulation of Peak Tension Loads in Subsea Power Cables during Installation (2021 IOP Conf. Ser.: Mater Sci Eng. 1201 012010)". In: *IOP Conference Series: Materials Science and Engineering* 1201.1 (Nov. 2021), p. 012089. ISSN: 1757-8981. DOI: 10.1088/1757-899x/1201/1/012089.

[23] Orcina. *OrcaFlex Manual Version 11.4a*. 2023. URL: https://www.orcina.com/webhelp/OrcaFlex/.

[24] OSPAR Commission. *Background Document on potential problems associated with power cables other than those for oil and gas activities*. Tech. rep. 2008.

[25] Ove Arup & Partners Ltd. *Review of Approaches and Costs of Decommissioning OffshoreWind Installations*. Tech. rep. 2018.

[26] T.A. Powell et al. "In-situ testing in trench backfill: Evidence of evolving backfill density". In: (2023).

[27] Ahmed M. Reda et al. "Compression limit state of HVAC submarine cables". In: *Applied Ocean Research* 56 (Mar. 2016), pp. 12–34. ISSN: 01411187. DOI: 10.1016/j.apor.2016.01.002.

[28] Svein Sævik. *Lecture Notes in Offshore Pipeline Technology*. Feb. 2017.

[29] Svein Sævik. *Lecture Slides TMR 4225 Flexible Pipes and Cables*. 2023.

[30] Bastien Taormina et al. *A review of potential impacts of submarine power cables on the marine environment: Knowledge gaps, recommendations and future directions*. Nov. 2018. DOI: 10.1016/j.rser.2018.07.026.

[31] Tennet. *About Tennet*. URL: https://www.tennet.eu/nl.

[32] Tennet. *The 2GW Program*. URL: https://www.tennet.eu/about-tennet/innovations/2gw-program.

[33] NI Thusyanthan et al. "Uplift Resistance of Buried Pipelines and DNV-RP-F110 Guidelines". In: *Proc. Offshore Pipeline Tech. Conf.* (2010).

[34] Eva Topham et al. "Challenges of decommissioning offshore wind farms: Overview of the European experience". In: *Journal of Physics: Conference Series*. Vol. 1222. 1. Institute of Physics Publishing, May 2019. DOI: 10.1088/1742-6596/1222/1/012035.

[35] Weiwang Wang et al. *Failure of submarine cables used in high-voltage power transmission: Characteristics, mechanisms, key issues and prospects*. May 2021. DOI: 10.1049/gtd2.12117.

[36] D White et al. "Free fall penetrometer tests in sand: Determining the equivalent static resistance". In: (2018).

[37] Thomas Worzyk. *Submarine Power Cables: Design, Installation, Repair, Environmental Aspects*. Vol. 39. 2009. ISBN: 9783642012693. DOI: 10.1007/978-3-642-01270-9.

A

Expert Interviews

The interviews with experts both within and outside of NKT gave valuable practical insights into the subsea cable industry and provided an overview of the current knowledge regarding cable decommissioning. I am thankful for all the friendly experts who were willing to share their experiences and ideas to improve the research and to go further than the scarce literature. Most interviews focused on technical and engineering aspects with some exceptions to also get an understanding of the legal, environmental, and economic context. This appendix sums up the main takeaways from all the interviews. An overview of the interviewees is given in Table A.1 below.

Name	Company	Function	Date
E. Impola	NKT	Senior Installation Manager	25/09/2023
R. Oor	NKT	Senior Marine Engineer	28/09/2023
J. Zheng-Lu	NKT	Offshore Project Engineer	29/09/2023
W. Snip	Primo Marine	Subsea Power Cable Consultant	02/10/2023
R. Andersen (1/2)	JD-Contractors	Chief Executive Officer	03/10/2023
M. Smalt	NKT	Commercial & Tender Manager	04/10/2023
J. Aas	Oceans5	Marine Operations Manager	05/10/2023
E. Heemrood	NKT	Project Installation Manager	12/10/2023
I. Buchan	NKT	Environmental Advisor	27/10/2023
R. Andersen (2/2)	JD-Contractors	Chief Executive Officer	15/11/2023
F. Bodesund	NKT	Senior Analysis Engineer	16/11/2023

Table A.1: Overview of expert interviews

A.1. Interview with Senior Installation Manager E. Impola

Company: NKT

Date: 25/09/2023

Focus: Technical perspective

Main takeaways:

• Near shore it is very difficult to decommission cables mainly due to the shallow water (< 10 m) which denies access to the large vessels. Next, the environmental impact would be relatively large. The burial depth is usually at least 1.5 m and no more than 8 m in the near-shore region.

• The interviewee has not heard of large-scale cable decommissioning projects at NKT. There are not many big cables that are out of service yet. It is expected that most of them will be left at the seabed

after their service time unless they are pipe-covered or can be extracted without touching the soil in another way.

• Wet storage of cable ends is a bit like decommissioning since a shallow buried cable will be retrieved later. However, burial depths are usually around 0.5 m which is less than for a typical offshore power cable that has to be decommissioned. Therefore the forces on the buried cable are way smaller in the case of wet storage.

• Reusing long DC export cables will be difficult since they are usually tailored to specific site parameters. Inter-array cables are shorter and therefore reusing makes more sense but it is still a serious challenge. The integrity of an offshore power cable is very important since unpredictable fixes are very complicated and expensive. Therefore the risks involved with reusing are high while the costs of retrieving the cables in a good state are also high.

• Hence, it is likely the decommissioned cable goes as scrap metal to a recycling company (e.g. Stena) instead of being reused. The requirements for scrap metal are low and thus the pull force on the cable can be far above the cable limit. This most probably increases the productivity and lowers the decommissioning costs.

• The economic goal is to decommission as much cable as possible in a minimal time. The two most important parameters here are 1) the time it takes to get the cable out of the water and 2) the time it takes to unload and deliver the cable to the recycling company. Both should be conducted in a safe manner and as quickly as possible. It could be interesting to discuss with a recycling company how to unload the cable efficiently.

A.2. Interview with Senior Marine Engineer R. Oor

Company: NKT

Date: 28/09/2023

Focus: Technical perspective

Main takeaways:

• With the Øresund project four power cables between Denmark and Sweden have been decommissioned. The big challenge of this project was the fact that the power grid had to be disconnected, resulting in a lot of time pressure. The four cables were 40 years old and oil filled which made the project even more difficult. Deburial was doable but when the cable pulling started, the cables failed because the armoured wires lost their strength.

• Another project was done using a relatively cheap pontoon without a turntable (20-30K per day). The cables were cut into pieces instead of keeping them together. It could be interesting to see whether inter-array cables can be decommissioned using a cheaper vessel.

• For the current research, it makes sense to leave the old-fashioned oil-filled cables out of the scope. Decommissioning oil-filled cables requires different methods due to the risk of environmental hazards. Besides, already 95% of the market is covered without taking oil-filled cables into account.

• A decommissioning project would entail three phases:

1. Deburial of the cable (at least at the start to connect to the cable), this would be the biggest engineering challenge

2. Connecting to the cable, the easiest option is using a diver but the industry prefers ROVs due to safety concerns

3. Pulling (and cutting) the cable, a relatively straightforward process

• The burial depth is increasing while the soil is also often harder, for example in clay soils. The reasons

are that the 'easy' spots are almost gone and that the industry has learned that the seabed mobility sometimes requires reburial.

• Deburial in shallow water can probably be done using MFE if necessary.

• Decommissioning the cables is probably more expensive than the income from recycling the materials. Therefore OWF owners may recommend the government to keep the cables in place.

• The amount of cables and other infrastructure in the North Sea is increasing fast. The seafloor will be congested soon if we don't decommission the offshore power cables. It already happens that NKT encounters out-of-service cables. Usually, they are only partly removed by making two cuts so the new cable can cross.

• A nice tool for deburial is a ring with water jets that you can lower down along the cable. The jets can fluidize the seabed right at the next spot of the buried cable.

• It is important to keep control of the operation. With pure pulling, there are more risks involved regarding the failure of the cable or the pulling device because the forces are larger compared to fluidizing the seabed. However, if pure pulling is possible it would be a relatively affordable and easy method for cable recovery.

• When a 150 m had to be retrieved after an experiment with a new plough design, it was very difficult to pull it back in with pure pulling (10-12 ton pulling strength). Although the burial depth was only 1.5 m and besides the seabed did not have time to settle. During another project at the Horn Sea, a cable at 1.0 m depth was impossible to pull out due to the clay soil.

• For the current research, it makes sense to limit the scope to sandy soils and leave out for example clay soils. When you would recover a cable from clay soil you would always have to remove the hard clay first with either a trencher or a plough. After deburial only soft clay or sand will settle down on top of the cable which could both be removed with a (sand) jetting tool.

• When you go to a scrap metal company with a complete cable, the company will pay you way less than when you split the cable before delivery (6-7 euros per kg). There might be splitting tools in the NKT factory. In the past, at VBMS we made a simple splitting tool.

• The cable splitting can be done onshore and would cost maybe 2k per day.

• It is likely that NKT has in-house data on the total cable market, for example at the business development department.

A.3. Interview with Offshore Project Engineering J. Zheng-Lu

Company: NKT

Date: 29/09/2023

Focus: Technical perspective

Main takeaways:

• To start decommissioning the cable you would probably start at one end of the cable. That could be for example the landfall, the substation platform or a wind turbine. You have to work together with the owner of these interfaces when you want to start decommissioning power cables. If the cables are not disconnected yet, you would need a platform team to release the end of the cable at the respective interface.

• Usually at the foundation of the interface you have a cable protection system (CPS) that secures the cable at the bottom. There are many different types of CPS. The old ones are difficult to detach but the alternative is to just cut the cable with a ROV at this point. After the CPS, inside of the platform or turbine, you would have a cable hang-off to secure your cable at the top.

• The cable can be detached from the hang-off relatively easily but then the cable needs to be lowered down the turbine tower or platform foundation. To lower the cable in a controlled and safe way you would need an extra winch or similar tool.

• When the cable finishes at a landfall, there might be a pipe covering the cable. If you also need to remove this pipe you could just cut the cable and leave it there until you recover the pipe, which would require a completely different process.

• With the current research, the focus should be on the deep- and intermediate-water-depth region, the area in between the cable ends. So there is no need for a detailed analysis of the turbine/platform interface or the landfall. This decision makes sense from both the engineering and the economic perspective because recovering the end of the cable is complicated and costly while the short amount of extra recycled cable length has little worth compared to the full length of the cable.

• It is important to know how much tension the cable can take and how much tension you have aboard the vessel. Once you cut the cable you recover it with a crane and clean it using two waterjets before you put it in the tensioner via the chute. When you remove the sand from the cable you have more friction and less slip.

• If you have enough tension capacity and your cable is not buried too deep you can just recover it out with pure pulling. When it is deeply buried or the soil settles very fast you need to continuously fluidize the sand with MFE while you keep the cable in tension until it pops out. You could use a ROV with a dredge pump, which works like a vacuum cleaner, for smaller cables with lower burial depth.

• Using a MFE/CFE (Controlled Flow Excavation) would require an extra vessel but using a newly designed tool, for example, an inverted trencher (with nozzles) could be an independently moving ROV on the seabed with tracks. It could be that such a tool would be faster than MFE and would probably also result in less environmental damage.

• Dealing with the burial depth and with very old cables are the biggest engineering challenges. When you are recycling it can be difficult to strip the cable.

• Good to add a small 'what if' scenario in case you find an old cable with a high-level flow chart with some steps you need to take. This will probably not happen often.

• Try to always also have tension on the final end of the cable. Without any back tension, you don't have control over the end of the cable. In case of a loose or broken cable, you can use for example an anchor to provide the back tension.

• You might be able to use platform supply vessels (50K per day) to do the decommissioning job if they have a crane. When they have older systems for dynamic positioning they might be cheaper.

• The cable decommissioning will not go faster than 4 m/s.

• Often the DC export cables are two cables together, sometimes attached to each other and sometimes separated.

A.4. Interview with Subsea Power Cable Consultant W. Snip

Company: Primo Marine

Date: 02/10/2023

Focus: Technical, legal, and economic perspective

Main takeaways:

• Sand waves form a big challenge for decommissioning because they might leave the cables buried deeper than during installation. They can move with a speed of dozens of meters per year, have wavelengths of 200-500 m, and wave heights from around a meter to a maximum of one-third of

the water depth. Dredging the sand wave is expensive (10 Euro per cubic meter) and might have a considerable environmental impact on the seafloor. MFE or a jet tool attached to the power cable could fluidize the sand wave as another easy, cheap, and effective option. When offshore, keep it as simple as possible, so do not go for ROVs or other complicated systems. The last option is to just pull until the cable breaks, which is also done with telephone cables.

• When the cables are less than 1.5 m deep in sand soil, pure pulling should be possible. The design pull force is usually a lot lower than the maximal pull force due to safety factors. The cable can likely withstand 20-30 ton pulling force.

• When using a cable-attached tool, it is better to have an underwater pump than a pump aboard the vessel. One advantage is having a more easily manoeuvrable and controllable power cable going down from the vessel instead of a water hose. Besides, the intake pressure in the pump is larger due to the positioning near the seafloor. The downside is the high price of the underwater pump.

• In the future the UN will make it mandatory to recover the subsea cables.

• Many cables contain lead. On relatively short time scales this lead can be contained within the cable. However, in the long term, the lead will end up the in soil and the sea. Leaving a lead-containing cable in place would thus eventually always be a short-term solution.

• It is possible to optimize the design of the cable for decommissioning and recycling. For example, the cable could be designed in such a way that it is easy to separate the materials in a recycling facility. To ensure that the cable still has enough of its strength after many years on the seafloor, the cable armour could be made of Dyneema or Kevlar instead of galvanized steel.

A.5. Interview 1/2 with Chief Executive Officer R. Andersen

Company: JD-Contractors

Date: 03/10/2023

Focus: Technical and economic perspective

Main takeaways:

• In the early years of the company, JDC, (power) cables were being decommissioned because of their scrap value. Most power cables were made of copper but nowadays a lot of cables are aluminium. Back in those days, there was no requirement at all to 'clean up after yourself' implying that cables were not commissioned based on legislation.

• For the last 10 or 15 years cable recovery has been part of the permit. When the cable goes out of service it has to be decommissioned to make the seabed return as close as possible to its former state. In Germany, the government has many rules for what tools and methods you can and cannot use to recover the cable. In other countries, there can be barely any rules in some situations.

• If you have any kind of lead or oil in your cable you need to make sure you don't have any kind of spillage.

• With a normal armoured cable, you would try to get it out by just pulling first. If that doesn't work you need to debury it. Deburial can damage the environment and therefore in some situations, it is better to leave the cable in place. For example in the Waddenzee, there is for some reason the requirement to bury the cable 5 m into the seabed. You normally do this with a vertical injector. If the cable is made out of metal and some polymer then the damage being done by the cable materials is quite small when you leave it in place. This is of course different from an oil-filled cable that could do a lot of harm. When designing a cable, you could choose the material such that it can do little harm when left in place when the cable goes out of service. The decommissioning method has to be evaluated case by case.

• The power cable owners, TSOs, and local power companies want to be in a good relationship with the

neighbours etc. and usually want to decommission the out-of-service cables.

• The cost of stripping the cables needs to be detracted from the metal value. Usually, this is done by the scrap dealers because they can do it way cheaper and safer regarding oil-filled or lead-containing cables than manually onboard the vessel. It is easiest to just deliver the cable as the smallest number of pieces as possible in the harbour. This is most effective for the operation because offshore time is expensive. We use a carrousel or drums and only make a cut when the carrousel is full. Keeping the cable as intact as possible, reduces the risk of polluting.

• Defining the scope of the project to be limited to offshore wind power cables in sandy soils in the North Sea makes sense because you have a limited number of regimes and similar weather conditions. There are special concerns regarding oil-filled and lead-containing cables and they have to be handled in a very different way than modern cables.

• By far the most efficient and least environmentally damaging decommissioning method is pure pulling. Water clouding will be minimized. As soon as you get to a depth of 1.5-2 m, having force enough to pull out the catenary-shaped cable is very challenging.

• Very often jetting with a jetting pig is the easiest way to free the cable at the touchdown point but it only works if you do need to remove large quantities of debris. Usually, it works for jetting away material for 0.5-1 m soil. In case of deeper burial, you need a mass flow excavator to remove large quantities. Authorities, e.g. Germany, usually prefer a suction tool that can remove the debris more locally. Damage is probably more local but still comparable to MFE effects. The worst-case scenario is when you need a dredger.

• At places where you have for instance cable crossings or some kind of mechanical protection like concrete matrasses (nice artificial reef) in place, it could be better to leave the cable in place either for environmental reasons or to protect the other asset that is crossing your cable. You can just cut the cable on both ends and continue decommissioning the other parts.

• The infrastructure is getting increasingly entangled and at the same time the cable lifetime is usually way longer than the OWF lifetime. It seems like a waste of resources to remove expensive infrastructure, especially the export cables, that are in place and fully functional. Ideally, how could you upcycle this infrastructure?

• There is a dilemma since on one side the OWF owners want to protect their assets as best they can to prevent any damage but this makes it more difficult to recover the cables afterwards while also making a bigger negative impact on the surroundings in case of decommissioning. Is it really necessary to bury the cables that deep or is it just because someone just decided this once in some sort of guideline? In case of damage risk due to a dynamic sea bed exposing the cable, you have to consider how the risk compares to the cost of the implications of burial depth. Increased depth also results in higher repair costs.

• More than 50% of the cable failures we see, cannot be proved to be caused by external factors. Very often something goes wrong during the production of the cable or in the way the cable is operated for example high temperature gradients in OWF power cables due to large power fluctuations.

A.6. Interview with Commercial & Tender Manager M. Smalt

Company: NKT

Date: 04/10/2023

Focus: Technical and economic perspective

Main takeaways:

• For offshore power cable tenders decommissioning is currently not considered. There is only a lifetime requirement, 25-30 years, which is equal to the OWF lifetime.

• It should be more important to also think about decommissioning during the tender process. Not in a way that upfront contracts should be signed for decommissioning 30 years later but in a way that cable design and installation take future decommissioning into account. When you design for decommissioning, for example, recycling could be more efficient. Installation for decommissioning e.g. reducing the burial depth, could make it easier to recover the cable in the future.

• Research is being done into using no more lead in cables because lead could be harmful to the environment.

• Legislation regarding decommissioning is largely based on previous oil and gas experiences. Things might change quite rapidly when for example organisations such as CIGRE or a TSO would conclude that OWF developers should recover offshore cables instead of leaving them in place.

• To retrieve an offshore cable a forceful pullout is probably the easiest option. Regular cable installation vessels could be used. Might be interesting to investigate whether the inverse cable laying technique is the best method. We have experience with recovering cables by pulling during cable repairs.

• Pulling out the cables takes more time than cable laying, which will make it an expensive operation. Say for example the vessel costs $200K per day. When it takes three times as much time to pull out the cables compared to lying the cables (10 weeks), the total cost would be around $40M ($200K x 210 days).

• When doing cable repairs sometimes Mass Flow Excavation (MFE) is used to fluidise or remove the soil to get the cable in a suspension resulting in easier cable recovery. The downside of this method is that you need an extra ship to operate the MFE tool which takes extra time and budget. The MFE has also a relatively low speed of around 3 meters per minute instead of 10 meters per minute. It is recommended to also talk to offshore specialists such as Juri Vogel.

• Most likely is the retrieved cable not suitable for reuse and can only be sold as scrap metal. It could be interesting to look for a specific cable recycling process to make the recycling more efficient. This is mainly interesting when large amounts of cables are being decommissioned.

• The main decommissioning cost is the time at sea. Offloading can be as fast as the onloading (2-3 weeks). The regular turn table can be used to store the recovered cable. The inter-array cables should be easy to recover because they are smaller and have less burial depth than the export cable.

• It should be possible to make a use case for cable decommissioning and recycling based on a NKT project. It would be interesting to calculate the extra forces needed for the cable pullout without MFE. Next, the impact of extra forces on the ship and the maximal recovery speed could be investigated. Another research direction could be to design an inverted plough that acts as a lever while placed under the cable. Try to find the most cost-efficient way to recover the cables out of for example three different methods.

• There might have also been a previous cable decommissioning project at Guernsey so try to look into that as well.

A.7. Interview with Marine Operations Manager J. Aas

Company: Oceans5

Date: 05/10/2023

Focus: Technical perspective

Main takeaways:

• So far there haven't been any rules or regulations that force the cable owners to decommission their cables once they are out of service. Those rules will come and I am surprised they are not here yet.

• You can pull out the cables without any problems when the burial depth is around a meter because you can damage the cable a bit without losing scrap value.

• It is very important to have a survey of the whole situation. You need data on the cable itself, the burial depth, the routing, and potential obstacles. Based on this overview you can determine your strategy for recovering the cable and request a permit for your project. With the permit, you can do the final planning and start decommissioning thereafter.

• You need to make sure that you will not waste time delivering the cable to the scrap metal company in the harbour.

• When you are using a barge for the decommissioning project you need to take into account that the barge will need more time to do the job. The process of anchor handling and moving the anchors to be able to move the barge is quite slow. A North Sea standard barge can move only 100 m at a time. However, you can save costs on the equipment because you can do the job with only a winch and a chute.

• A better alternative to an expensive installation vessel would be using a cheaper vessel such as a PSV (Platform Supply Vessel). You could just put a turntable, a chute, a couple of winches, and a tensioner on there. Your capacity will be smaller, so you probably have to go back and forth to the harbour more often.

A.8. Interview with Project Installation Manager E. Heemrood

Company: NKT

Date: 12/10/2023

Focus: Technical and legal perspective

Main takeaways:

• The most important parameters are the soil type and the burial depth. For example, Tennet wants to bury the cable very deep, 5-6 m, to make sure there will be no need for any seabed maintenance. In case of lower burial depths, it might be necessary to perform maintenance in the form of sand or rock dumping. The burial depth is usually also dependent on the environment, for example near major shipping routes, the required burial depth is larger. To determine the necessary depth, we perform a Cable Burial Risk Assessment (CBRA).

• When cables are buried very deep, say more than 5 m, mass flow excavations may not be sufficient to free the cable. In that case, you would need to dredge the cable which damages the seafloor severely and comes along with high emissions.

• It would be interesting to give an overview of the burial depth requirements for the different countries adjacent to the North Sea. It is likely that the requirements are similar but there could be differences as well.

• The material of a cable is partly selected based on the burial depth because deeper buried cables heat up more easily due to the isolation of the sand cover. For cables that heat up more, because of larger burial depth but also because of more power, the preferred material is usually copper.

• Calculating the cost of decommissioning is quite complex. For example, you have to take the weather into account, do you just cut the cable halfway when you need to return to the harbour while you are in the middle of your decommissioning project? It might also be difficult to assess the mechanical properties of an old cable. In case it just breaks every couple of meters, decommissioning will be way more expensive. However, if you have a couple of general cases of cables at certain locations, we are able to put a price for decommissioning.

• Current permits (in the Netherlands) aim for the methods that are the best solution for the environment today. However, those methods might not be the best solutions for the environment in the long term. For example, burying the cables very deep could be a great short-term solution to prevent negative environmental impacts from maintenance. In the future, this may result in a mission impossible

regarding cable decommissioning.

A.9. Interview with Environmental Advisor I. Buchan

Company: NKT

Date: 27/10/2023

Focus: Environmental perspective

Main takeaways:

• For a cable decommissioning project you would have to do a bespoke EIA wherein you identify impacts and mitigation and minimization measures.

• When it is possible to justify leaving the cable in situ, people will try to make a case. It is possible to find arguments both for complete decommissioning and for leaving the cable in place.

• Society determines how far decommissioning should go and society's opinion is subjected to change constantly. When there is an energy crisis, permits for fossil fuels are suddenly being given out again. Judgements on all individual cases will be made in the future based on factors that can change a lot over time, such as societal attitudes, policy, and available technology. You can only base your methods on what you know today. Generally, things get more strict and stringent in the future but not always.

• The general rule is that if you were allowed to bury the cable in the first place, it should be allowed to decommission it with a reverse operation.

• When you are speaking of deburial you have to consider the loss and disturbance of seafloor habitat. The impact is not massive, since you only have a small footprint and are operating in the same area as where similar damage was being done during installation. In the case of for example stone coverage, the impact could be bigger because you could be dealing with reef structures.

• To determine what method to use for decommissioning, you need to assess it for each individual case. For example, vulnerable areas near the cable could be affected by MFE but not by a jetting pig. Generally, the more local is the impact, the better. You should try to minimize footprint and blasting material up in the water column.

• To select a method option, you should score each type on technical, commercial, health and safety, and environmental criteria.

• Usually, the engineers propose a method and then the environmental manager will assess the impact.

A.10. Interview 2/2 with Chief Executive Officer R. Andersen

Company: JD-Contractors

Date: 15/11/2023

Focus: Technical perspective

Main takeaways:

• You would decommission the entire bundle at once because the cables are entangled and they cannot easily be untangled on the seabed. You need to recover the bundle as a whole till the surface. Aboard you can untangle the bundle and store the fibre optic cable on a drum and the power cables in separate turntables or in coils if the cables are coilable. The bundle is heavier and wider than a single cable which makes the decommissioning more complicated.

• Decommissioning with MFE/CFE is the easiest and quickest way to debury the cable. Suction would

cause less harm because it is more local but would be way slower. For burial depths up to 1.5 m, it could be possible to perform a direct pull-out on the cable bundle.

• You usually know the breaking load of the cable, it should be specified by the cable producer. You perform a pull-out with a pulling force just under the breaking load, for example up to 90% of the cable breaking load. You can make some conservative estimations on the reduction in breaking load depending on the age of the cable system.

• The maximum tension load is different than the breaking load. The maximum tension determines how much force you can pull without damaging the cable. During decommissioning for recycling, we do not care about the full cable integrity.

• The breaking load is a combination of the armour and the conductor strength. For example, strangled conductors can be quite strong. It might be a challenge, however, to find suitable equipment for pulling up till the breaking load. In case the breaking load is e.g. 100 tons and you need 100 tons for deburial, you would have to find a winch that can pull 100 tons.

• Ideally you would have a capstan wheel to pull out the cable. As far as he knows there is no capstan that can withstand 100 tons. Most of the capstans are used for pipe laying and go up to 40-50 tons of tension.

• Normally the joints, either repair or planned joints, are considered the weak points in the cable. If you do not have a specification of the breaking load of the joint, you need to make assumptions.

• A flexible pipeline can collapse relatively easily compared to a power cable because the pipeline does not have a conductor inside. This makes decommissioning of a cable easier than a flexible pipeline. The armouring of flexible pipes is flat which makes the minimal bending radius larger compared to cables with round armour wires. However, the bending radius is still important because it adds to the friction. The more you bend the cable, the more friction you have. Therefore you also use the chute.

• When the risks related to a breaking cable are small for example for fibre optic cables, you can go over the break load and take the risk it breaks. If the cable holds, you have a faster decommissioning process and if it breaks in a controlled way because the cable is contained in rollers there is no big risk involved. After breakage, you can decide to leave the rest of the cable in situ or you can connect it again and probably conduct some deburial to continue decommissioning. This would be different for e.g. an oil-filled cable with which you could cause considerable environmental damage if you break the cable after going over the break load.

• OrcaFlex is based on calculating the catenary in water where you have little friction. As soon you have to pull something out of the seabed it is not a catenary and the cable would behave completely differently. Nobody has really any values on that but this friction will have a large impact on the operation.

• Modelling the part from the vessel to the seabed is relatively easy but from the seabed down to where the cable is rested is very complicated. You need to challenge what parameters you can put in your model.

• You would need to do two calculations, one for the part in the seabed and one for the part in the water column because the two scenarios are very different. The second part is only a matter of angles and tension. You could also calculate what the bottom tension would be at the seabed but what is required further down is complicated.

• When you are doing the deburial of the sand you have to take into account that you need to have at least a 45-degree angle to prevent the sand from collapsing and burying the cable again. The trench you create with your CFE needs to be 15 to 20 m wide.

A.11. Interview with Senior Analysis Engineer F. Bodesund

Company: NKT

Date: 16/11/2023

Focus: Technical perspective

Main takeaways:

• In OrcaFlex the seabed is just a surface with friction. The seabed is thus not deformable or viscous. Therefore, you need to work around this if you want to model a buried cable.

• The DNV literature could be used to model the stiffness of the soil.

• There are alternative simulation methods where you could model the soil better. However, these methods are very complex simulations and therefore advanced and computationally heavy. They also require a lot of different parameters.

• Probably it is not possible to model a buried cable using the nonlinear soil model option in OrcaFlex because the soil (at least the elastic seabed model) acts as a spring that pushes the cable out as soon as you take away the pressure that forces the cable to penetrate the seabed.

• However, there are tools in OrcaFlex that you could experiment with in order to try to 'build a cover seabed' on top of the cable.

• For example you have the 'solid shapes'. It might be difficult to capture the soil stiffness correctly by using the solids. The shapes are not affected by the environment and are usually used e.g. for chutes.

• You could also use 'links'. They act like strings and are given a nonlinear behaviour that depends on how far they are elongated. You could have a series of links pulling the cable down mimicking the soil resistance when you start pulling on the cable. The links are probably more suitable for getting a nonlinear behaviour. For example, up until you have reached a certain tension of X, the links are linear, thereafter they would completely fall mimicking the cable breaking through the surface.

• In OrcaFlex you do not have a 3D mesh of the whole cross-section and do a global analysis. This is of course different than a local analysis that you could perform in e.g. Abacus or SolidWorks.

• The cable bundles should be decommissioned as a whole and modelling the individual cables in the bundle is possible but computationally heavy and simulations could take weeks. Therefore, it is more efficient to simplify the cable bundle as a single cable. The mechanical properties of the three individual cables can be added to model this single cable.

• The fibre optic cable can be disregarded because it is small compared to the other cables in the bundle and is not supposed to take any tensile loads.

B

Planned Projects of the Tennet 2GW Program

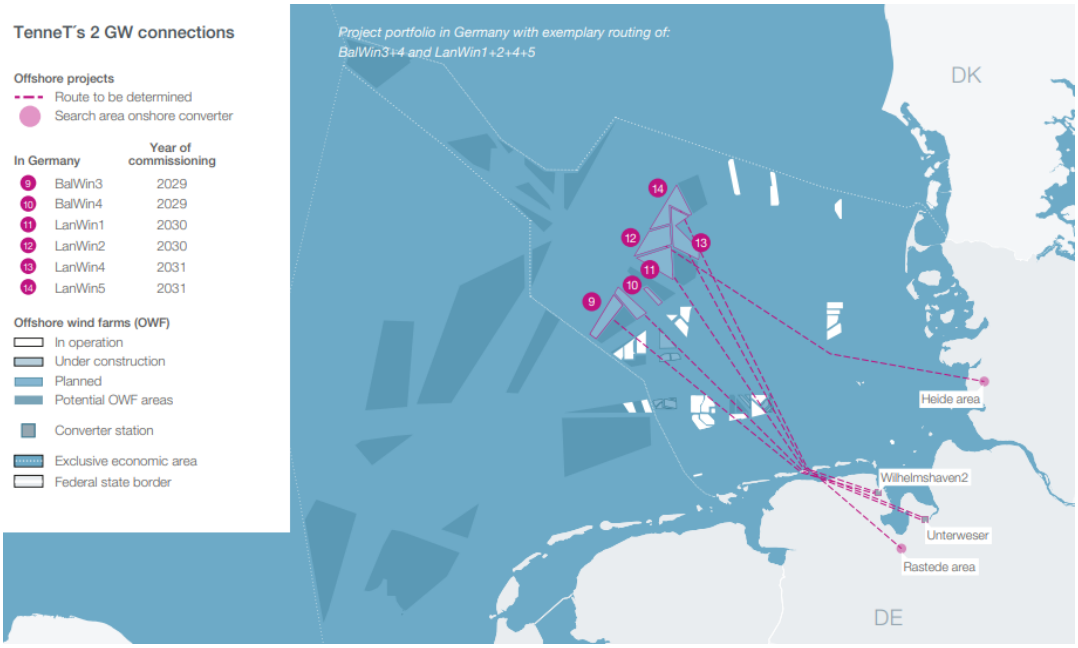

Figure B.1: Tennet 2GW Program's six German offshore grid connection systems BalWin3+4 and LanWin1+2+4+5 [32]

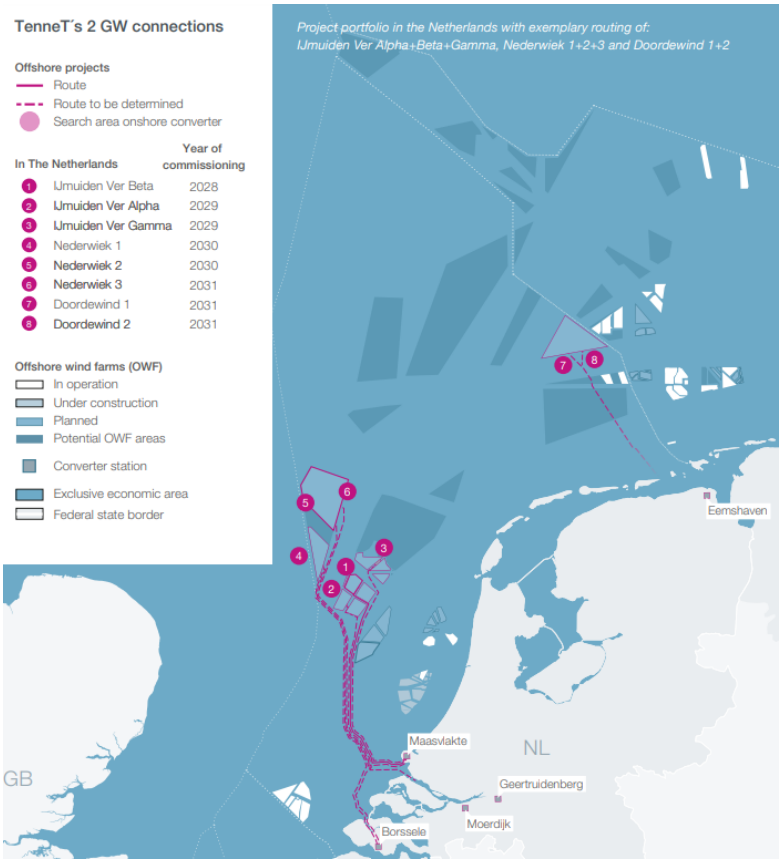

Figure B.2: Tennet 2GW Program's eight Dutch offshore grid connection systems IJmuiden Ver Alpha+ Beta+Gamma, Nederwiek 1+2+3, and Doordewind 1+2 [32]

C

Simulation Results Sensitivity Analyses

C.1. Simulation Results Segment Length of 0.1 m

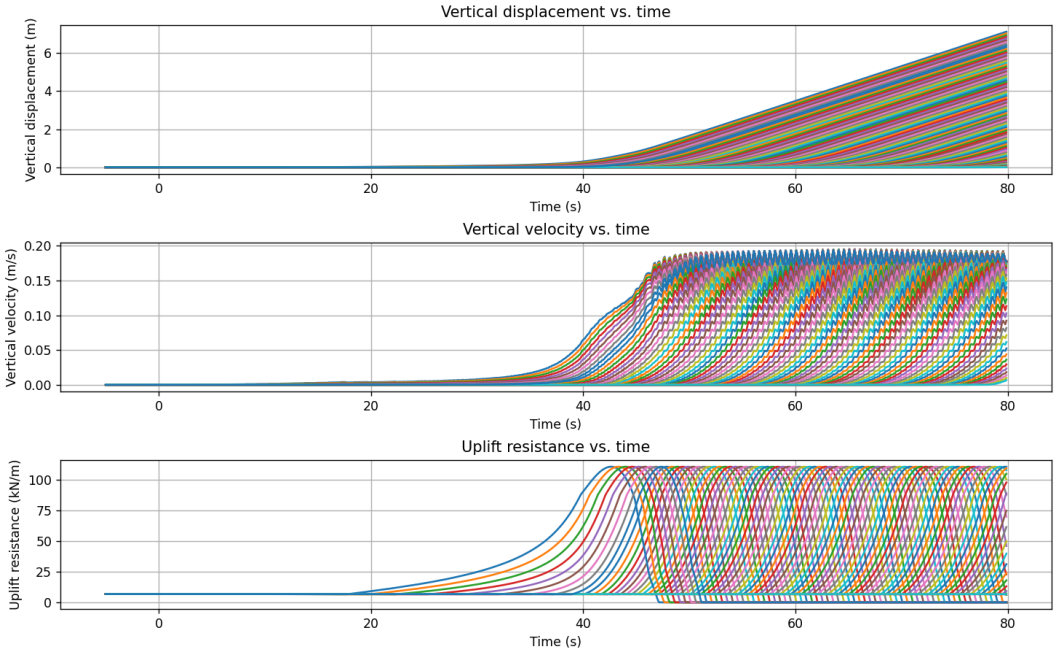

Figure C.1: Resulting vertical displacement, velocity, and uplift resistance as computed by the external Python function for each node of the cable with $L = 0.1$ m, $H_0 = 1$ m, and $I_D = 0.5$

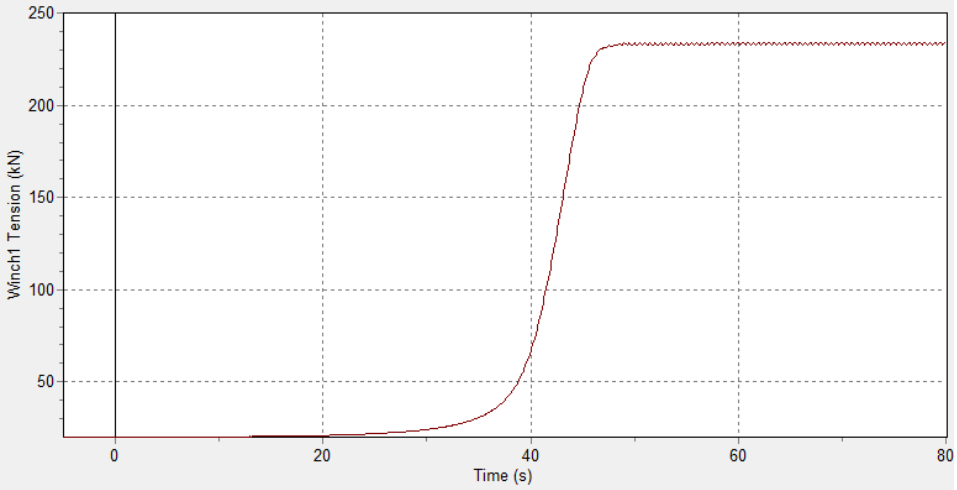

Figure C.2: Time history graph of the winch tension

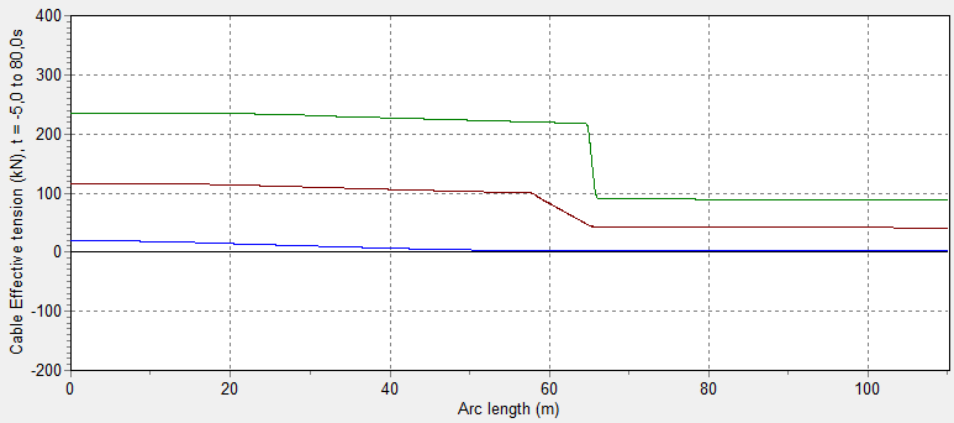

Figure C.3: Range graph of the cable tension with blue as minimum, red as mean, and green as maximum tension

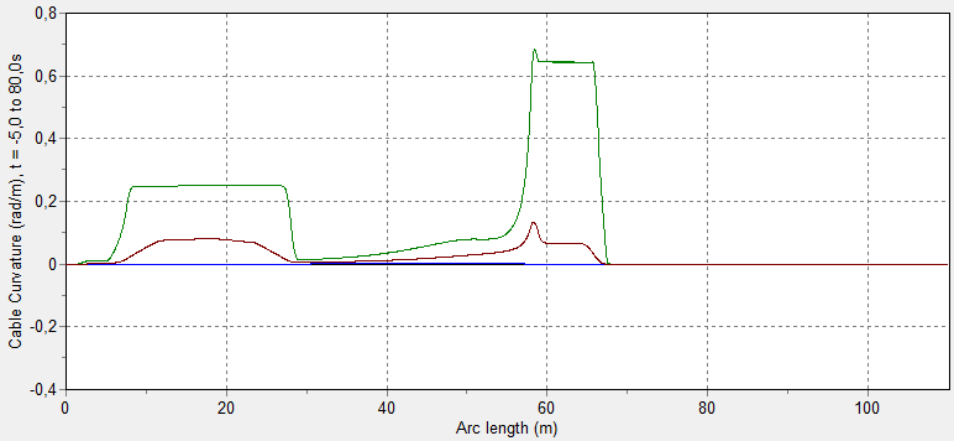

Figure C.4: Range graph of the cable curvature with blue as minimum, red as mean, and green as maximum curvature

C.2. Simulation Results Segment Length of 1 m

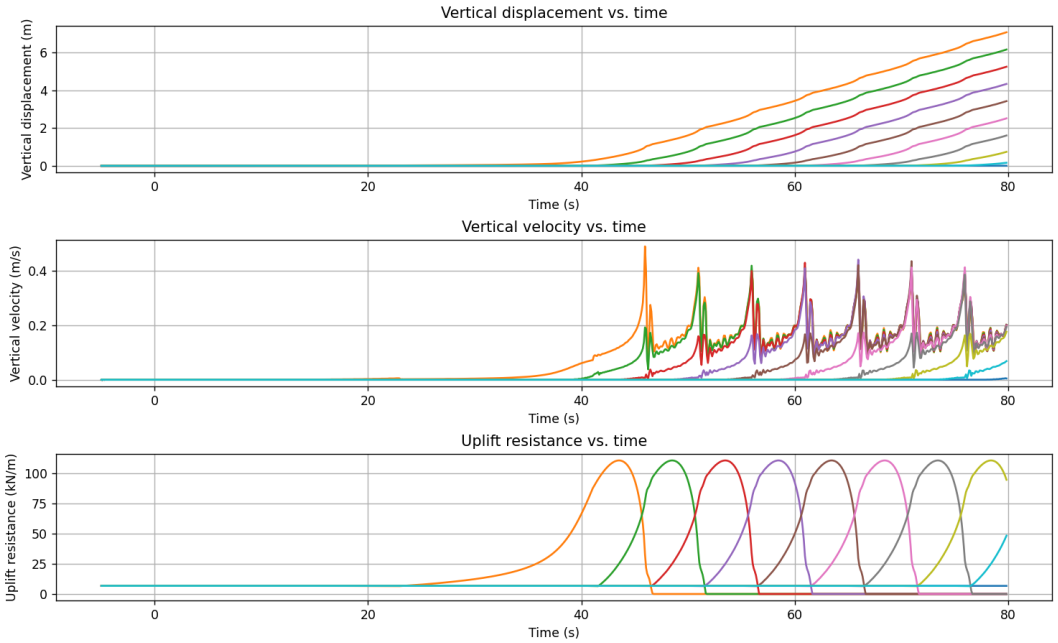

Figure C.5: Resulting vertical displacement, velocity, and uplift resistance as computed by the external Python function for each node of the cable with $L = 1$ m, $H_0 = 1$ m, and $I_D = 0.5$

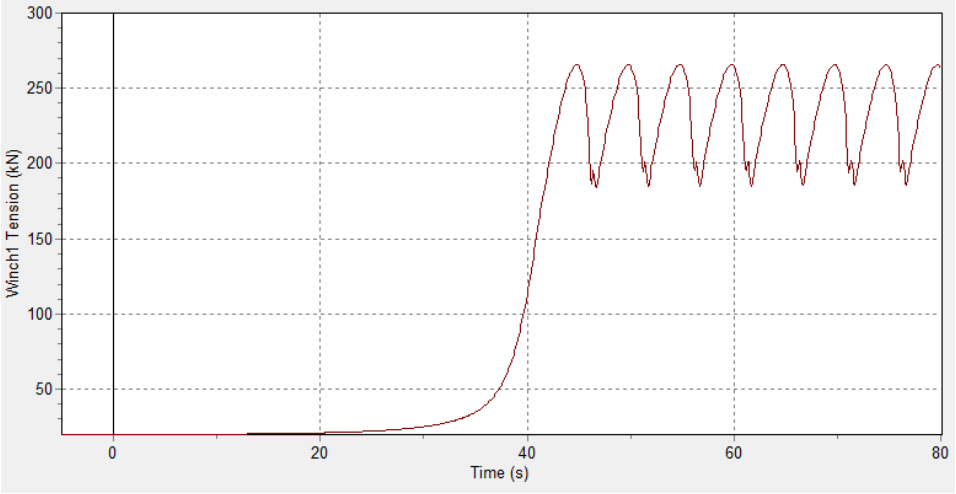

Figure C.6: Time history graph of the winch tension

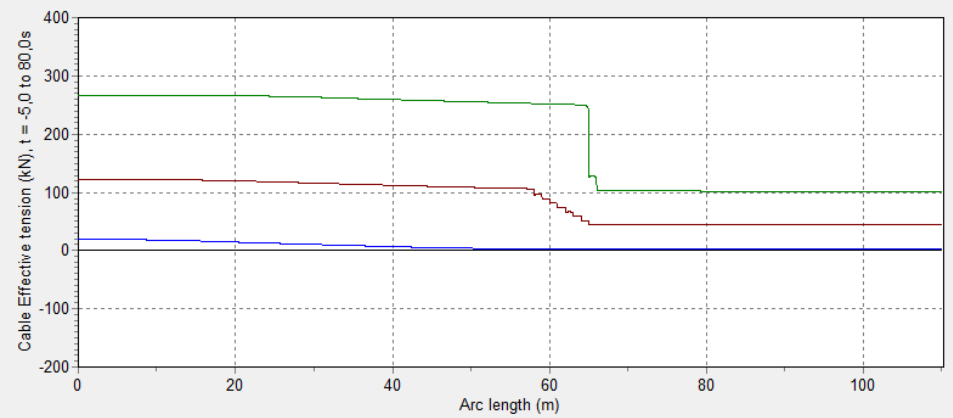

Figure C.7: Range graph of the cable tension with blue as minimum, red as mean, and green as maximum tension

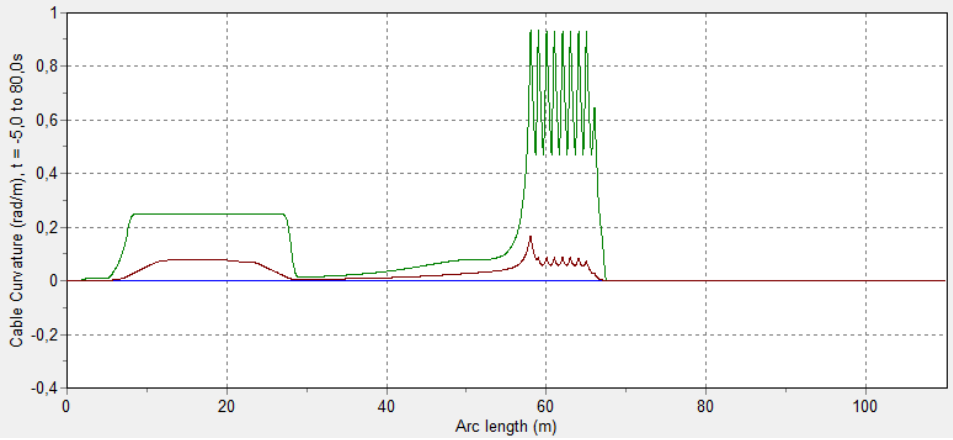

Figure C.8: Range graph of the cable curvature with blue as minimum, red as mean, and green as maximum curvature

C.3. Simulation Results Time Step of 0.001 s

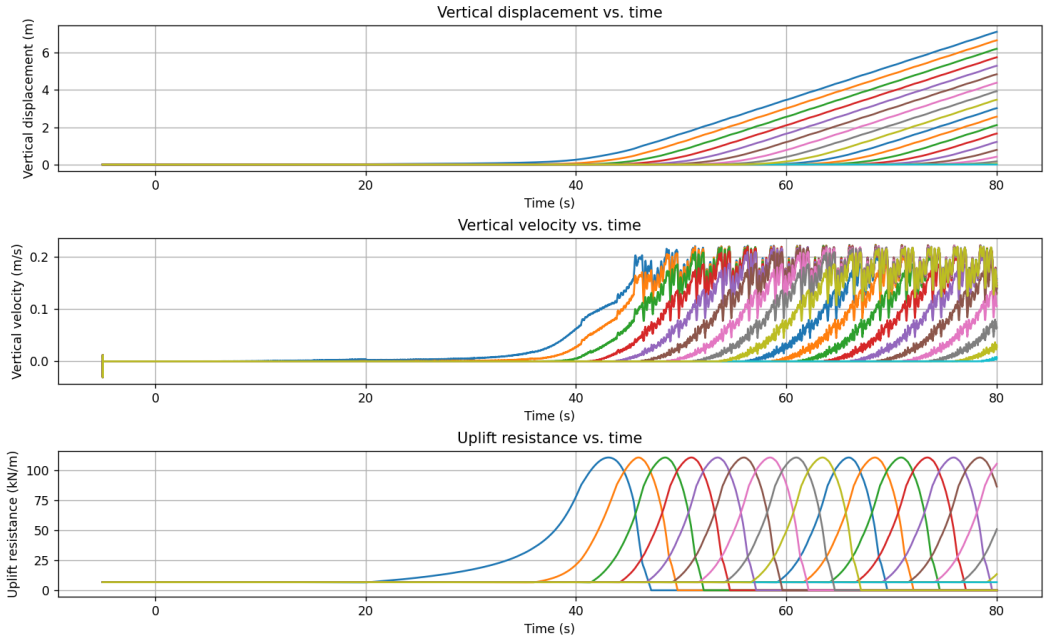

Figure C.9: Resulting vertical displacement, velocity, and uplift resistance as computed by the external Python function for each node of the cable with $t = 0.001$ s, $H_0 = 1$ m, and $I_D = 0.5$

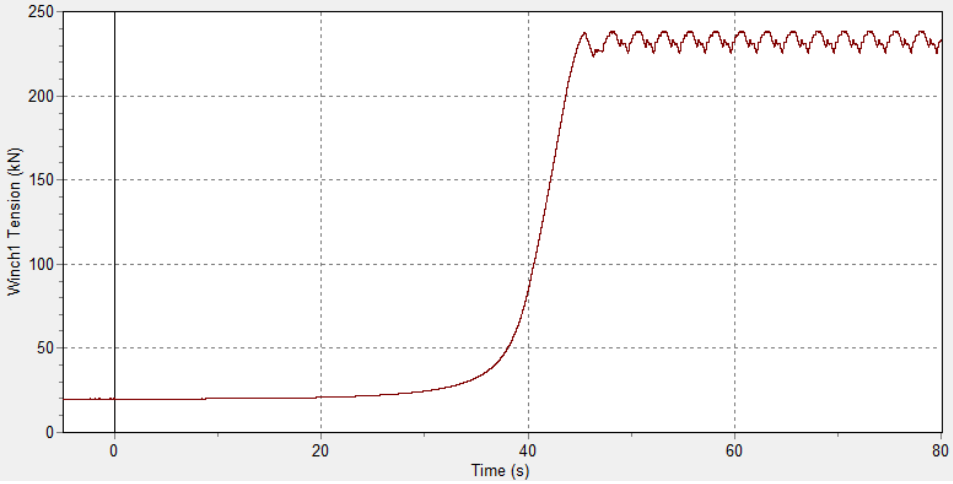

Figure C.10: Time history graph of the winch tension

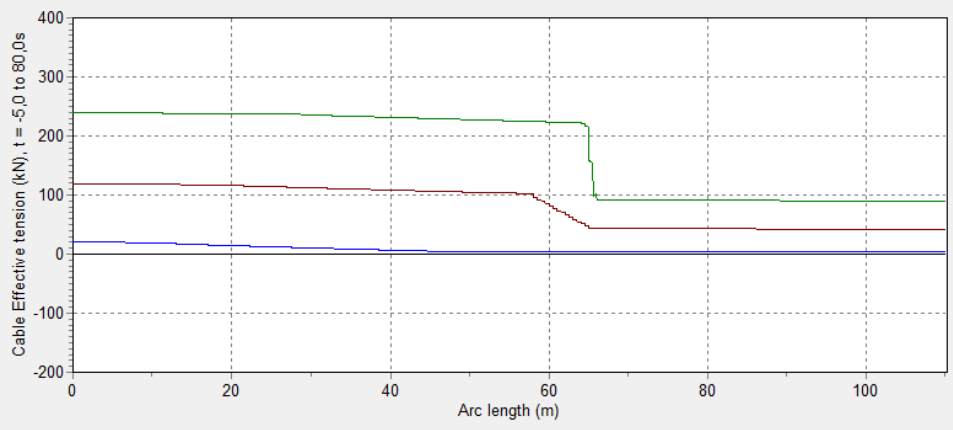

Figure C.11: Range graph of the cable tension with blue as minimum, red as mean, and green as maximum tension

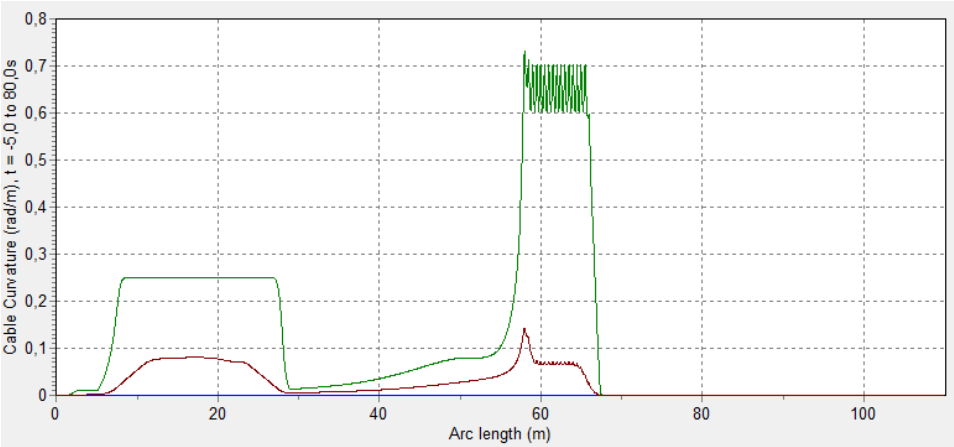

Figure C.12: Range graph of the cable curvature with blue as minimum, red as mean, and green as maximum curvature

C.4. Simulation Results Time Step of 0.1 s

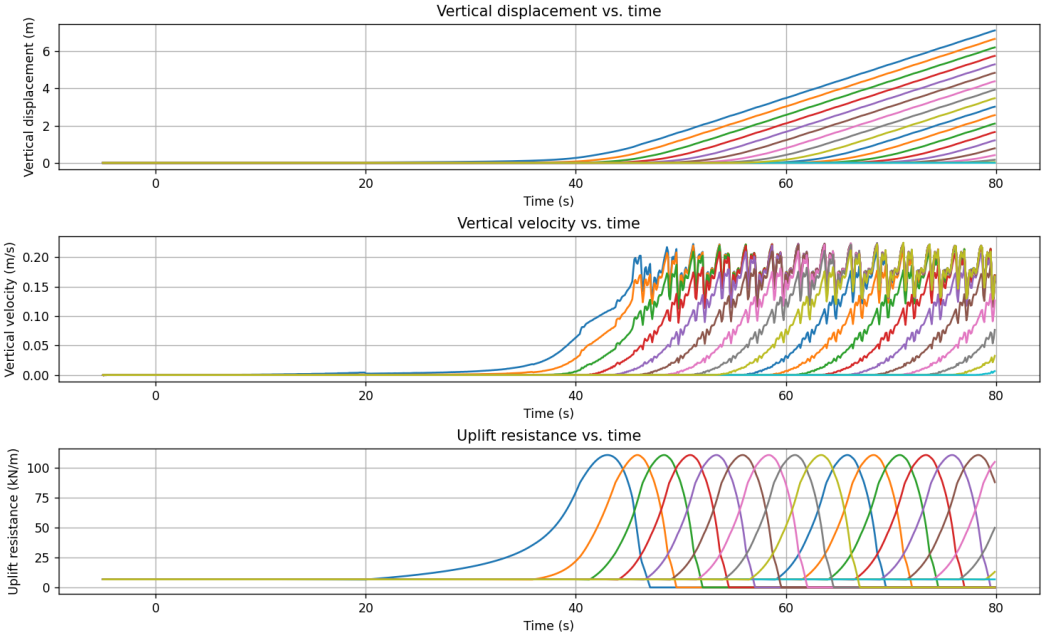

Figure C.13: Resulting vertical displacement, velocity, and uplift resistance as computed by the external Python function for each node of the cable with $t = 0.1$ s, $H_0 = 1$ m, and $I_D = 0.5$

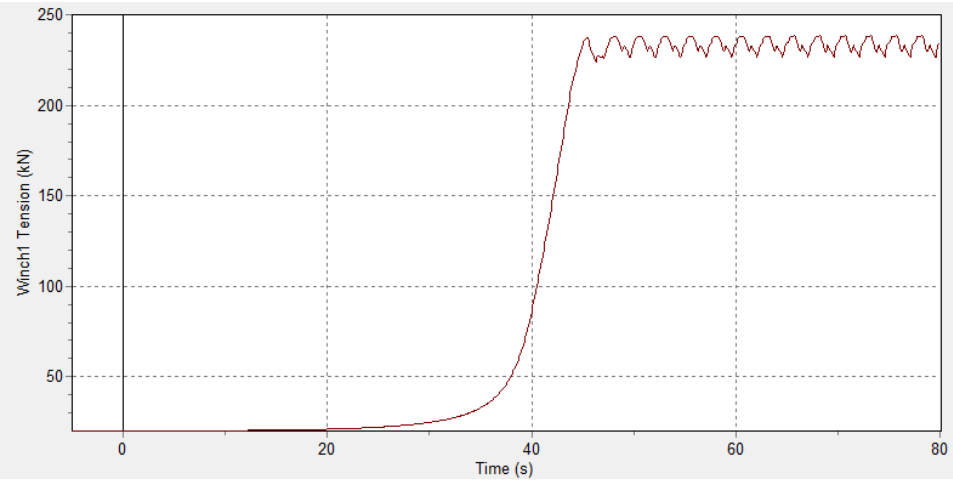

Figure C.14: Time history graph of the winch tension

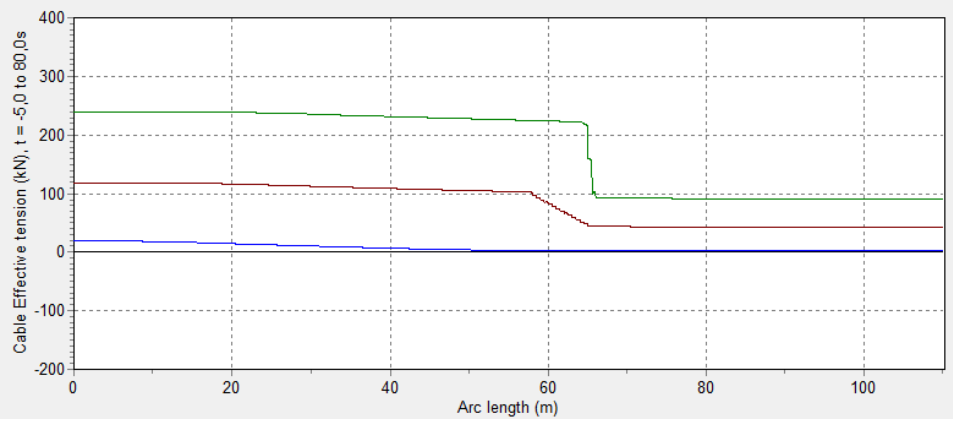

Figure C.15: Range graph of the cable tension with blue as minimum, red as mean, and green as maximum tension

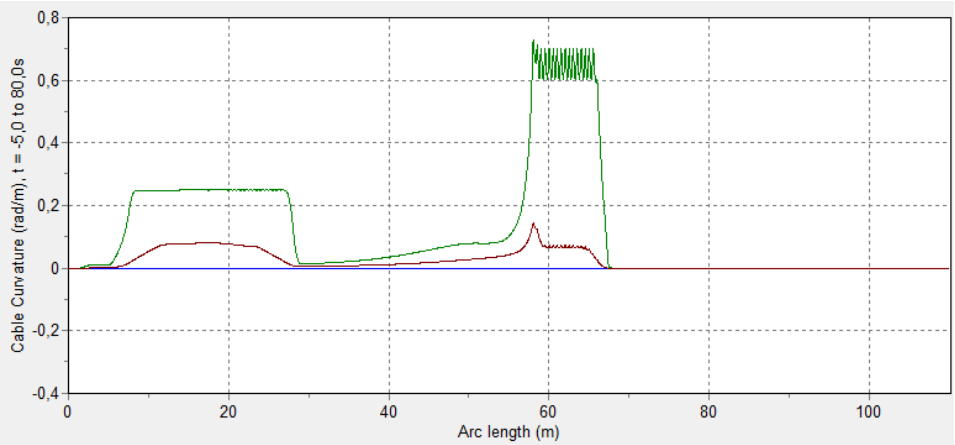

Figure C.16: Range graph of the cable curvature with blue as minimum, red as mean, and green as maximum curvature

C.5. Simulation Results Coefficient of Consolidation of 3e8 m^2/year

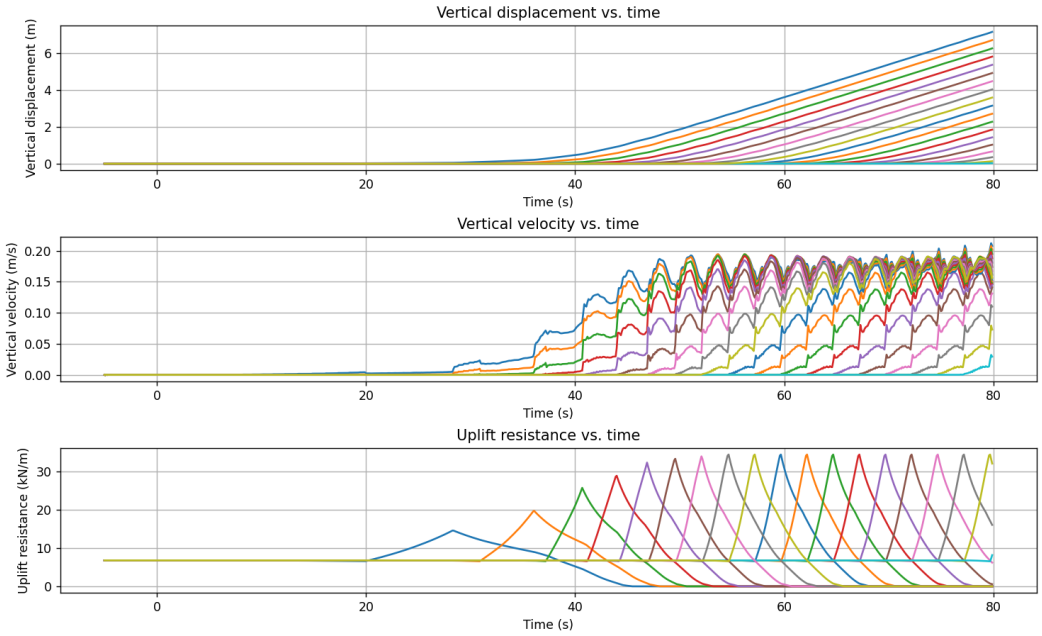

Figure C.17: Resulting vertical displacement, velocity, and uplift resistance as computed by the external Python function for each node of the cable with c_v = 3e8 m^2/year, t = 0.1 s, L = 0.5, H_0 = 1 m, and I_D = 0.5

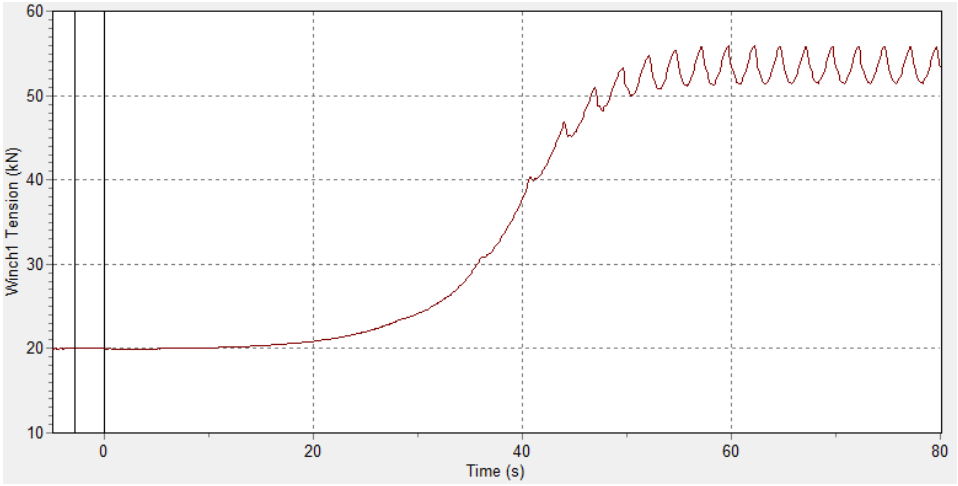

Figure C.18: Time history graph of the winch tension

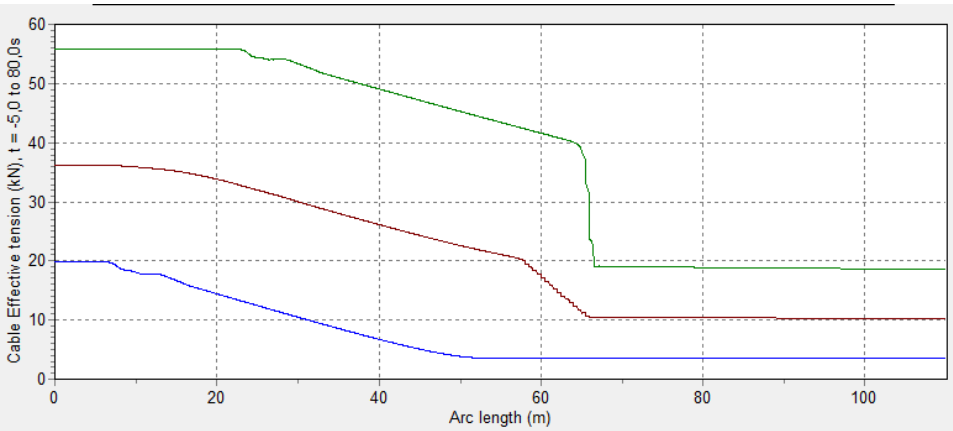

Figure C.19: Range graph of the cable tension with blue as minimum, red as mean, and green as maximum tension

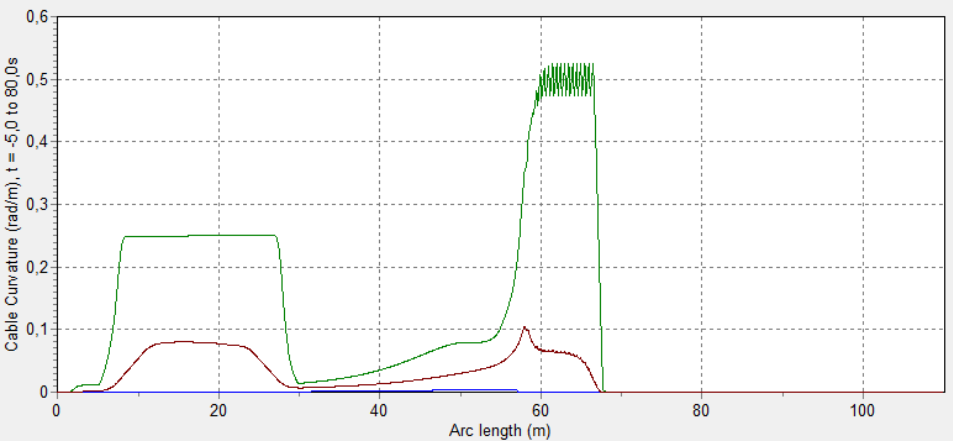

Figure C.20: Range graph of the cable curvature with blue as minimum, red as mean, and green as maximum curvature

C.6. Simulation Results Coefficient of Consolidation of 3e10 m^2/year

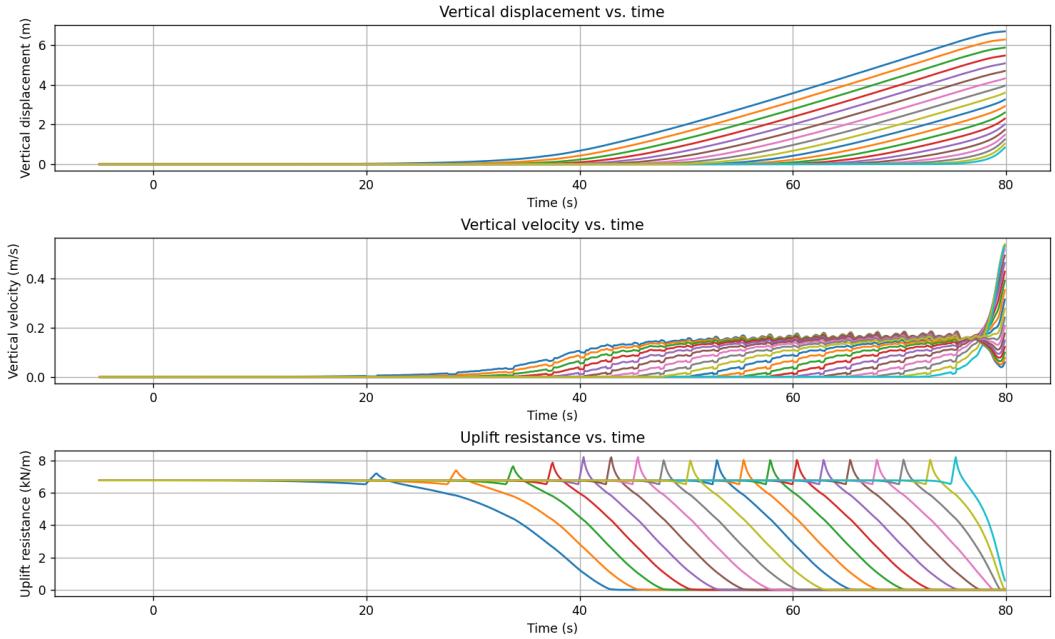

Figure C.21: Resulting vertical displacement, velocity, and uplift resistance as computed by the external Python function for each node of the cable with c_v = 3e10 m^2/year, t = 0.1 s, L = 0.5, H_0 = 1 m, and I_D = 0.5

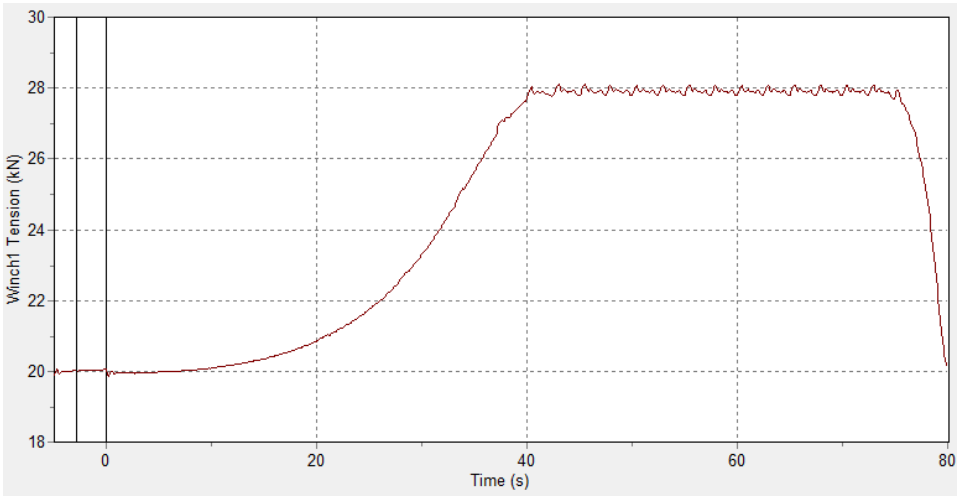

Figure C.22: Time history graph of the winch tension

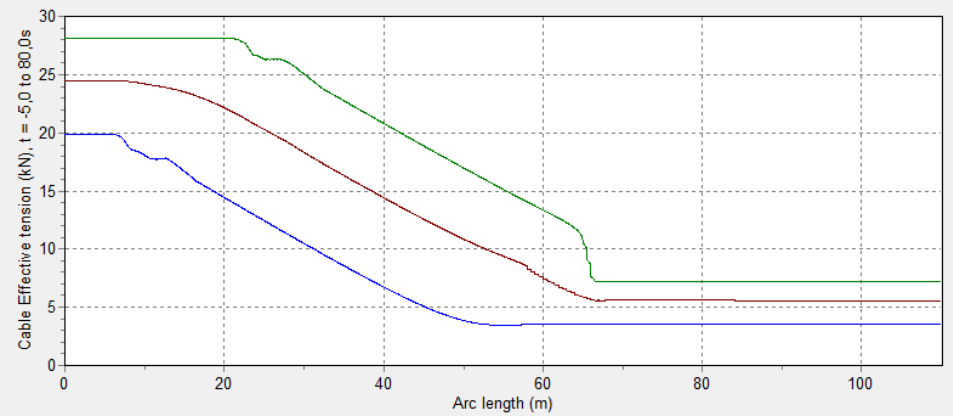

Figure C.23: Range graph of the cable tension with blue as minimum, red as mean, and green as maximum tension

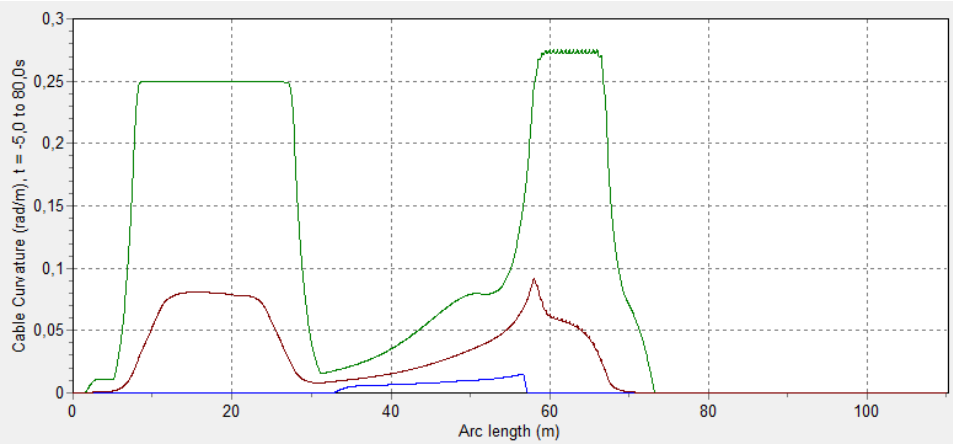

Figure C.24: Range graph of the cable curvature with blue as minimum, red as mean, and green as maximum curvature

C.7. Simulation Results Vessel Velocity of 2 m/s

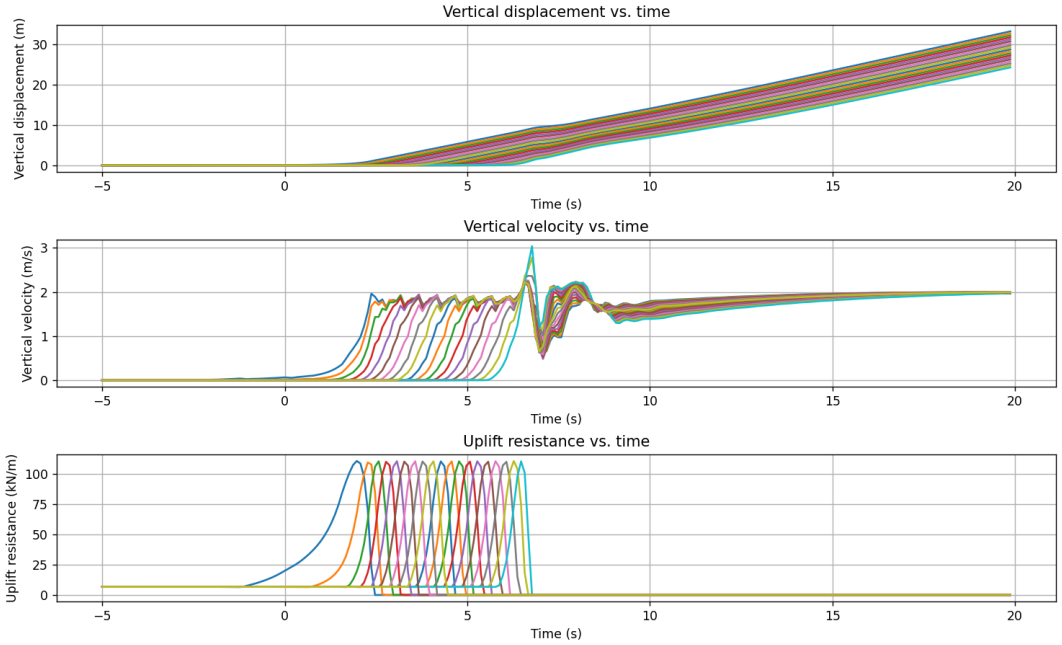

Figure C.25: Resulting vertical displacement, velocity, and uplift resistance as computed by the external Python function for each node of the cable with $v = 2$ m/s, $t = 0.1$ s, $L = 0.5$, $H_0 = 1$ m, and $I_D = 0.5$

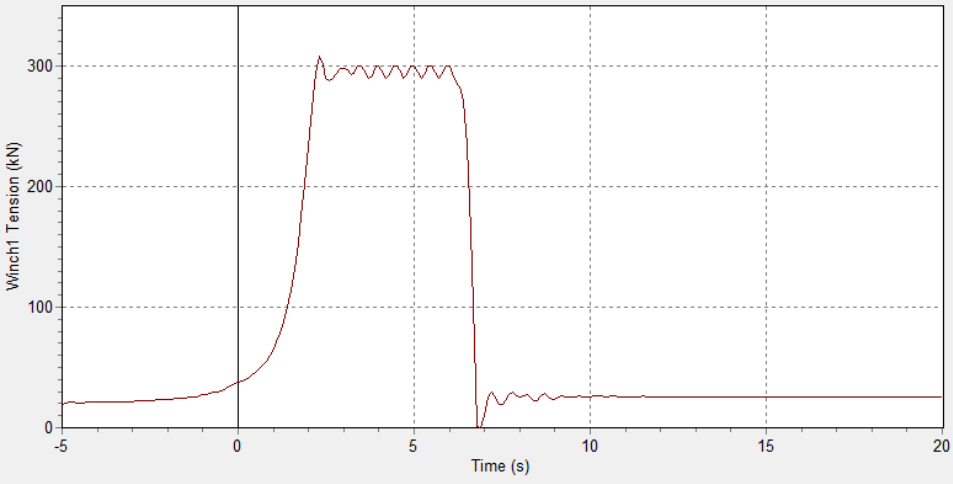

Figure C.26: Time history graph of the winch tension

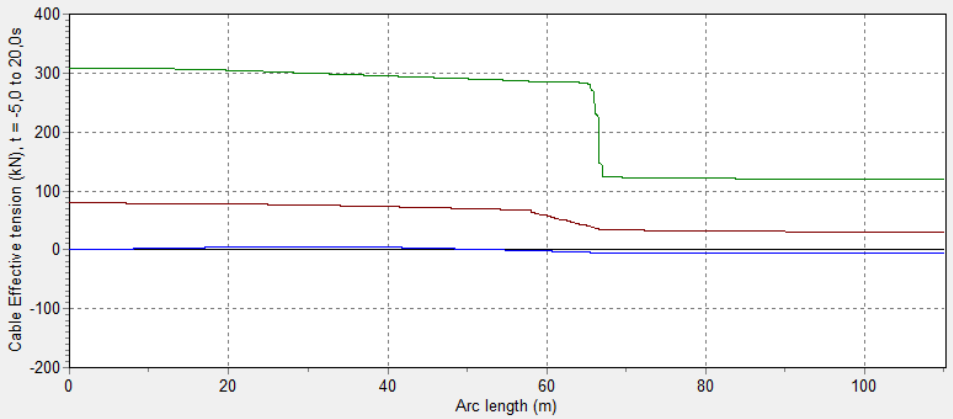

Figure C.27: Range graph of the cable tension with blue as minimum, red as mean, and green as maximum tension

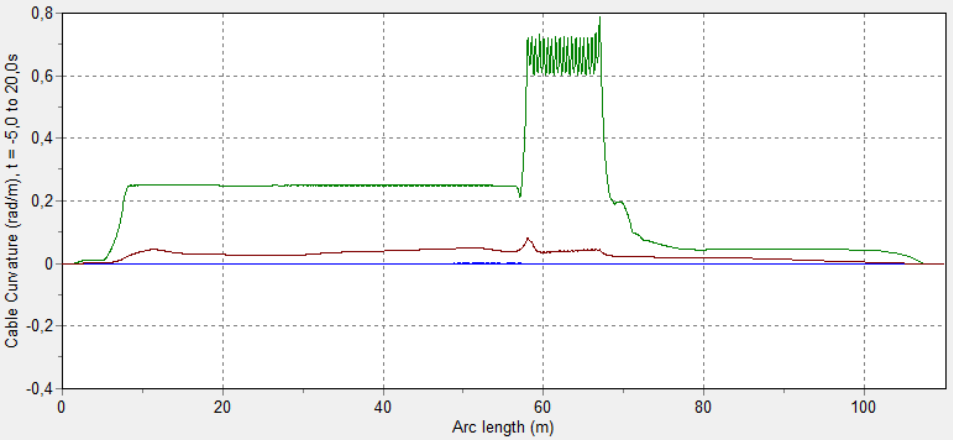

Figure C.28: Range graph of the cable curvature with blue as minimum, red as mean, and green as maximum curvature

D

Simulation Results Varying Burial Depth and Relative Density

D.1. Simulation Results Burial Depth of 1.5 m and Relative Density of 0.5

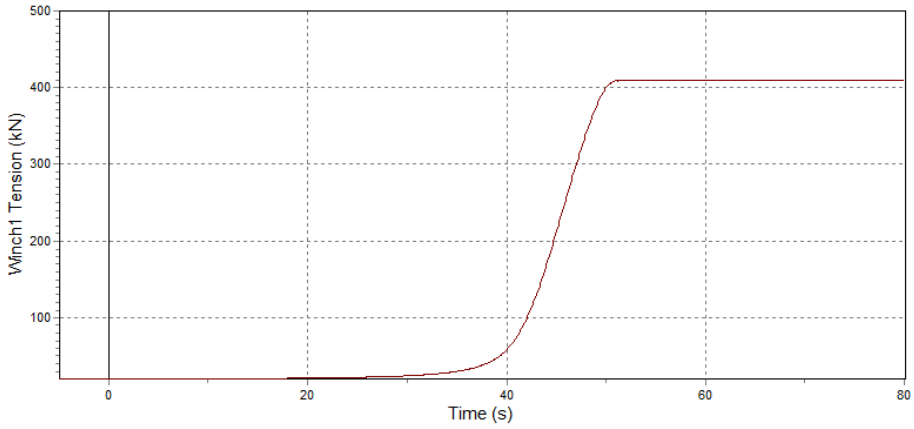

Figure D.1: Time history graph of the winch tension

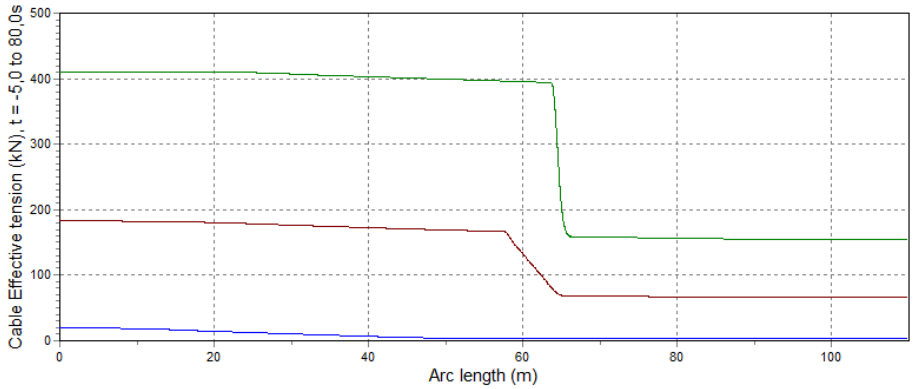

Figure D.2: Range graph of the cable tension with blue as minimum, red as mean, and green as maximum tension

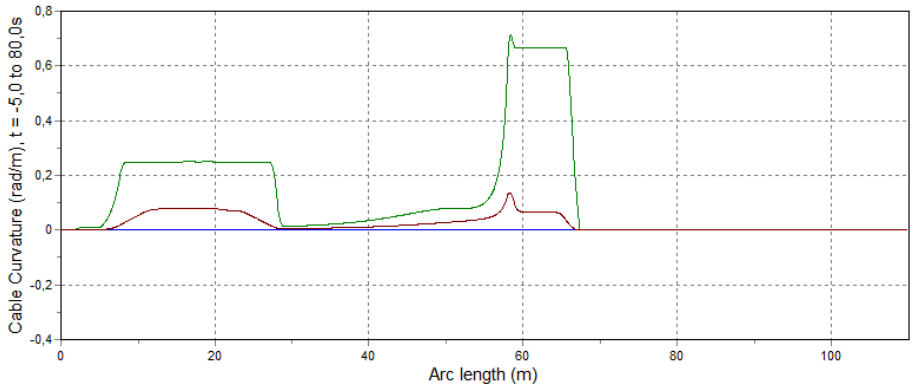

Figure D.3: Range graph of the cable curvature with blue as minimum, red as mean, and green as maximum curvature

D.2. Simulation Results Burial Depth of 2 m and Relative Density of 0.5

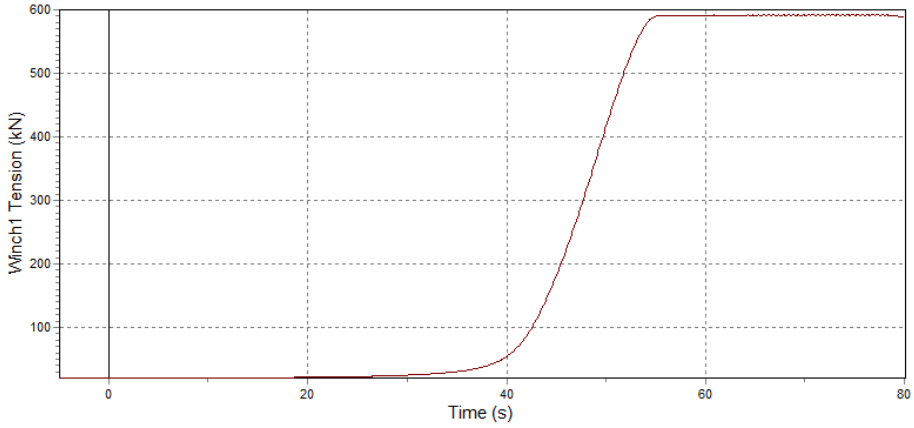

Figure D.4: Time history graph of the winch tension

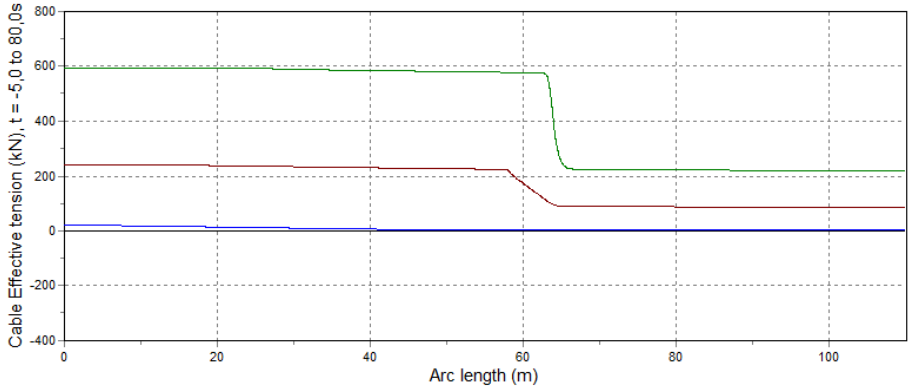

Figure D.5: Range graph of the cable tension with blue as minimum, red as mean, and green as maximum tension

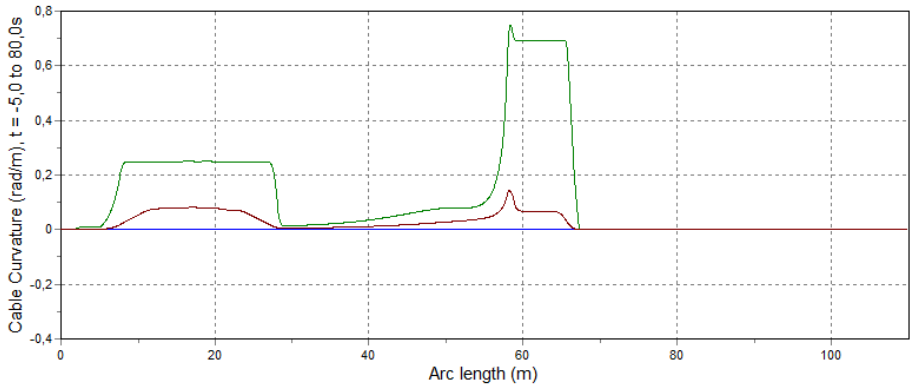

Figure D.6: Range graph of the cable curvature with blue as minimum, red as mean, and green as maximum curvature

D.3. Simulation Results Burial Depth of 3 m and Relative Density of 0.5

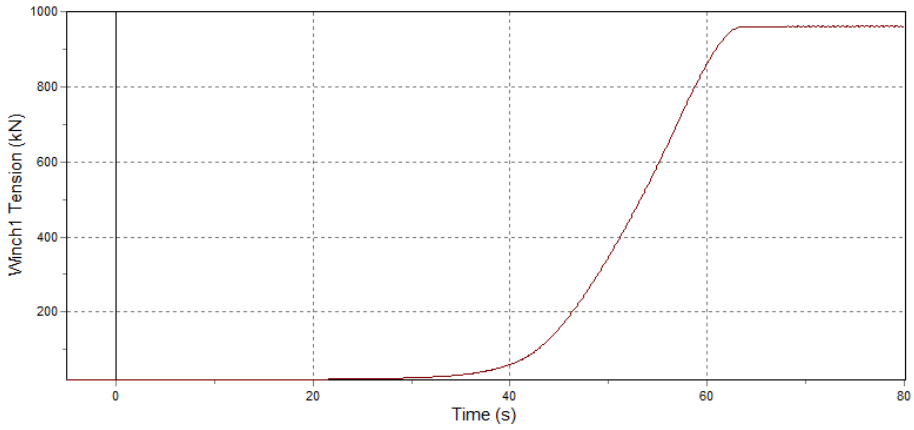

Figure D.7: Time history graph of the winch tension

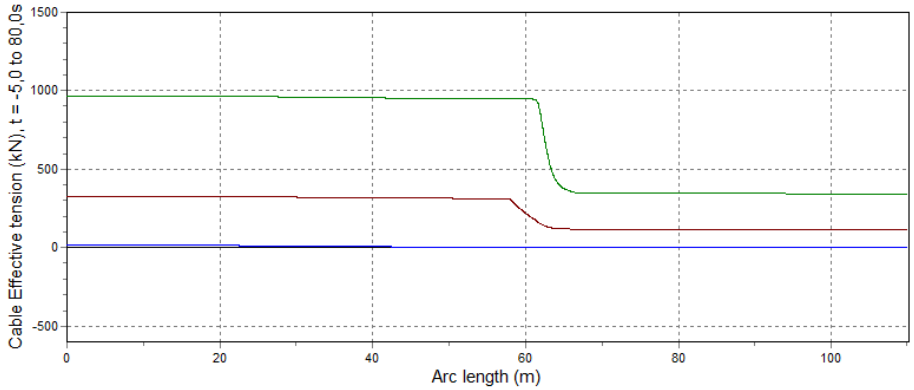

Figure D.8: Range graph of the cable tension with blue as minimum, red as mean, and green as maximum tension

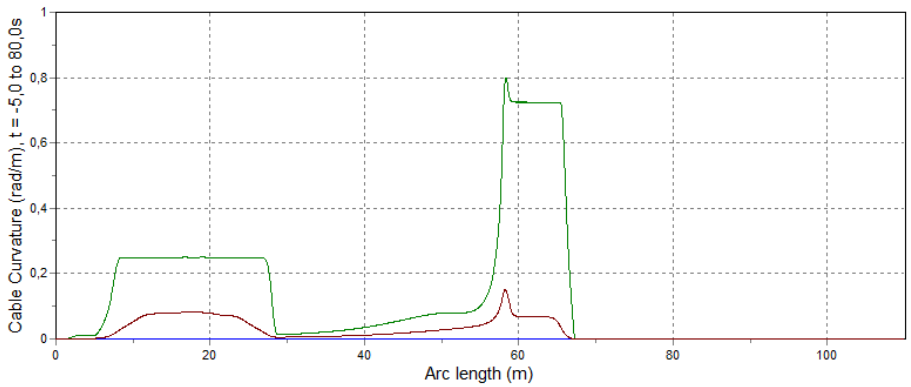

Figure D.9: Range graph of the cable curvature with blue as minimum, red as mean, and green as maximum curvature

D.4. Simulation Results Burial Depth of 4 m and Relative Density of 0.5

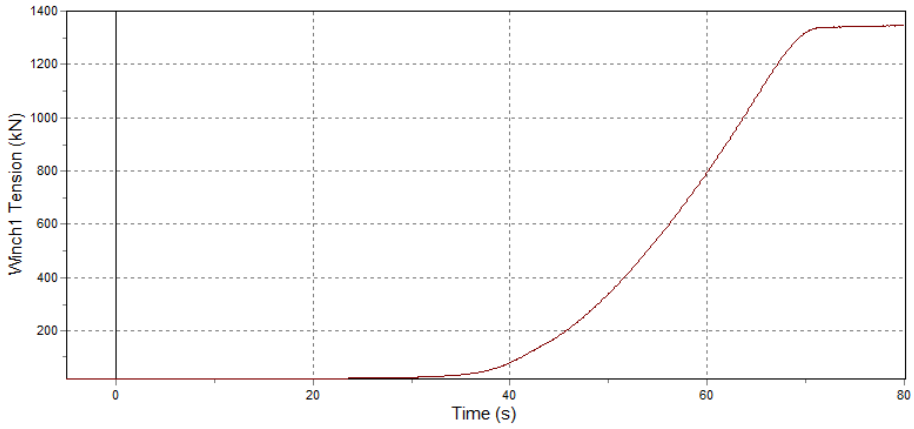

Figure D.10: Time history graph of the winch tension

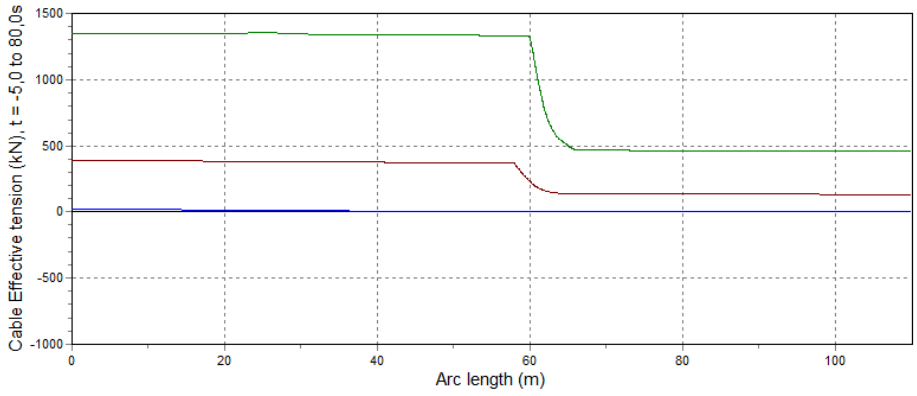

Figure D.11: Range graph of the cable tension with blue as minimum, red as mean, and green as maximum tension

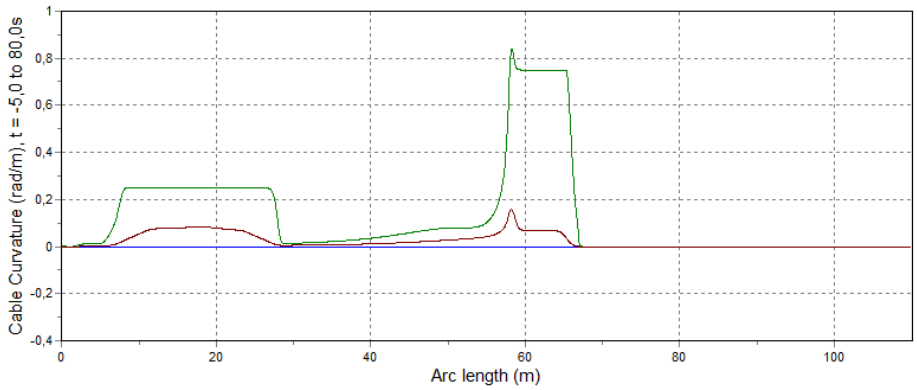

Figure D.12: Range graph of the cable curvature with blue as minimum, red as mean, and green as maximum curvature

D.5. Simulation Results Burial Depth of 1 m and Relative Density of 0.8

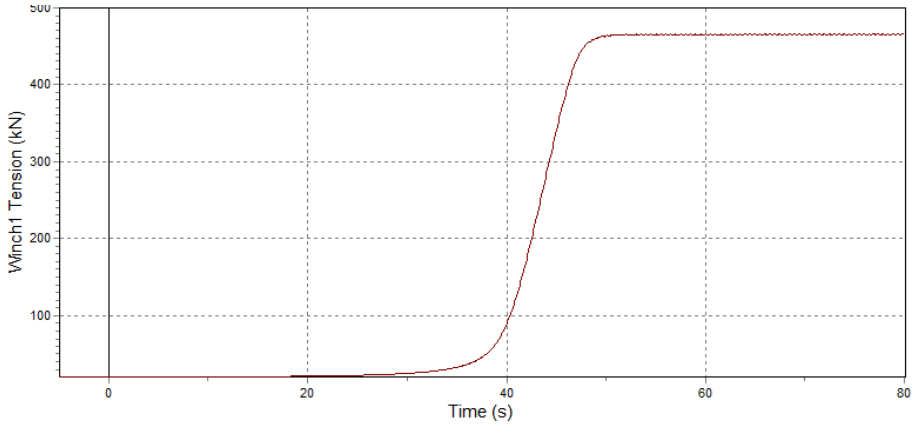

Figure D.13: Time history graph of the winch tension

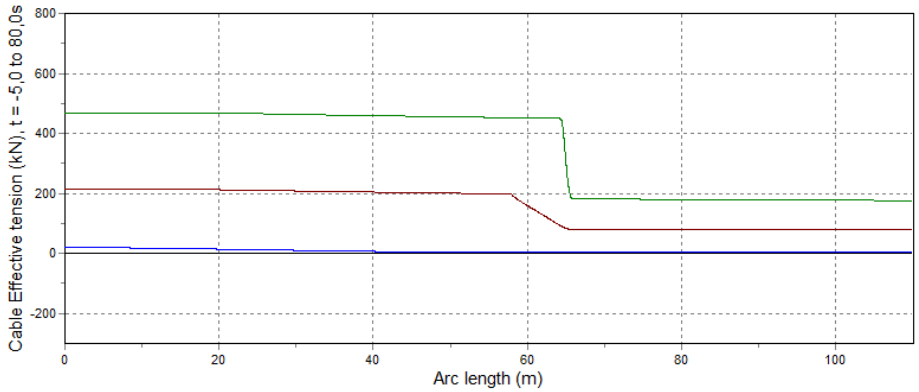

Figure D.14: Range graph of the cable tension with blue as minimum, red as mean, and green as maximum tension

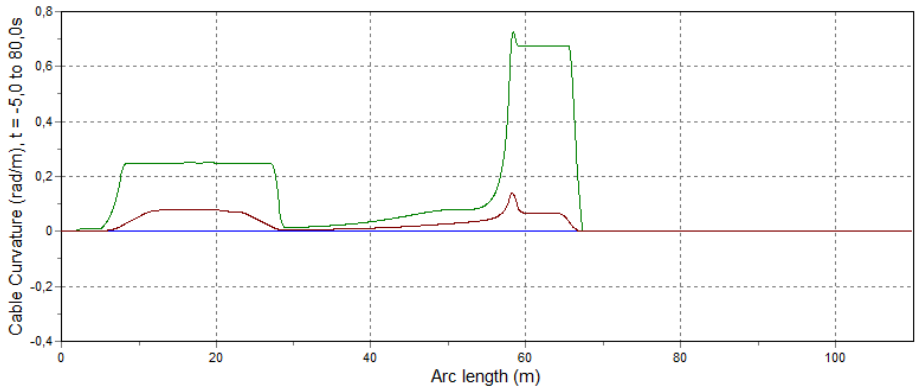

Figure D.15: Range graph of the cable curvature with blue as minimum, red as mean, and green as maximum curvature

D.6. Simulation Results Burial Depth of 1.5 m and Relative Density of 0.8

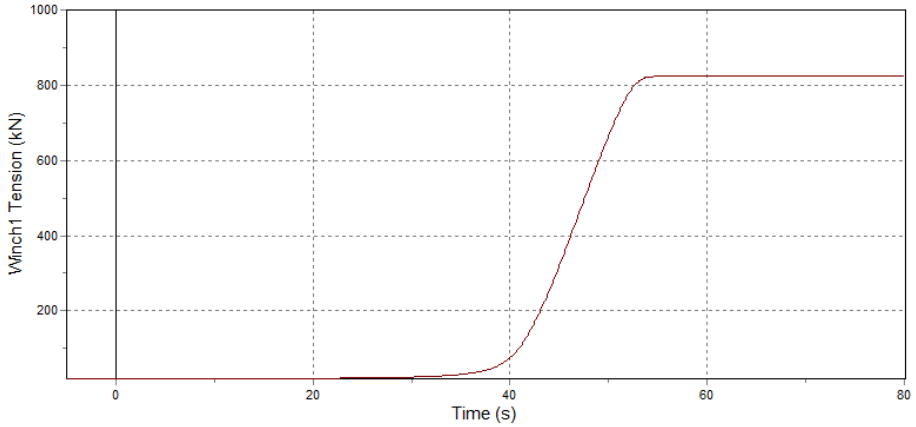

Figure D.16: Time history graph of the winch tension

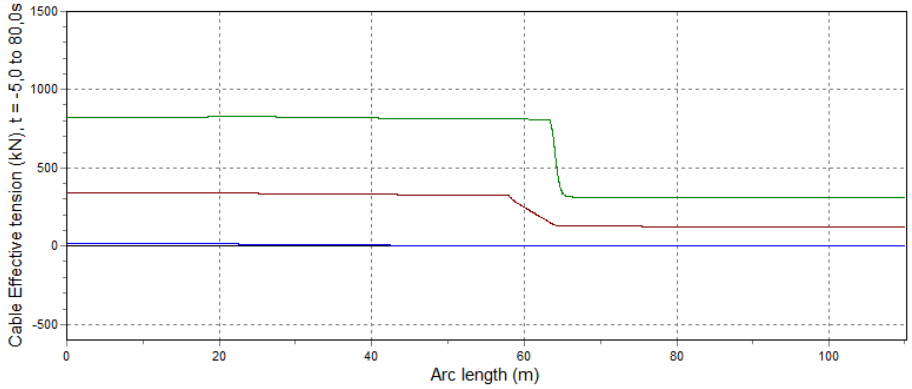

Figure D.17: Range graph of the cable tension with blue as minimum, red as mean, and green as maximum tension

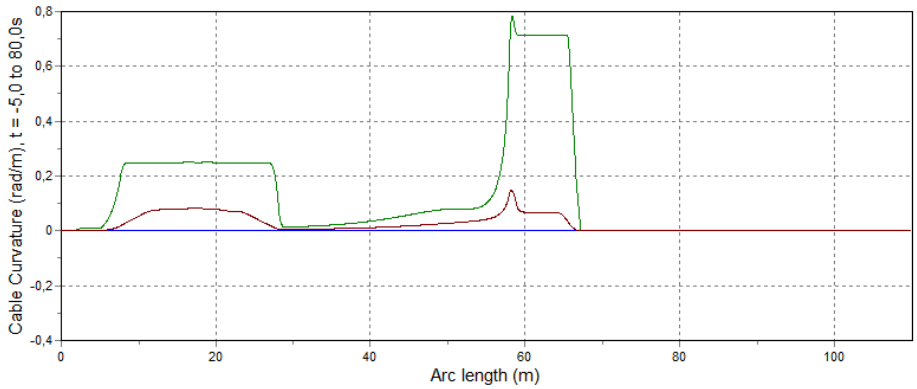

Figure D.18: Range graph of the cable curvature with blue as minimum, red as mean, and green as maximum curvature

D.7. Simulation Results Burial Depth of 2 m and Relative Density of 0.8

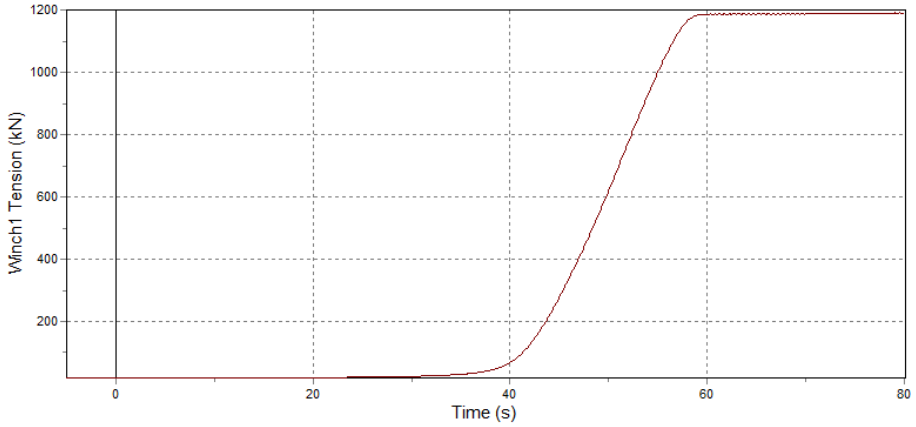

Figure D.19: Time history graph of the winch tension

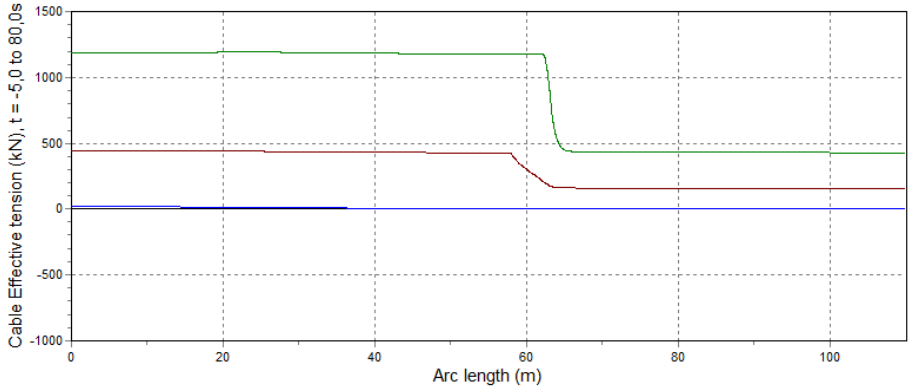

Figure D.20: Range graph of the cable tension with blue as minimum, red as mean, and green as maximum tension

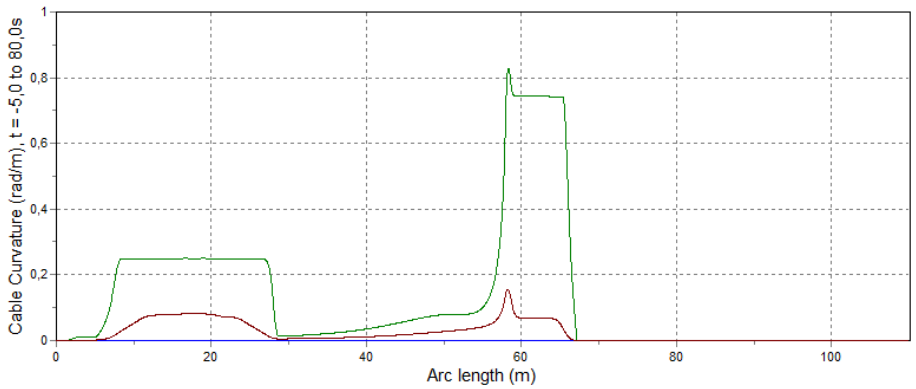

Figure D.21: Range graph of the cable curvature with blue as minimum, red as mean, and green as maximum curvature

E

External Python Function for Soil Modelling

```python
import numpy as np
import matplotlib.pyplot as plt
import math
import os

class Uplift_resistance(object):
    def Initialise(self, info):
        line = info.ModelObject
        self.logfileName = (os.path.splitext(info.Model.latestFileName)[0] + "_" + line.name
            + "_" + info.DataName + ".log")

        # Open a log file for writing
        self.log_file = open(self.logfileName, "w")
        # Header
        self.log_file.write("Time,z,Velocity,Resistance\n")
        self.log_file.flush()

        # Track the current time
        self.current_time = None
        self.last_log_entry = ""

        # Cable parameters
        self.D = 0.149 # cable diameter in meters

        # Soil parameters
        self.gamma_prime = 10
        self.I_D = 0.5 #relative density
        self.H0 = 1 # initial burial depth
        self.c_V = 3000000/(365*24*3600) # coefficient of consolidation

        if self.I_D < 0.15: # very loose
            self.f = 0.29 # DNV RP F114 Table 5-1
        elif self.I_D < 0.85:
            self.f = 0.29 + (self.I_D - 0.15) * (0.62 - 0.29) / (0.85 - 0.15)
        else: # very dense
            self.f = 0.62

        self.Q = 10
        self.phi_cv = 32 / 180 * math.pi
        self.p_f_prime = math.exp(self.Q - 1 / self.I_D)
        self.s_u = 0.5 * self.p_f_prime * (6 * math.sin(self.phi_cv)/(3 - math.sin(self.
            phi_cv)))

        self.N_c = 10.5 # Brandsby 2009

```

```
        self.m = 1
        self.V_50 = 0.01

        # OrcaFlex variables
        self.WD = 30 - self.H0 - self.D # virtual water depth, 30 m = OrcaFlex water depth
        self.Z0 = - self.WD - self.H0 - 0.5 * self.D

        self.segment = 0.1 # segment length

        # Time
        self.InitialFailureTime = None

    def Calculate(self, info):
        if True: # use if info.NewTimeStep: to only compute for the first iteration of each timestep
            node_data = info.InstantaneousCalculationData
            position = node_data.Position  # Tuple: (X, Y, Z)
            velocity = node_data.Velocity  # Tuple: (Vx, Vy, Vz)

            v = velocity[2]

            z = - self.Z0 + position[2]

            if True:
                D = self.D
                H = self.H0 - z  # depth of cover in m
                if H < 0:
                    H = 0
                    D = self.D + self.H0 - z
                    if D < 0:
                        D = 0

                term1 = self.gamma_prime * H * D
                term2 = self.gamma_prime * D**2 * (1/2 - math.pi/8)
                term3 = self.f * self.gamma_prime * (H + D/2)**2
                F_uD = term1 + term2 + term3

                term3 = 2 * self.s_u * (H + D/2)
                F_global = term1 + term2 + term3

                F_local = self.N_c * self.s_u * D - self.gamma_prime * math.pi * D **2 / 4

                F_uU0 = min(F_global, F_local)

                t = 0
                if self.InitialFailureTime is not None:
                    t = info.SimulationTime - self.InitialFailureTime
                T = self.c_V * t / self.D **2
                n = 1
                T_50 = 0.5
                F_uU = F_uD + (F_uU0 - F_uD) * (1/(1 + (T/T_50) ** n))

                V = v * self.D / self.c_V
                F_u = F_uU + (F_uD - F_uU) * (1 / (1 + (V / self.V_50) ** self.m))

                z_mob = 0.1 * self.H0 # 0.1 is based on Bransby
                k = F_uU0 / 100 / z_mob
                F = F_uD
                if k * z > F_uD:
                    F = min(k * z, F_u)

                if v <= 0.001:
                    F = F_uD

                if F > min(F_uD,F_uU0):
                    if self.InitialFailureTime is None:
                        self.InitialFailureTime = info.SimulationTime



            log_entry = f"{info.SimulationTime},{z},{v},{F}\n"
```

```
114
115
116             if self.current_time is not None and self.current_time != info.SimulationTime:
117             # If the timestep changed, write the last recorded entry to the file
118                 self.log_file.write(self.last_log_entry)
119                 self.log_file.flush()
120
121             # Update the current time and last log entry
122             self.current_time = info.SimulationTime
123             self.last_log_entry = log_entry
124
125
126
127             # Set the force to be applied
128             info.Value =  -F * self.segment
129
130     def Finalise(self):
131         # Write the last entry upon finishing the simulation
132         if self.last_log_entry:
133             self.log_file.write(self.last_log_entry)
134             self.log_file.flush()
135         # Close the log file
136         self.log_file.close()
```